AN ABSTRACT OF THE DISSERTATION OF

Brie J. Lindsey for the degree of Doctor of Philosophy in Oceanography presented on August 27, 2013.
Title: Bioenergetics and Behavior of the Krill *Euphausia pacifica* in the California Current System off the Oregon Coast

Abstract approved: _____
Harold P. Batchelder

Euphausia pacifica, the North Pacific krill, is a key grazer in the California Current System and an important prey item for consumers such as salmon, seabirds, and whales. As a crucial link between phytoplankton and higher trophic levels, it is essential to understand both the behavior and bioenergetics of this species in the context of its physical environment in order to anticipate distributions in time and space. The second chapter of this dissertation explores an hypothesis of differential transport of larval stages at the Oregon coast with an analysis of previously-collected and staged samples of *E. pacifica*. A metric was proposed to quantify the fraction of migrating late larval stages in net tows and how it was anticipated to vary with upwelling on an event-length time scale, due to differential cross-shelf transport. While the data from one year were consistent with the hypothesized relationship, the other years in the analysis did not conform to expectations. Results suggest there may be other confounding factors operating in the Oregon upwelling zone that prevent the direct observation of differential transport of larvae with field samples. The third chapter discusses egg transport between the Oregon coast shelf break and the inner

shelf region. Modeling of egg trajectories demonstrated that females spawning at or beyond the shelf break are unlikely to be the primary source of eggs found at an inner shelf station. Years with strongly positive (warm) Pacific Decadal Oscillation index values are not likely to be years with large fluxes of *E. pacifica* eggs to the nearshore region if they originate at the shelf break or seaward, as a result of increased egg development rate. Finally, the fourth chapter introduces an individual based model (IBM) of *E. pacifica* bioenergetics and explores the potential for the species to maintain its position in a region off Oregon, as well as the assumption that repeated sampling in the region is resampling the same *E. pacifica* population over a period of months. Optimistic (i.e. no mortality) trajectories of individuals modeled off Oregon suggest that cohort analyses of juvenile and adult *E. pacifica* in the region may not always violate the assumption of resampling a single population, especially if samples are taken during the fall or krill are caught in mesoscale features such as eddies. In these special cases, cohort analysis may be useful for estimating *in situ* growth rates, which might not be expected for a region as dynamic as the Northern California Current. There are still significant gaps in our understanding of fundamental biological processes for *E. pacifica*, such as how it responds to an ocean environment with generally insufficient food, whether overwintering metabolism is greatly reduced, how consumption rates by larval stages change when multiple food types are available, what mechanisms cause the variability in larval stage diel-vertical migration, and what the impact of different qualities of food might have on egg characteristics such as buoyancy. Addressing these unknowns and how well *E. pacifica* copes under non-ideal conditions will facilitate a fuller understanding of the dynamics of this species.

Bioenergetics and Behavior of the Krill *Euphausia pacifica* in the California Current System off the Oregon Coast

by
Brie J. Lindsey

A DISSERTATION

submitted to

Oregon State University

in partial fulfillment of
the requirements for the
degree of

Doctor of Philosophy

Presented August 27, 2013
Commencement June 2014

Doctor of Philosophy dissertation of Brie J. Lindsey presented on August 27, 2013.

APPROVED:

_____

Major Professor, representing Oceanography

_____

Dean of the College of Earth, Ocean, and Atmospheric Sciences

_____

Dean of the Graduate School

I understand that my dissertation will become part of the permanent collection of Oregon State University libraries. My signature below authorizes release of my dissertation to any reader upon request.

_____

Brie J. Lindsey, Author

ACKNOWLEDGEMENTS

First and foremost, I wish to thank the members of my Ph.D. committee for moving through this process with me. Each has supported me in a different way and all have contributed to my development as a scientist and a member of academia. Since the day I first met him, I have been impressed by how easily Hal can carry a conversation with almost anyone, regardless of his enormous pile of commitments. Hal has a remarkable ability to remain focused on minute details for long periods and then quickly pull back to see the larger picture, and I can only hope that I've absorbed some of that talent by working with him. Even if that isn't the case, I know that he has taught me a lot through conversations and lots and lots of red ink. I cannot express enough how important his support of me in the final year of my Ph.D. contributed to my confidence as a scientist. Yvette has been a source of not only interesting science conversation and modeling background, but also valuable advice on work/life balance and how to exist comfortably in academia. Though Bill is one of the most expert experts I've ever met, he never tried to make me feel like an idiot for not knowing things that an observationalist working in the area for decades would know in his sleep. I am grateful to Ted for his encouragement during some of the scariest parts of this process, when his words were able to calm me when nothing else would. My biggest regret looking back on my graduate education is that I did not lean on these remarkable people more. Together, they have provided me with one of the most important lessons I will have learned in graduate school: not to let my respect and admiration of remarkable people turn to intimidation and keep me from taking advantage of the opportunity to learn from them. I look forward to continuing to develop relationships with all of them in the coming years.

Chapters 3 and 4 would not have been possible without the modeling efforts of Drs. Christopher Edwards and Jerome Fiechter of University of California, Santa Cruz, who developed and ran the ROMS and NEMURO models used in this research. Both have been very generous not only in sharing the fields but also with their time when answering my many questions about forcing fields, boundary conditions, and other aspects of both models.

I owe the privilege of working with these scientists to several funding sources. Support for my first year came from the Diversity Pipeline Fellowship through Oregon State University. For several years afterward, my student funding and conference travel was provided by the U.S. GLOBEC program, NOAA, and NSF, as well as teaching assistanceships that also allowed me to develop my teaching skills and philosophy. My final stretch was funded by the Richard D. Mathews Memorial Scholarship and generous support from the Chipman Downs fund.

Many friends and colleagues I have met along the way have made the journey that much more rewarding. I have to thank Toby Garfield and Julie McClean for introducing me to oceanography in the first place, without them I might never have taken this path. Bren, my first Batchelder lab mate, helped me put lots of things into perspective! Aaron, Brandon, and Amanda, were fantastic office mates who inspired me on a daily basis and I enjoyed our mutual encouragement sessions. Karen, my study buddy for the written exams, made that part a lot more bearable than it might have been. Maria was my rock throughout some of the hardest parts. I miss having her as a writing partner and a life- and career-path analyzer. She continues to inspire me from across the country.

I could never have gotten this far without the love and support of my brothers Daniel and Josh, and my mom and dad. And I can't possibly say enough about how wonderful and supportive my husband and best friend,

Tristan has been throughout. I know that without him, I wouldn't have eaten as well, played as often, or felt as believed-in if he weren't here. I am grateful to him for staying so long in Corvallis so I could finish, and for having enough faith in me for the both of us until I did.

TABLE OF CONTENTS

TABLE OF CONTENTS (Continued)

LIST OF FIGURES

Figures Page

Figures Page

Figures Page

Figures Page

Figures Page

Figures Page

LIST OF TABLES

I dedicate this dissertation to my boys. I am so very proud of you and I love you so, so much.

1.0 Introduction

Euphausiids (krill) are a key trophic pathway for food webs in the world ocean. They are an energetic link between lower trophic level organisms, such as phytoplankton and smaller zooplankton (Ohman, 1984), and higher trophic level organisms, such as fish, baleen whales, and seabirds (Ainley *et al.*, 1996). There is evidence that some euphausiids may bypass the microbial loop and feed directly on nano- and picoplankton under certain conditions (Passow and Alldredge, 1999). The variability in abundance of some krill associated with El Niño/Southern Oscillation events (Lavaniegos-Espejo *et al.*, 1989) and the overall decline in biomass of California Current System zooplankton with upper-ocean warming (Roemmich and McGowan, 1995) establishes krill as a potentially useful bioindicator organism. And krill play direct roles in biogeochemical cycling in the water column, actively transporting carbon to depth while migrating (Steinberg *et al.*, 2000). As such influential members of the plankton assemblage, an understanding of krill spatial distributions and bioenergetics is important in a broader context than just euphausiid biology.

Krill spatial distributions are thought to be influenced by their behavior, which in turn likely depends on their development through a series of dramatically different morphological stages on their way to adulthood. These life stages span a range of abilities related to changing appendages (Boden 1950; Mauchline and Fisher 1969). The typical progression for a euphausiid is through 15 stages from egg to adult (Figure 1.1). An egg hatches into the first of two naupliar stages. In the naupliar stage, a euphausiid has an unsegmented, oval body with no compound eyes and few, simple limbs. A single metanauplius stage follows, during which there is

some rearrangement of limbs (some, like the mandibular legs, are lost) and budding of other appendages begins. Next, the euphausiid develops through three calyptopis stages, the first of which includes the development of feeding appendages, allowing the larva to feed for the first time. Development continues through up to seven separate furcilia stages. It is during this time that features such as the antennae and compound eyes become more fully developed and complex behaviors such as diel-vertical migration commonly begin to be expressed (Vance 2003; Feinberg *et al* 2006). The final molt out of furcilia 7 and into the juvenile stage produces an individual that closely resembles an adult. Finally, after many molts, the individual is a reproductively mature adult (Mauchline 1971).

One of the most well-studied krill species in the world is *Euphausia pacifica*, the North Pacific krill described by Hansen in 1911 (Hansen 1911). This species is found in a remarkably wide array of ecosystems around the North Pacific basin (Figure 1.2), from subarctic to subtropical biomes and oceanic regions to fjords. Their ability to thrive in such diverse environments is a testament to the plasticity of their life history, and sustains interest in them as a study species.

Field workers have been exploring aspects of *E. pacifica*'s life history and physiology since the 1950's. Boden (1950) described the development of larval stages from samples off southern California. Nemoto (1957) presented growth rates for *E. pacifica* off Japan, while Smiles and Pearcy (1971) estimated growth from cohort analyses off Oregon. Brinton (1976) estimated growth rates from observations of cohorts off southern California, as well as reproductive output and survivorship of various life stages. Lasker (1966) explored feeding rates and resources and resulting growth rates in the laboratory. Ohman (1984) added to reports and considerations of the

crustacean's omnivory. In the early 1980's, Ross presented measurements of energetics and full carbon and nitrogen budgets (1982*a* and *b*) to the efforts of Lasker (1966) and Pearcy and Small (1968). Ross *et al* (1982) observed spawning and estimated fecundity for *E. pacifica* in Puget Sound, Washington. More recently, much effort has been put into understanding variations in spawning capacity, timing and intensity (Tanasichuk 1998, Feinberg and Peterson 2003, Pinchuk and Hopcroft 2006, Feinberg *et al.* 2007, Gómez-Gutiérrez *et al.* 2007) and estimating growth rates in relation to spatial, interannual and seasonal variability (Pinchuk and Hopcroft 2007, Shaw *et al.* 2010).

As a zooplankter that straddles the definitions of true zooplankton in its early larval stages and what some might consider micro-nekton by its adult phase, *E. pacifica*'s distributions and behaviors have also been of great interest to researchers since the mid-twentieth century. Brinton reported on their horizontal distribution across the North Pacific (1962) and their vertical distribution in the water column (1967). Other observations of vertical distribution and swimming behavior (Bollens et al 1992, Iguchi *et al.* 1993, DeRobertis 2002, Vance *et al.* 2003) have led to discussions of how its behavior might influence its distribution (Lamb and Peterson 2005, Keister *et al.* 2009).

One place *E. pacifica* calls home is the Northern California Current, (NCC) in the upwelling region off the Oregon coast, where it is the numerically dominant euphausiid species (Brinton, 1962; Gómez-Gutiérrez *et al*, 2003; Feinberg and Peterson, 2003). The California Current system is an extremely productive coastal upwelling system with strong interannual, seasonal, and multi-day scale variability. Seasonal alongshore equatorward winds move water offshore in the surface Ekman layer, which is replaced by

colder, saltier water that flows onshore near the bottom to upwell near the coast. California Current coastal upwelling is strongest during the spring and summer. On event time scales (order 3-10 days), upwelling can be interrupted by changes in wind direction that cause reversals in shelf current directions at the surface and along the bottom. All of these dynamics have implications for krill distribution and their ability to maintain populations in the highly advective NCC.

Gómez-Gutiérrez *et al.* (2005) report from data obtained in 1970-1972 that *E. pacifica* larvae were ubiquitous across the shelf off of Newport, Oregon, but adults were found in highest abundances near the shelf break (about the 200m isobath). Feinberg and Peterson (2003) mentioned a similar inshore larvae/offshore adults trend for data collected between 1996 and 2001. Diel-vertical migration, which is a stage- or size-dependent behavior in *E. pacifica*, has been suggested as a retention mechanism for species occupying coastal upwelling regions (e.g. Batchelder *et al.* 2002), and it has been generally assumed that different life stages are retained differentially in dynamic coastal systems (see discussion in Brinton 1976). The second chapter of this dissertation explores a hypothesis of differential transport of larval stages of *E. pacifica* collected at the Oregon coast in an effort to link distributions of various portions of the population to changes in wind stress.

Despite the amount of research effort that has been devoted to understanding *E. pacifica*, there remain unanswered questions about where and when eggs are released. In particular, it is unclear how (or if) high abundances of eggs sampled at an inshore station off Oregon (Feinberg and Peterson 2003) arrive there from where they are presumably released at the shelf break, where large numbers of gravid females are found (Gómez-Gutiérrez *et al.* 2010). The third chapter pairs a particle-tracking model with

a temperature-based model of *E. pacifica* egg hatching to evaluate the likelihood that eggs found in the nearshore region are, in fact, from the shelf break.

The fourth chapter presents an individual-based development and bioenergetic model that pulls together many of the aspects of krill physiology and behavior mentioned above to give an estimate of juvenile stage duration in *E. pacifica* under a range of food and temperature conditions likely to be found near the Oregon coast. In addition, the chapter includes a particle-tracking model with behavior and development to explore the validity of the assumption that a population of krill sampled repeatedly for cohort analysis in a region as dynamic as the California Current remains in place.

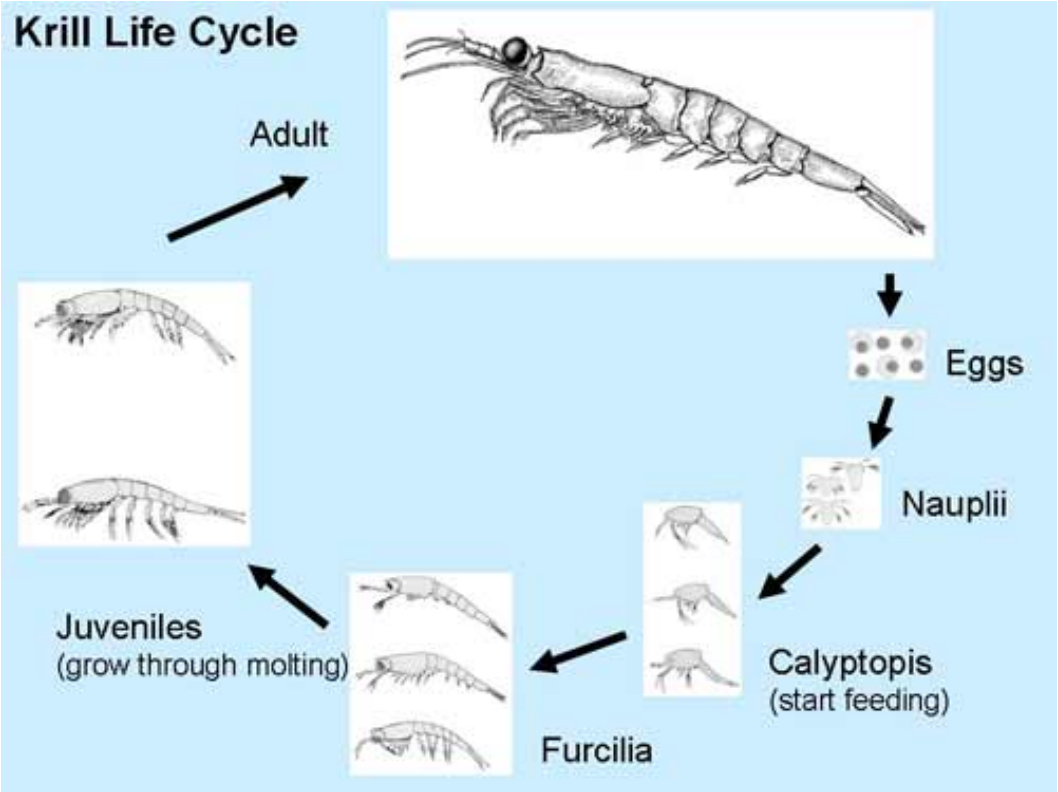

Figure 1.1. Typical life cycle of a euphausiid. A typical progression is through 15 distinct stages, with multiple instars in the naupliar, calyptopis and furciliar stages. In this figure, the metanauplius is grouped with the nauplii. Figure by Jillian Worssam. Illustrations from Boden 1950.

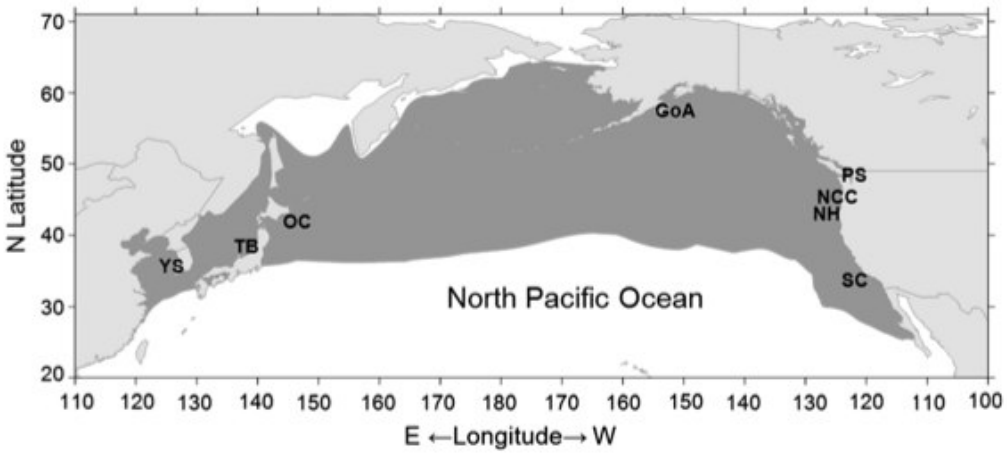

Figure 1.2. Pan-Pacific distribution of *Euphausia pacifica*. From Feinberg *et al* (2013). Letters in the figure denote regions from which data came for their excellent synthesis of geographical variability in brood size, interbrood period, and fecundity.

Cross-shelf distribution of *Euphausia pacifica* in the Oregon coastal upwelling zone: Field evaluation of a differential transport hypothesis

Brie J. Lindsey and Harold P. Batchelder

Journal of Plankton Research
www.plankt.oxfordjournals.org
Volume 33, Number 11, Pages 1666-1678
June 30, 2011

2.0 Cross-shelf distribution of *Euphausia pacifica* in the Oregon coastal upwelling zone: Field evaluation of a differential transport hypothesis

2.1 Abstract

The frequent upwelling events characteristic of Oregon's summer may make nearshore retention challenging for early, non-migrating euphausiid life stages inhabiting the surface layer. In contrast, later, vertically migrating life stages spend more time below the strongest offshore flow, and are moved offshore less rapidly. We hypothesize that population stage structure will vary in predictable ways as a result of differential transport, a function of occupied depth (and therefore life stage). MOCNESS samples have indicated early *Euphausia pacifica* calyptopes (stages 1-2) are non-migrators, while late furcilia (stages 4-7) are migrators. We develop a metric (Fraction of Migrators, F_M) of relative densities of these larval stages within a sample to examine potential differential transport with alongshore winds on short timescales (0.5 to 7 days), for data collected during upwelling seasons from 2000 to 2002 at two stations off Oregon. F_M and northward winds had a significant negative relationship in 2002 at the inshore station, indicating differential transport. Upwelling condition-classified sampled densities at nearshore and offshore stations also suggested differential cross-shelf transport, but trends were not always consistent with the hypothesis, suggesting the cross-shelf distribution of non-migrators was not consistent throughout the study period. Several other factors, such as spawning, might also contribute to significant trends observed in F_M. The results of this analysis suggest relationships exist between *E. pacifica* larvae distributions and wind events in the Oregon upwelling region, but that the distributions may be too complex to predict at the event scale without more sophisticated tools, such as biological-physical coupled models.

2.2 Introduction

In the northern California Current System (CCS), the response of biological distributions to many physical influences at various temporal scales is often pronounced. Interannual influences might include multi-month duration events, such as the 1997-1998 El Niño, when phytoplankton concentration off Oregon was abnormally low when warm, nutrient-poor waters were advected into the region and weak upwelling prevented the normal influx of new nutrients to the surface waters (Corwith and Wheeler, 2002). The Oregon upwelling season is typically characterized by strong, intermittent equatorward winds that advect water in the Ekman layer (~10-40m) offshore and upwell deep, cold, nutrient-rich water to the surface near the coast. This contrasts strongly with wintertime conditions when winds blow northward and downwelling conditions prevail. These seasonal shifts in current direction and strength can change the zooplankton assemblage from homogeneous across the shelf and slope in the winter to sharply segregated in the summer, when northern waters carry boreal species equatorward along the coast (Keister and Peterson, 2003).

However, physical circulation alone cannot entirely explain zooplankton spatial patterns; in many cases, the behavior (e.g. vertical migration or swarming) of zooplankton is also important. Various behaviors influence zooplankton depth in the water column, which can play an important role in the horizontal distribution of the population in a region of dynamic circulation on seasonal and shorter timescales. For instance, ontogenetic variations in preferred depth of several copepod species off Oregon were observed to lead to species-specific seasonal cross-shelf distributions in the upwelling zone (Peterson *et al.*, 1979).

Diel vertical migration (DVM), a behavior expressed by krill and other

zooplankton species, is the migration between surface and deeper waters over a daily cycle. The behavior can be influenced by physical factors, such as temperature, density, and light intensity (Mauchline and Fisher, 1969) and by biological factors ranging from reproductive strategies to food availability or predation pressure (Bollens *et al.*, 1992; Tarling *et al.*, 1999). Keister *et al.* (2009) showed that distributions of small, weakly-swimming copepods closely resembled physical fields (e.g. sea surface height) in the CCS, whereas the distribution of other zooplankton, such as larger copepods and krill, did not mimic physical circulation patterns, suggesting that biological processes, such as vertical migration behavior, may have been important in determining their distributions.

DVM has been suggested as a mechanism for the nearshore retention of some species in coastal upwelling regions (e.g. Pillar *et al.*, 1989; ; Peterson, 1998; Dorman *et al.*, 2005; Lamb and Peterson, 2005). As a zooplankter descends out of the surface layer during an upwelling event, it enters depths where offshore flow is more sluggish (or moves onshore in deeper waters). Since the Ekman layer is rapidly displaced offshore during active upwelling, any time spent away from the surface reduces offshore transport, and may benefit organisms that require the denser prey fields often available near the coast. Batchelder *et al.* (2002) demonstrated the theoretical effectiveness of DVM in retaining a population nearshore with an individual-based copepod model coupled to a 2-D cross-shelf circulation model. Marta-Almaida *et al.* (2006) developed a crab larvae model which showed that depth-dependent differential advection could retard offshore loss of larvae.

While these studies have focused on whether zooplankton behavior impacts horizontal distribution in environments with strong upwelling

circulation, they have not addressed how developmentally-related changes in behavior in a single species may impact the cross-shelf distributions. The life cycles of many zooplankton consist of a sequence of life stages with varying physiological or morphological developments that affect the zooplankter's vertical swimming competencies and behaviors. This shifting expression of behavior with developmental stage may have subtle effects on the species' cross-shelf distributions and may be important for understanding the mechanisms controlling the distribution of species near the coast.

One species in the Oregon upwelling region with such a complex life history is the numerically dominant and well-studied krill, *Euphausia pacifica*. This species passes through several developmental stages, moving from egg through two nauplius stages (N1-N2), a metanauplius stage (MN), three calyptopis stages (C1-C3), up to seven furcilia stages (F1-F7), and a juvenile phase on its way to adulthood (Feinberg *et al.*, 2006; Suh *et al.*, 1993; Ross, 1981; Mauchline and Fisher, 1969; Boden, 1950). As the krill develop through early furcilia stages, additional appendages are added and its swimming ability improves, allowing deeper daytime migration (Suh *et al.*, 1993; Knight, 1984). Vance *et al.* (2003) reported that, among *E. pacifica* larval stages, late-stage furcilia are found deepest in the water column during the day, while earlier larval stages (e.g. calyptopes) are found closer to the surface. If offshore transport of krill in a coastal upwelling region is reduced by an interaction between DVM and upwelling circulation, one would expect less motile, surface-dwelling stages to be transported offshore more rapidly during upwelling than are more motile stages that undertake larger amplitude DVMs. If DVM amplitude is a function of life-history stage, the resulting cross-shelf distributions of early and late life-stages might differ under various wind conditions.

A small number of studies present evidence to support this hypothesis. Pillar *et al.* (1989) reported differential transport of early versus later life stages of *Euphausia lucens* during two hydrographic regimes in the Benguela current system. However, the data represented only a brief period (two cruises over two months in 1973), covering only one upwelling event and one relaxation period. Gómez-Gutiérrez *et al.* (2005) described a persistent cross-shelf separation of *E. pacifica* life phases near the Oregon coast from samples collected in the 1970's (also evident in data from the 2000's; Lamb and Peterson, 2005): adults dominated the shelf break whereas the earliest larval stages were more abundant nearshore. While Gómez-Gutiérrez *et al.* (2005) and Gómez-Gutiérrez (2003) found a weak relationship between all early larval stages (nauplii through furcilia) and upwelling events using the Bakun Upwelling Index, they did not discuss whether the influence of upwelling varied between these stages or how important it might be in shaping the cross-shelf distribution of *E. pacifica* early larval stages over the narrow shelf. Therefore, it is difficult to know how upwelling may have influenced the distributions of *E. pacifica* larvae across the shelf in the short term, or how the differential DVM amplitudes of different life stages contributed to any potential nearshore retention.

Understanding how differing *E. pacifica* larval behaviors and wind-forced circulation on the Oregon shelf interact on the scale of wind events should help to better identify the processes leading to the overall cross-shelf distribution of this species. Because the Oregon coast experiences upwelling-favorable winds that are more episodic than farther south in the CCS, it is an ideal location to study event-scale effects of upwelling circulation on *E. pacifica* distributions. The objective of this analysis is to quantify the short-term (0.5- to 7-day) effects of alongshore winds on the cross-shelf

distribution of *E. pacifica* larvae, using a metric of relative abundances of vertically migrating and non-migrating larval stages.

2.3 Methods

Data collection and processing

As part of the U.S. GLOBEC program, sampling along a cross-shelf transect was generally conducted biweekly off the Oregon coast, USA, during the April-October upwelling seasons of 2000, 2001, and 2002 along the Newport Hydrographic (NH) Line (Latitude 44.65° N). Samples used in this analysis were collected day and night with 0.5m diameter, 202μm mesh ring nets towed vertically to the surface from the shallower of 5m above the bottom or 100m. A TSK flowmeter in the mouth of the net provided estimates of filtered volumes. Samples were preserved in 5% buffered formalin-seawater. *E. pacifica* from samples collected at station NH15 (124.41°W, 92m water depth) and farther offshore at station NH25 (124.65°W, 297m water depth) were counted and identified to development stage in the laboratory. Further details of collection and staging can be found in Feinberg and Peterson (2003).

The National Data Buoy Center (NDBC; www.ndbc.noaa.gov) database provided hourly wind data for 2000-2002 at NDBC station 46050 (44.64°N, 124.50°W; 123m water depth), located 22 miles due west of Newport, OR, and at Coastal-Marine Automated Network (C-MAN) station NWPO3 (44.61°N, 124.07°W; 9.1 m above sea level), located on the south jetty at Newport. Gaps in the NDBC 46050 wind data were filled using estimates from a linear regression relation between NDBC 46050 and NWPO3 (R^2=0.64, 0.72, and 0.63 for 2000, 2001, and 2002, respectively). In rare instances (less than 1% of the data record), winds were not available from

either station.

Definitions

Cumulative Wind Stress. Wind stress was calculated hourly according to the method of Large and Pond (1981). Northward (alongshore) cumulative wind stress (CWS) prior to the collection of the plankton sample was used to represent recent wind energy input to the upwelling system. CWS[t] was calculated from hourly wind stress for various durations (t=0.5,1, 3, and 7 days) prior to each sample to provide descriptive wind histories for each sample at several short timescales.

Upwelling classifications. Upwelling classes were determined for each of the four durations described above. Plankton samples were considered to be obtained after upwelling if the CWS[t] for the sample was equivalent to that resulting from an average of -5 m s^{-1} (i.e. 5 m s^{-1} wind speed to the south) over the same period. Because alongshore wind is highly variable during the upwelling season, a single plankton sample might be classified differently (as upwelling or not upwelling – relaxed or downwelling) depending on the time span (t) considered. That is, a sample may be classified as upwelling when CWS is calculated from a short time span (e.g. 1 day), but non-upwelling when calculated from a longer time span (e.g. 3 day). Given that wind direction in the northern CCS often changes within a few days, classification based on longer periods generally results in fewer upwelling-classified samples.

Migrators and non-migrators. Migrators and non-migrators are defined as the larval stages of *E. pacifica* that are *clearly* capable and incapable of vertical migration, respectively, as previously determined by differences in vertical positions of stages between day and night Multiple Opening/Closing Net and Environmental Sampling System (MOCNESS)

plankton samples from the NH Line (Vance *et al.*, 2003; Figure 2.1). Calyptopis 1 and 2 (C1 to C2) are able to swim, but their small size and undeveloped pleopods diminish their ability to determine their vertical position (Brinton *et al.* 1999). Therefore, they are considered "non-migrators," while late-stage furcilia (F4-F7) are "migrators." Because the extent of migration by intermediate larval stages (F1 through F3) is not clearly distinguished from that of later and earlier stages in the MOCNESS samples, these stages were not included in the analysis. *Euphausia pacifica* juveniles and adults are very strong migrators but were excluded because they are known to avoid daytime capture by small diameter ring nets (Brinton, 1967), resulting in sampled densities not representative of *in situ* numbers when daytime samples are included, as they are here.

Migrator fraction. The proportion of migrators in the sample, or the Migrator Fraction (F_M), is based on log transformed abundances captured in a single plankton sample:

$$F_M = \frac{\log_{10}(a_M + 1)}{(\log_{10}(a_M + 1) + \log_{10}(a_N + 1))}, \quad a_M = \sum_{j=11}^{14} a_j \text{, and } a_N = \sum_{i=5}^{6} a_i \text{,}$$

where a_M is the sum of densities (individuals m^{-3}) of all migrating stages (j = stages 11 through 14, or F4 through F7) and a_N is the sum of densities (individuals m^{-3}) of all non-migrating stages (i = stages 5 through 6, or C1 through C2) in a given sample. Summed densities were log-transformed to account for non-normal distribution. Some samples lacked one or more categories of interest; the F_M metric was designed to avoid mathematically undefined values when either migrators or non-migrators are absent in a sample. F_M ranges from 0 to 1: F_M=0 when migrators were absent in the sample, F_M=1 when non-migrators were absent in the sample, and F_M=0.5 when migrators and non-migrators are equally abundant. Because earliest

larval stages are typically more numerous than late larval stages, samples are expected to have a high frequency of $F_M<0.5$.

Differential Transport Hypothesis and Analysis. The Differential Transport Hypothesis (DTH) proposed here predicts that F_M will vary systematically in response to an observed time-integrated strength of wind forcing. Migrating larval stages spend less time in the highest cross-shelf velocity regions of the near surface Ekman layer than do non-migrating larval stages, and will therefore experience different cross-shelf transport during active upwelling or downwelling. Shelf station samples are expected to have highest (lowest) F_M values when wind stress histories favor upwelling (downwelling), while slope station samples show the opposite trend, primarily as a result of increased (decreased) offshore transport of non-migrating krill from shelf to slope. Likewise, when collected on the same date, shelf station samples are expected to have higher (lower) F_M than slope station samples when recent winds were upwelling (downwelling) favorable, primarily as a result of greater offshore (onshore) transport of non-migrating larval stages.

The DTH was tested in two ways. First, mean migrator and non-migrator densities were compared for upwelling and non-upwelling categories classified by the same periods for which CWS was calculated, for within-station and across-shelf patterns. Second, the relationship between F_M and CWS was explored both within station and across the shelf. Because wind-driven upwelling is very dynamic in this region, the F_M-CWS relationship was examined for each of four periods prior to sampling.

Significance of differences between sampled densities classified by CWS were determined with the non-parametric Mann-Whitney U test, which is robust to outliers, common in samples collected from patchy

environments. Pearson correlation coefficients were calculated to evaluate relationships between F_M at each station and CWS(t) or yearday. Linear CWS(t)-F_M relationships were calculated to illustrate coherence with the DTH. Finally, Fisher's exact test was used to determine significance of same-date F_M classifications across the shelf. Two-tailed p-values are reported.

2.4 Results

Wind. CWS from the beginning of the year shows interannual wind variability (Fig. 2.2). In the northern CCS, the spring transition to the upwelling season can be reliably linked to alongshore wind events (Holt and Mantua, 2009). This physical transition, shown here as the point at which the slope of CWS becomes consistently negative, began much later in 2000 (12 June) than in 2001 (30 April) or 2002 (16 April). The earliest physical autumn transition (return of poleward winds) occurred in 2000 (11 Oct, 121-day season), with later autumn transitions in 2001 (20 Oct, 173-day season), and 2002 (3 Nov, 202-day season). These transition dates are consistent with those provided for 2000-2002 by daily-averaged CWS products (Pierce *et al.*, 2006). Net CWS during the upwelling season was similar for 2001 and 2002 (-128.2 $Nm^{-2}h$ and -133.4 $Nm^{-2}h$, respectively), and lowest for 2000 (-98.6 $Nm^{-2}h$).

Distributions of zooplankton density data. Euphausia pacifica were identified to stage for 69 samples obtained at NH15 and NH25 during the upwelling seasons of 2000-2002. Of these, four (three from NH15 and one from NH25) lacked both migrating and non-migrating life stages, and were excluded. More samples were available from NH15 (10, 19, and 14 from 2000, 2001, and 2002, respectively) than from NH25 (9 and 13 from 2001 and 2002, respectively) in each year. No staged *E. pacifica* samples from

NH25 in 2000 were available for this analysis.

Migrating life stages were significantly less abundant than non-migrators over the study period (NH15: U=1344, $n1$=$n2$=43, p<<0.001; NH25: U=342, $n1$=$n2$=22, p=0.02). There were no significant interannual differences in mean migrator or non-migrator abundance at either station.

Larval densities with upwelling. Upwelling effects on mean larval densities were variable between years and dependent on the time scale of the upwelling classifications (Fig. 2.3). For 2001 and 2002 together, mean non-migrator density at NH25 was lower during upwelling than non-upwelling (for t=0.5 days: U=110, $n1$=10, $n2$=13, p=0.004; for t=1 day: U=101, $n1$=9, $n2$=14, p=0.02). The significance of the pooled result can be mainly attributed to the same pattern in 2001, which is only significant for the 0.5-day classification (U=18, $n1$=3, $n2$=6, p=0.02); a similar pattern could be seen in the non-migrator densities of 2002, but was not significant. Similarly, several patterns appeared in 2002 at NH15 (notably, higher non-migrator densities during non-upwelling times), but due to the high variability in the abundance data, these also were not significant. Though in the pooled data (2000-2002 for NH15 and 2001-2002 for NH25) migrators appeared to be more abundant at both stations during upwelling, there were no significant differences in migrator densities between classes at either station, for any period of classification. (The patterns described above were generally preserved in both the 3- and 7-day classifications, but since no significant differences were found for any comparison, these classes are omitted from Figure 2.3 for simplicity.)

As for cross-station comparisons, the classification periods that yielded significant results for cross-shelf larval density comparisons were 0.5- and 1 day. After upwelling-classified periods in 2001, there were higher

densities of non-migrators at NH15 than at NH25 (for t=0.5d: *U*=56, *n1*=11, *n2*=6, p=0.018; for t=1d: *U*=59, *n1*=12, *n2*=6, p=0.029). Post-upwelling density of migrators did not differ significantly across the shelf for any period in any year. Both migrators and non-migrator densities were virtually identical across the shelf after non-upwelling periods in all years for all classification periods.

F_M and CWS. F_M of NH15 samples (Fig. 2.4) from 2002 showed a significant negative correlation with CWS[7 days] (Pearson's r =-0.55, p=0.04), largely driving a significant correlation between the pooled (2000-2002) NH15 F_M and CWS[7d] (Pearson's r=-0.31, p=0.04). Pooled (2001-2002) NH25 samples yielded a nearly significant (Pearson's rho=-0.39, p=0.07) negative correlation between F_M and CWS[1 day], but the individual years lacked a clear relationship with recent winds (Fig. 2.5). While F_M was not significantly correlated with CWS for any other periods at either station, likely due to small sample size and a high number of samples lacking migrators (e.g. F_M=0), all trends were negative.

While aggregated data illuminate patterns for within-station comparisons of F_M under different forcing, another test of cross-shelf differential transport of migrators and non-migrators is possible when both the nearshore and the offshore stations are sampled on the same day; presumably, both stations have experienced similar recent wind forcing. During 2001-2002, there were 15 instances when samples containing both classes of *E. pacifica* larvae were obtained at NH15 and NH25 during a single transect. F_M values for all same-date samples sorted into a 2 × 2 contingency table according to the same upwelling classification periods as above showed no significant patterns across the shelf. F_M values were higher at NH15 than at NH25 about as often as otherwise in all upwelling cases (CWS[0.5 day]:

4/10 dates; CWS[1 day]: 6/11 dates; CWS[3 day]: 3/6 dates; CWS[7 day]: 4/7 dates), and were higher at NH15 than at NH25 at least as often as otherwise in all non-upwelling cases (CWS[0.5 day]: 5/5 dates; CWS[1 day]: 3/4 dates; CWS[3 day]: 6/9 dates; CWS[7 day]: 5/8 dates).

2.5 Discussion

Determining how *Euphausia pacifica* behavior might interact with physical phenomena at many timescales in the Oregon upwelling region is a necessary step toward understanding what mechanisms are most important in influencing alongshore and cross-shelf distributions of this species. An improved understanding of the role of behavior in the distribution of this species will aid in identifying spawning locations and provide insight into potential locations and mechanisms responsible for retention.

Those studies in the CCS that have specifically focused on zooplankton life stage abundances at upwelling event time scales have produced varying results. Papastephanou *et al.* (2006) discovered very clear patterns with upwelling events for *some* copepod species, but Bernal and McGowan (1981) reported no apparent influence of upwelling on cross-shelf distributions of various copepod life stages. Dorman *et al.* (2005) reported rapid responses of a Northern California *E. pacifica* population to wind forcing, including sharp decreases in larval abundance during upwelling events, presumably due to offshore transport of these weaker migrators. Similarly, Lu *et al.* (2003) found higher concentrations of *Thysanoessa spinifera* and *E. pacifica* larvae offshore of adults during generally upwelling conditions and onshore of adults during generally downwelling conditions off Vancouver Island, also suggesting that the adult ability to migrate to deeper depths retarded their cross-shore transport in either direction, relative to less motile stages.

Neither of these compared concentrations or transport of early versus late euphausiid larval phases, however.

With the aim of determining whether *E. pacifica* larvae at different developmental stages collected at the same stations along the NH Line are advected differentially, this study attempted two types of measures. The first examined differences based on collected densities of the migrating and non-migrating larvae after upwelling periods and non-upwelling periods. The second was the development of a novel metric, the Migrator Fraction (F_M), designed to be more robust to the variability expected from zooplankton density data. Cross-shelf patterns of stage density and F_M were compared with and examined in relation to CWS, which quantified the time-integrated winds for periods spanning 0.5-7 days.

A priori predictions of the DTH were that non-migrator densities at NH15 would be lower after upwelling periods and higher after non-upwelling periods. Secondarily, the hypothesis predicted higher non-migrator densities at NH25 after upwelling periods and reduced non-migrator densities at NH25 after non-upwelling periods. Strong differences in migrator abundances between upwelling and non-upwelling periods were not expected because even the later furcilia stages are unlikely to migrate deep enough to be transported in the opposite direction of the surface Ekman layer.

Few comparisons in this analysis yielded results required to accept the DTH as stated, especially as it depended on the assumption that non-migrator densities are consistently higher over the shelf, or increase shoreward from NH25. In their analysis of *E. pacifica* data collected along the NH Line between 1970 and 1972, Gómez-Gutiérrez *et al.* (2005) presented an Indicator Species Analysis which revealed *E. pacifica* calyptopes as good

indicators for the inshore region (NH1-10, or 1-10 nautical miles from shore). However, strength of region indication does not necessarily imply a difference in sampled biomass (Mouillott *et al.* 2002); the same study also mapped distributions of calyptopes for the three years and it is clear that, while these life stages may be typical of the inshore region over the entire study period, on shorter timescales their distribution can vary widely across the entire shelf and seaward of NH25. Since the current study focuses on event-scale periods and makes use of densities on a per-sample basis, the assumption of a typical higher density of non-migrators inshore of NH25 probably does not hold in every case.

Lower mean densities of non-migrators at NH15 after upwelling than non-upwelling periods (in 2000 and 2002, CWS[0.5 day]; in 2002, CWS[1 day]) is a pattern consistent with the DTH; however, the densities were so variable that the results were not significant. A better comparison might have been performed for NH15 with samples categorized by winds favorable for active upwelling versus winds favorable for active downwelling, since the downwelling might cause the non-migrators to aggregate over the shelf, provided they are buoyant enough (or sufficiently strong swimmers) to resist the downwelling action of the Ekman layer they inhabit (e.g. Franks, 1992). However, very few samples were collected after periods of strong and sustained northward winds (downwelling), so the possibility cannot be adequately explored here.

The only significant density comparisons were directly counter to what the DTH would predict: significantly higher mean densities of non-migrators at NH25 after non-upwelling periods (for pooled data with full- and half-day classification, and for 2001 for the half-day classification). This result might be explained by the violated assumption discussed above; if the

mechanism most responsible for influencing non-migrator density at NH25 is wind-driven advection, the result would imply higher non-migrator densities offshore of NH25 in 2001 but not in 2002 (when there was no significant difference between samples collected after upwelling or after non-upwelling). Also counter to the DTH prediction, for both half- and full-day classifications, mean non-migrator density was significantly greater at NH15 than at NH25 after upwelling periods in 2001 (and for both years, but this result is clearly driven by the 2001 samples). If cross-shelf, wind-driven transport of surface non-migrators is the responsible process, then these results suggest that non-migrators are more dense inshore of NH15, with a relatively low concentration between the stations. Together, these results suggest a non-migrator distribution with two peaks: one nearshore and one offshore. The maps of Gómez-Gutiérrez *et al.* (2005) show the distribution of calyptopes in 1971 have a large peak inshore of NH15 and a more modest presence at and seaward of NH25. Additionally, Gómez-Gutiérrez *et al.* (2010) showed that *E. pacifica* reproduction occurred all along the NH Line during this time, suggesting non-migrators can be present anywhere across the shelf or offshore.

It is tempting to use density data to explore differences in distributions across the shelf. This direct measure allows one to see exactly what was found and make inferences about the mechanisms involved in distributing the zooplankton. However, the variability common to plankton samples may result in coefficients of variance up to several hundred percent, even for same-day hauls from fixed stations (e.g. Barnes and Marshall, 1951). The larval samples in this study, taken together, have a coefficient of variance of 247%. Separately, the migrators are more variable (349%)than the non-migrators (193%). This pattern stands at odds with the findings of Decima *et*

al. (2010), who reported higher spatial patchiness for the calyptopis phase than for larger larval stages (e.g. furcilia) of *E. pacifica* in the southern California Current.

The F_M metric was designed with an eye toward reducing this variability by taking a ratio of the log-transformed migrator densities to the log-transformed densities of the non-migrators. Indeed, the coefficient of variance for F_M was lower than for the densities (113% rather than 349%), though still quite high, likely because many samples (22 of 65) were missing (or have extremely low densities of) migrators and consequently have F_M values of or very near zero, and the coefficient of variance is sensitive to the mean value.

The significant negative relationships between F_M and CWS[7 days] at NH15 (2002 and all years combined; Fig. 2.4) support the stated DTH, regardless of whether non-migrator densities increase offshore or higher densities of non-migrators are more frequently at NH15 than offshore, if migrators are either uniform across the shelf or more abundant offshore of NH15. But the fact that these relationships were only significant for a single classification period (7 days) reveals the clear influence of the two F_M values of 1 on the correlation; when the same F_M values are shuffled around for different CWS periods, the significance vanishes – a weakness of this method.

If a significant positive correlation between F_M and CWS at NH25 had been found, and the assumption that non-migrator density is always higher inshore of NH25 than offshore is met, it would be straightforward to conclude that the DTH is robust. But as discussed above, the assumption of a typical non-migrator distribution with respect to these stations and on a per-sample basis cannot be met. Accordingly, no significant (or otherwise) positive correlations between F_M were found at either station for any year.

With the understanding that the non-migrator densities can be relatively high both over the shelf and offshore, the NH25 requirement becomes fairly unrestrictive. A negative relationship could be found if non-migrators are more dense offshore of NH25, or no trend at all, if non-migrators and migrators are evenly distributed in either direction from NH25, and both of these relationships would be in agreement with the DTH; this is an obvious weakness in the F_M metric for this purpose.

A confounding factor in the interpretation of the significantly negative relationship between CWS and F_M is the flux of non-migrators in relation to upwelling events, as a result of upwelling-influenced spawning. A large number of calyptopes arriving at the inshore station within 7 days of the onset of a relaxation would drive F_M down when CWS is high, mimicking the expected trend. The length of time from egg release to the first calyptopis stage is on the order of 8 days at typical temperatures for the region (Feinberg *et al.*, 2006); if an upwelling event stimulates a large release of eggs, this scenario could occur and influence F_M trends. Feinberg and Peterson (2003) were unable to find a significant event-scale relationship between upwelling and egg abundance, but Gómez-Gutiérrez *et al.* (2007) did report an increase in eggs per brood when chlorophyll-*a* concentrations were high, indicating some connection between upwelling events and concentration of eggs sampled. However, the latter study does not report the gravid female distribution at the time of spawning, so an accurate estimation of the overall effect of an upwelling/relaxation event cannot be made. Without knowing how *E. pacifica* adult distribution *and* spawning are influenced by upwelling events, it is difficult to make a strong assertion about where the youngest larvae are likely to be under different upwelling conditions.

One reason the expected relationship between CWS and F_M might be absent from most comparisons is that the two groups chosen to represent non-migrators and migrators may not have been different enough in their ontogeny to have very differential transport in this region, such that either the migration amplitude of the group described here as migrators was not different enough from that of the non-migrators. Other factors, both external and internal, have been observed to affect DVM, such as water temperature (Taki 2008), food availability (Nakagawa, *et al.* 2003), population density (Burrows and Tarling 2004), or molting and reproduction (Endo and Yamano 2006), so perhaps not all the migrators migrated together. Either of these situations would result in a lack of differential transport between the groups. If, instead, early calyptopis stages had been considered non-migrators, while the migrator group had been composed only of juveniles, much clearer separations between the groups might have been noted.

Finally, an important factor not considered in this analysis is the time required for non-migrators to develop/molt into the migrating stages. While the gap in development time between the migrators and non-migrators established two groups with different migration behaviors, the development time between them also means that their members, sampled at the same time and the same location, have potentially very different transport histories and originating dates. In other words, this analysis compares non-migrators and migrators as though they both originated from the same place and have always had different behaviors. However, the time to develop from a 2nd-stage calyptopis to a 4th-stage furcilia is on the order of 30 days at 10°C, based on the median time to stage of *E. pacifica* reared in the laboratory (Feinberg *et al.*, 2007). With near-surface, southward flow in the northern

CCS as swift as 0.35m s^{-1} in the core of the upwelling jet (Barth, 2003), 30 days worth of transport is quite considerable.

To illustrate the significance of these facts, an individual-based model of *E. pacifica* development and behavior (Lindsey and Batchelder, unpublished) was run backward in time from 4 June 2002, a date when both non-migrators and migrators were present at both stations in the data (Fig. 2.6). The Regional Ocean Modeling System (ROMS) physical model for the Oregon coast in 2002, described in Koch *et al.* (2010), provided the 3-D velocity and temperature (necessary for the development model) fields. Three particles (representing stages F4/5, F6, and F7) were initialized at NH15 and at NH25 (six particles total). These particles were allowed to reverse-develop (from furcilia stages toward calyptopes) using a Belehradek function, while their trajectories were tracked backward in time (Batchelder, 2006). Meanwhile, each particle exhibited a DVM behavior based on day length, such that they occupied surface layers during the night and deeper layers (determined from Figure 2.1) during the day. From the NH line, all particles encountered the northern boundary of the model domain at 47.5°N before regressing in stage to C2, suggesting that migrators found at NH15 and NH25 on 4 June 2002 were non-migrators at 47.5°N or farther north. The migrating larvae sampled on the NH line had vastly different transport histories from the non-migrating larvae in the same sample; their cross-shelf locations may speak more to the various influences controlling spawning location and alongshore transport than to recent wind-forced cross-shelf transport.

2.6 Conclusion

A case may still be made for differential transport of larvae, but the assumption that differential transport of these larval stages will always occur, or will always appear the same, cannot be met. What seemed at first like a straightforward and testable idea of a local system is, in hindsight, a very complex question that involves not only cross-shelf but also alongshore transport, development time, individual variability in behavior, and ultimately, spawning locations north of the sampling locations. The variability in the density data breaks confidence in the few trends that were found. On the other hand, the F_M metric proposed here failed to clearly demonstrate the degree to which differential DVM behavior by *E. pacifica* larvae might impact cross-shelf distribution in an upwelling region. Decisive evidence of differential transport due to ontogenetic differences in DVM was not found in the analysis of this data set due to the potential confounding interactions of time- and location-dependent spawning and strong alongshore (including cross-isobath) transport with wind-forced cross-shore Ekman transport. It is unlikely that sufficient sampling in space and time would be available to discriminate wind-forced cross-shore Ekman transport from these other processes. Individual-based modeling of development and behavior, coupled with particle tracking provided by well-validated physical model representation of ocean fields, might provide a means to quantify and partition the relative importance of these processes in determining the cross-shore shifts of ontogenetic stages.

Acknowledgements

The authors acknowledge W. Peterson, L. Feinberg, T. Shaw, C. Morgan, and many other scientists for collecting and processing the data

used here; W. Peterson for the use of unpublished data; Y. Spitz for comments on early drafts of the manuscript; and an anonymous reviewer whose close reading and comments had a tremendous hand in shaping the final version of the manuscript. This is contribution number 702 of the U.S. GLOBEC program, jointly funded by the National Science Foundation and National Oceanic and Atmospheric Administration.

Figure 2.1. Vertical Distributions of *Euphausia pacifica* larvae. Sampled depths of calyptopis stages 1-3 at shelf stations (A) and slope (B) stations; intermediate furcilia (stages 1-3) at shelf (C) and slope (D) stations; and late furcilia (stages 4/5-7) at shelf (E) and slope (F) stations. Adapted from Vance *et al.* (2003).

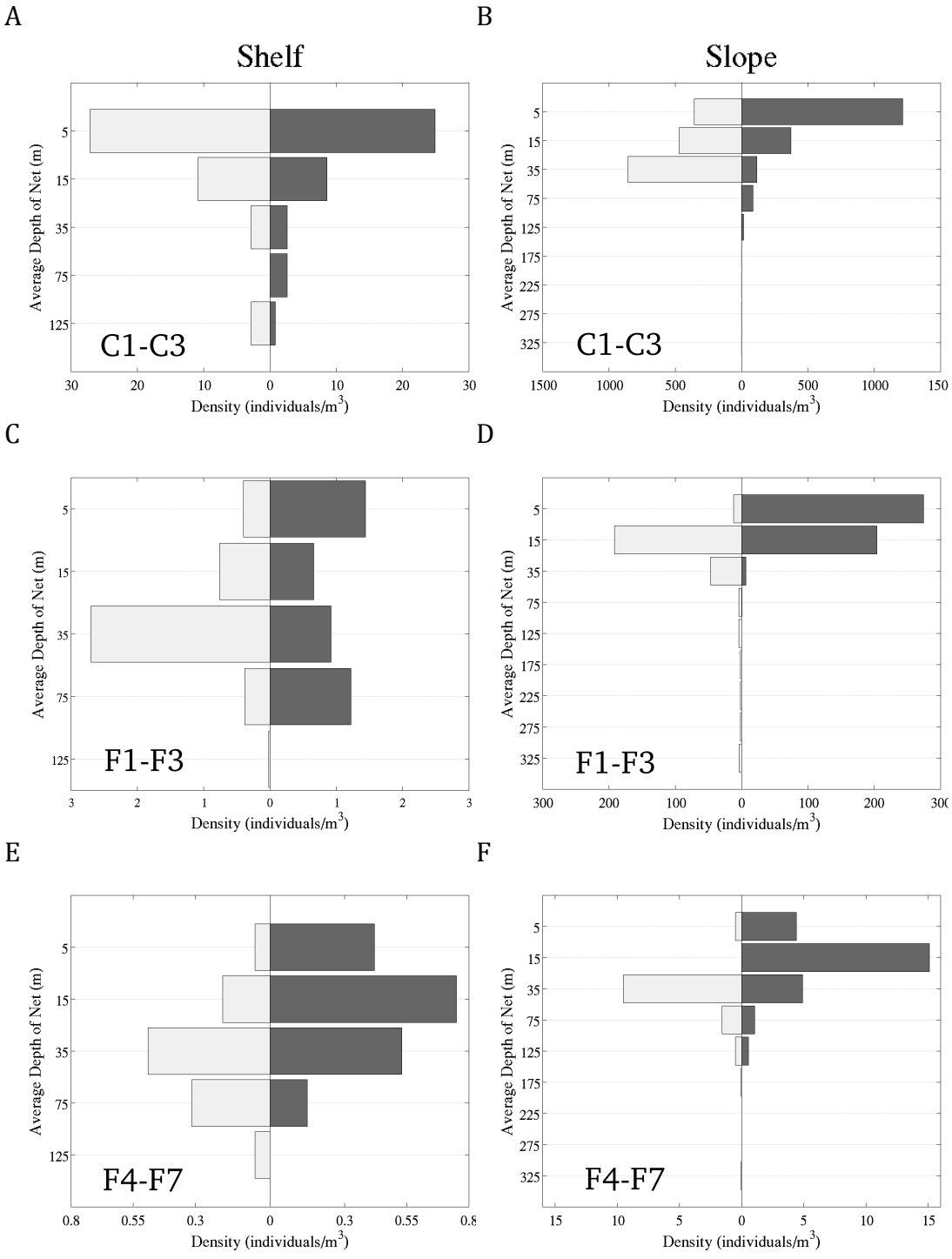

Figure 2.1. Vertical Distributions of *Euphausia pacifica* larvae.

Figure 2.2. Hourly cumulative alongshore wind stress (CWS) from Jan 1 of 2000 (top panel), 2001 (center panel), and 2002 (bottom panel). For reference, sample dates are indicated with an open triangle; apex direction denotes upwelling/not upwelling according to CWS[1d] (≤ –0.84 $Nm^{-2}h$: upwelling, pointing up; > –0.84 $Nm^{-2}h$: not upwelling, pointing down). Filled symbols are samples containing either migrators or non-migrators that were collected from both stations within 24 hours, as discussed in the text.

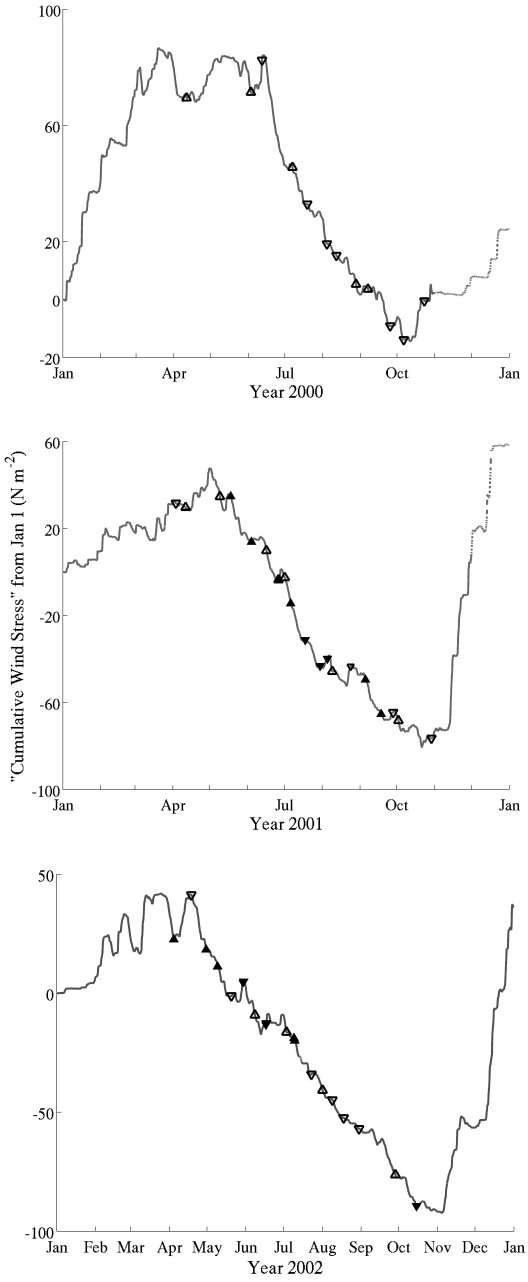

Figure 2.2. Hourly cumulative alongshore wind stress (CWS) from Jan 1 of 2000 (top panel), 2001 (center panel), and 2002 (bottom panel).

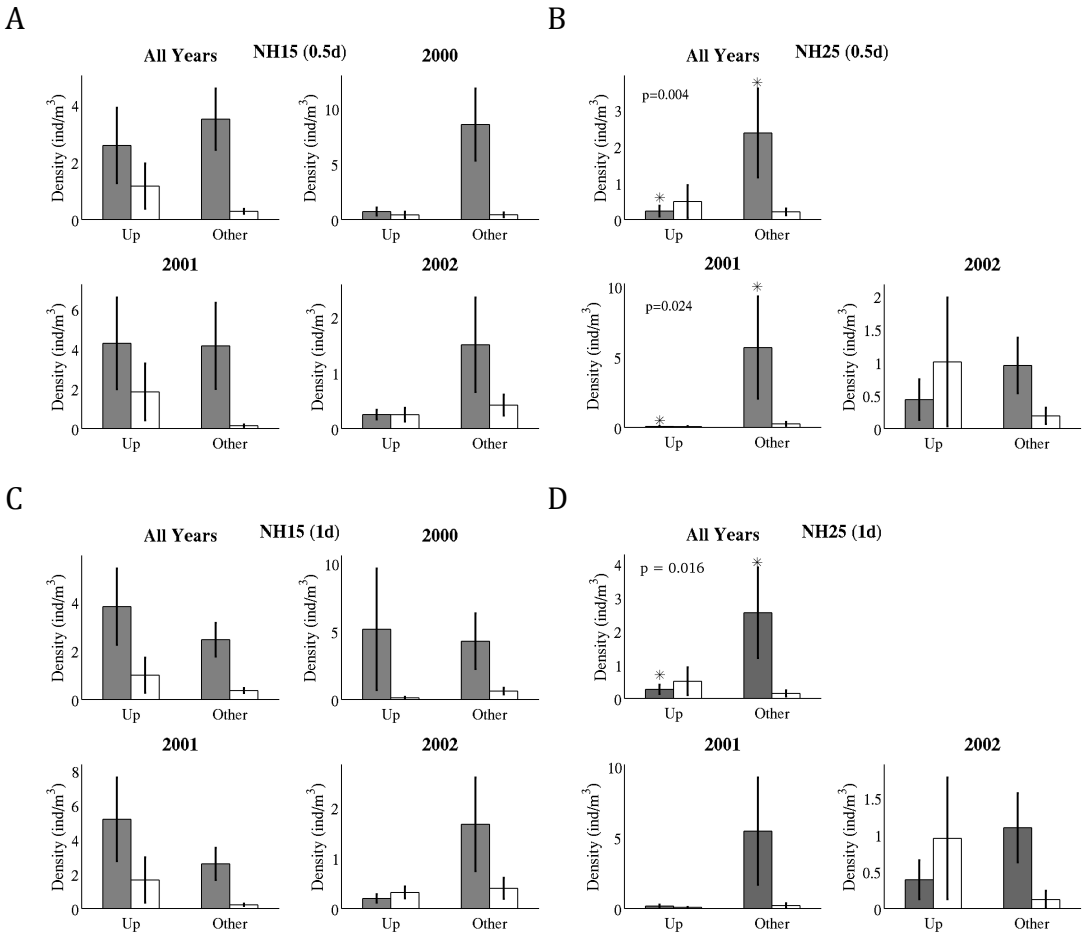

Figure 2.3. Mean Larval Densities after upwelling and non-upwelling conditions. Mean (± standard deviation) larval densities (individuals m^{-3}) are shown for non-migrators (gray) and migrators (white) for different upwelling classifications at NH15 (CWS[0.5d], A; CWS[1d], C) and NH25 (CWS[0.5d], B; CWS[1d], D). "Up" refers to upwelling, and "Other" refers to both weak upwelling (≥ 5m s^{-1} time-averaged winds to the south) and downwelling conditions (< 5m s^{-1} time-averaged winds to the south) Significant pairs are denoted by an asterisk and p-values are printed when significant.

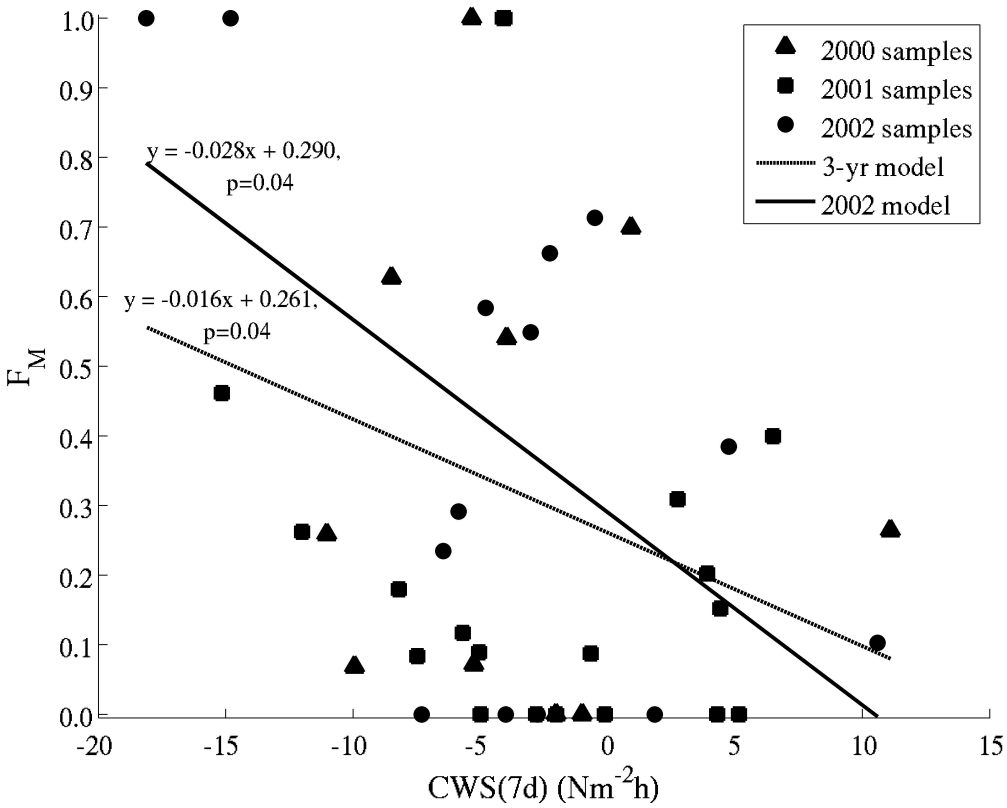

Figure 2.4. F_M vs. CWS at NH15. F_M at NH15 is plotted for 2000-2002 according to CWS[7d]. Linear models for 2002 values (solid) and pooled values (dashed) are plotted.

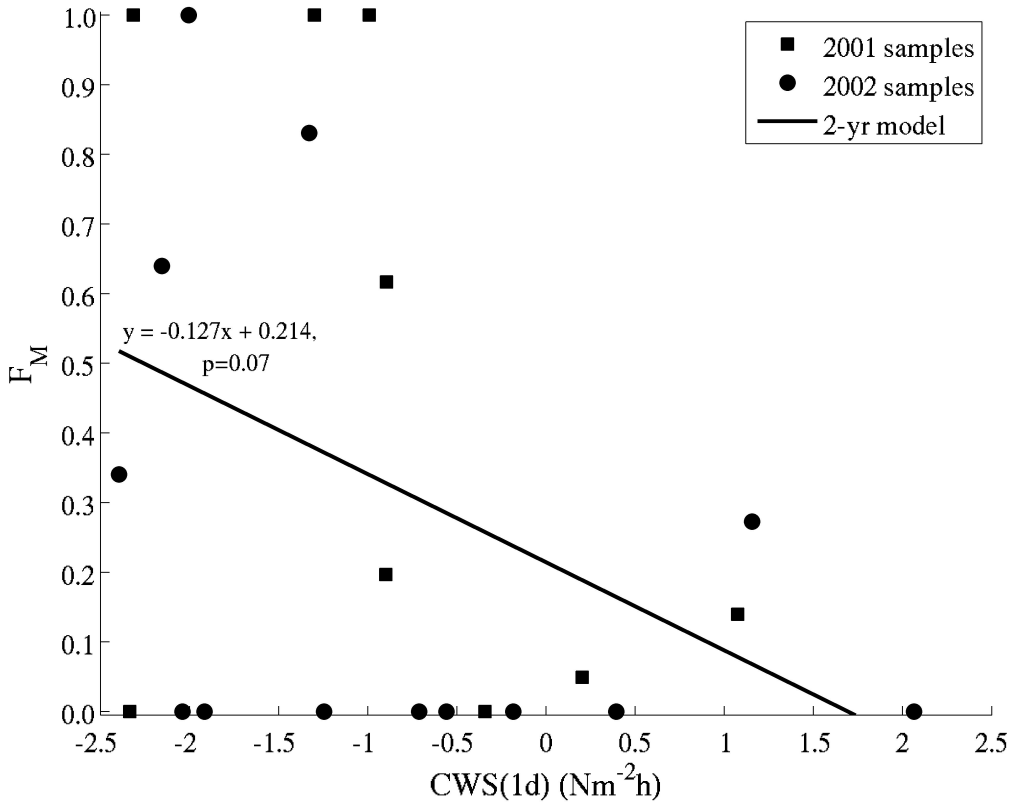

Figure 2.5. F_M vs. CWS at NH25. F_M at NH15 is plotted for 2001-2002 according to CWS[1d]. A linear model for 2-year pooled values is plotted.

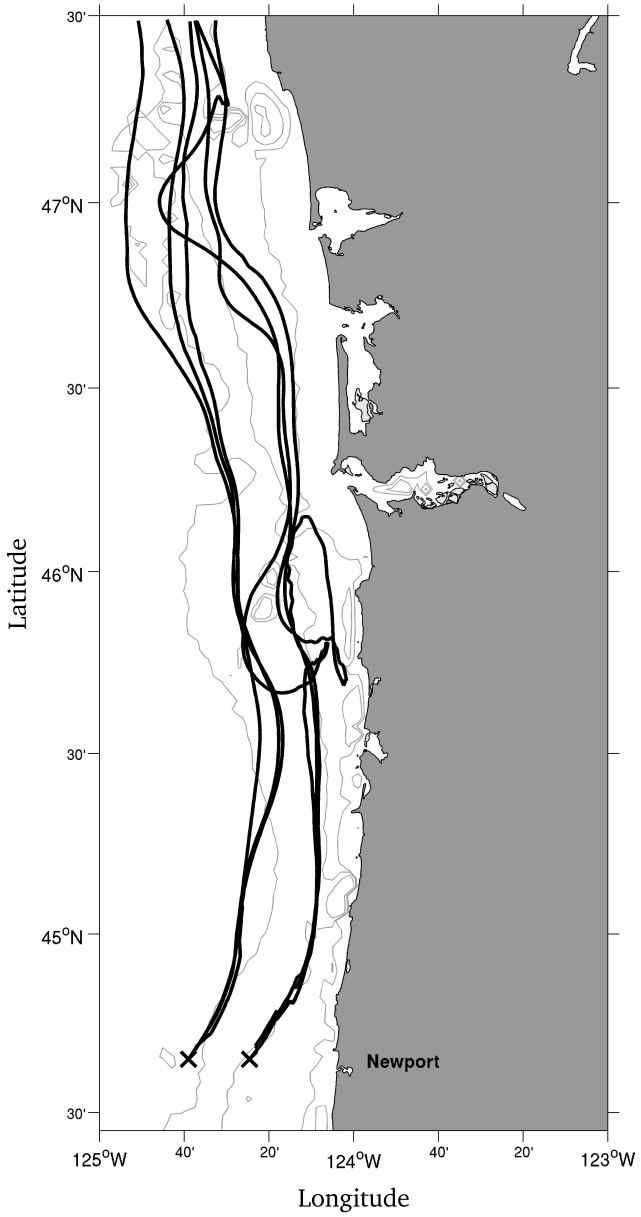

Figure 2.6. Backward-in-time migrator trajectories. Six backward-in-time trajectories show that migrators sampled at NH15 (inshore "x") and NH25 (offshore "x") would have traveledto the NH Line from north of 47.5°N, where they would have been non-migrators.

3.0 *Euphausia pacifica* eggs at the Oregon coast: a modeling study of potential spawning locations

3.1 Abstract

Euphausia pacifica is a well-studied, important trophic link in the California Current System. Despite many laboratory and field studies, however, specifics of its reproductive behaviors, such as where and when eggs are released, remain unclear. In particular, eggs sampled at an inshore station (NH05) on the Newport Hydrographic Line off Newport, Oregon, during the upwelling season, are far inshore of the shelf break (here defined as the 180m isobath), the region many observers believe to be the primary source of eggs during spawning events. A 3D Regional Ocean Modeling System circulation model was used to force a particle tracking and development model both backward in time and forward in time to explore the likelihood of the shelf break as a potential spawning location of eggs found on the inner shelf in 2000-2004. While passive eggs in backward simulations showed extremely rare connection between the shelf break and the inner shelf station (in 2001 only), passive and sinking eggs in forward simulations showed none. Further examination of eggs that were transported inshore of the 60m isobath (but not to NH05) from the shelf break revealed interannual differences in the number of eggs transported that can be linked to the Pacific Decadal Oscillation. In general, passive eggs at the surface at the 180m isobath were transported most reliably to the inner shelf region when released during upwelling relaxations, and all other eggs (passive deep eggs or any sinking eggs) were more often transported to the inner shelf region when upwelling was strong.

3.2 Introduction

Euphausia pacifica is found across the North Pacific basin, from the Yellow Sea to the Gulf of Alaska and in the California Current. Its importance as a prey item, its adaptability to various environments, and its relative hardiness in the laboratory have made it a common subject of study, from its description in 1911 (Hansen, 1911) to population studies off Southern California (Brinton, 1976), body nitrogen and carbon budgets for *E. pacifica* from Washington (Ross, 1982a and 1982b), development stage descriptions for the Yellow Sea (Suh *et al.*, 1993), and growth estimates for adults sampled off Oregon (Shaw *et al.*, 2010). While studies of this species—the numerically dominant krill species off the coast of Oregon—have been undertaken for more than a century, some aspects of its life history remain unclear, including specifics of its spawning. Despite numerous studies of spawning potential (Ross *et al.*, 1982; Gómez-Gutiérrez *et al.*, 2006; Pinchuk and Hopcroft, 2006; Feinberg *et al.*, 2007), and information on spawning seasons in various regions—March-October off Oregon (Feinberg and Peterson, 2003); nearly year-round off Southern California (Brinton, 1976); July-October in the Gulf of Alaska (Pinchuk and Hopcroft, 2006); April-May in the Puget Sound, Washington (Ross *et al.* 1982); and February-May in Toyama Bay, Japan (Iguchi et al, 1993)—the actual locations and behaviors associated with *E. pacifica* spawning *in situ* are not yet clearly understood. Specifically, when and where, precisely, do females release their eggs?

Off Oregon, a long period of sampling (1970-1972, Gómez-Gutiérrez *et al.*, 2005; 1996-2001, Feinberg and Peterson, 2003; 2001-2009, Shaw *et al.*, 2010; and W. Peterson, unpublished data) along the Newport Hydrographic Line (NH-Line, a transect at 44.65°N beginning at 1 nautical mile (nm) offshore and extending seaward, see Huyer *et al.* 1983) has shown a

consistent pattern of highest adult *E. pacifica* concentrations at the shelf break and beyond, with few reproductively mature individuals captured inshore over the shelf. Peak abundance of *E. pacifica* at the shelf break has been reported from other coastal regions, such as the Gulf of Alaska (Coyle and Pinchuk, 2005) and British Columbia (Lu *et al*., 2003). Mackas *et al.* (1997) observed spatial patterns that suggest horizontal aggregation of adult and juvenile euphausiids at the shelf break can arise from the interaction between shelf break upwelling and light-mediated diel vertical migration (DVM) behavior.

But while adults and juveniles are aggregated at the shelf break in these systems, their larvae are not necessarily coincident. Prior observations of *Euphausia pacifica* in upwelling regions have documented a cross-shore separation between the juveniles and adults and the larval stages (Lu *et al.*, 2003; Mackas *et al.* 1997; Gómez-Gutiérrez *et al.*, 2005). A similar spatial pattern is known for krill in the Benguela upwelling system (Pillar 1989). This cross-shelf separation has been suggested as beneficial because it reduces the likelihood of cannibalism (Brinton, 1976), and is often attributed to differential transport of larvae and adults, due to their different DVM behaviors. Lu *et al.* (2003), in their study of the cross-shelf distribution of *E. pacifica* off Vancouver Island, British Columbia, Canada, found that the magnitude and direction of the spatial offset between peak abundances of early larvae and adults (about 5-10 km) were consistent with expectations of cross-shelf transport of surface material calculated from recent wind histories.

Farther south—at the NH-Line—eggs are even more displaced from the locations of high adult abundances. While eggs at the NH-Line are found near the shelf break, they are also found in high abundances at stations far

inshore over the shelf, where adults are rarely found. Gómez-Gutiérrez *et al.* (2010) reported that, while high concentrations of eggs were found as far inshore as NH01 (1 nmi west of the coast), gravid females were "virtually absent" inshore of NH15 (15 nmi west of the coast); the pattern in egg abundance did not scale with the pattern of adult abundance. Feinberg and Peterson (2003) found a similar pattern of high egg abundances at station NH05 in samples taken in 1996-2001, and continue to sample eggs at this station, ~20 nautical miles (37.2km) inshore from the peak abundances of adults (Feinberg, unpublished).

That physical transport of eggs would result in separation from the adult distribution is not entirely surprising, since *E. pacifica* is a broadcast spawner (Mauchline and Fisher, 1969) and adults are capable of large-amplitude diel-vertical migrations that eggs are not. But the fact that *E. pacifica* spawn most intensely from July-September (Gómez-Gutiérrez, 2010)—during the upwelling season, when surface waters are pushed offshore—makes the observed pattern of eggs inshore of adults unexpected. A reasonable explanation to link inshore eggs and adults at the shelf break during the upwelling season is that wind relaxation events cause surface waters carrying eggs to "slosh" shoreward (Lu *et al*., 2003). The typical spatial separation from the adult concentration to the larval concentration reported by Lu *et al.* (2003) for British Columbia was order 5-10km, and peak egg concentrations were spatially closer to the adults than the larval peak (Lu *et al.*, 2003). Feinberg and Peterson (2003) found that *E. pacifica* eggs tended to be present in higher abundances at NH05 following cold water events, or *after* upwelling, implying transport in surface water moving back toward shore during lulls in the southward winds. The cross-shelf offset between *E. pacifica* adults and eggs in central Oregon is close to 30 km, which

is much greater than offsets documented farther north. Thus, for Oregon it seems unlikely that wind relaxations alone could create the observed separations.

In addition to horizontal source locations, depth of egg release by the adults may be an important factor determining the distance and direction of egg transports from their spawning locations. *E. pacifica* eggs are presumed to be released near the surface (Gómez-Gutiérrez *et al.*, 2010; Feinberg and Peterson, 2003; Lu *et al.*, 2003), but while eggs are most often found in highest abundance in surface waters, instances of eggs found at depths of 90 to 250m seaward of the shelf break (Vance *et al.*, 2003) have led to the suggestion that they may be released at depth in some cases (W. Peterson, personal communication). The eggs in these observations may also have reached these depths by sinking, which has been estimated in the laboratory to be as swift as 128 m d^{-1} (Gómez-Gutiérrez, 2003). Spawning depth and sinking rate influence the mechanisms Oregon coast researchers have hypothesized to connect adults at the shelf break to high abundances of eggs found at inner shelf stations (e.g. NH05). For instance, if eggs are released in surface waters, they may be carried toward shore during relaxation events (Gómez-Gutiérrez *et al.*, 2010), or they may sink into onshore-flowing deep waters during upwelling events (Ju *et al.*, 2006). If eggs are spawned near bottom at the shelf edge, they may be transported shoreward during upwelling without first sinking into the onshore-flowing waters near the seafloor (W. Peterson, personal communication).

Feinberg and Peterson (2003) argue that the *E. pacifica* egg development duration (time from spawn to hatch) is too short for eggs to accomplish the 20 nm journey from adult peak (near NH25) to the inner shelf station NH05. Only about 40 hours elapse between spawning and hatching

into the first larval stage at typical surface temperatures of 10ºC in spring and summer (Gómez-Gutiérrez 2010; Feinberg *et al.* 2006). Accordingly, they posit that adult females may be transported inshore near the bottom at their deepest migration extent during the day and release their eggs nearer shore. Alternatively, Gómez-Gutiérrez (2010) suggests that females may be transported inshore at night while they occupy surface waters during a relaxation event.

Excluding the direct onshore transport of the gravid females, three hypotheses have been advanced to explain the high egg and naupliar concentrations on the inner shelf:

1. Eggs are transported from the shelf break to inner shelf stations in surface waters during relaxation events
2. Eggs are transported from the shelf break to inner shelf stations in deep waters during upwelling events
3. Eggs are not transported from the shelf break to inner shelf stations, but are in fact released closer to the inner-shelf locations than available observations indicate

These alternative explanations are difficult (if not impossible) to evaluate with field data alone. Models can be used to track the transports of eggs from their site of spawning until they hatch. This study uses an individual-based development and particle tracking model forced by the velocity, mixing and temperature fields from a physical circulation model off the Oregon coast to determine which explanation best fits the observations to date.

3.3 Methods

This study explored possible sources of the *Euphausia pacifica* eggs frequently observed at an inner shelf station (NH05) along the Newport Hydrographic line, (5 nautical miles offshore at 44.65°N, 124.18°W) during the April-September upwelling seasons of 2000-2004. Eggs were tracked for the duration of the egg stage within a 3-dimensional physical circulation model. The duration of each egg was controlled by temperature experienced along its trajectory.

A straightforward method of particle-tracking is to begin with a starting location or distribution and follow particle drift patterns by recording their positions as time marches forward, or forward-in-time tracking (FITT; Batchelder 2007). This approach is useful when the question being asked is concerned with where particles go: oceanic regions through which organisms might be advected as they develop (e.g. Baums *et al.* 2006, Pfeiffer-Herbert *et al.* 2007); ultimate destinations of organisms when the initial distribution is known (e.g. Weibe *et al.* 2011) or the connectivity between two or more regions (e.g. Kim and Barth 2011). But this approach may not be ideal for the reciprocal question: knowing their positions now, where did these organisms originate?

Backward-in-time tracking (BITT) of passive particles is another method of investigating trajectories, which may be more suitable for identifying sources when destination distributions or locations are known. While there is agreement that advection—transport of the particles as a direct result of the fluid's bulk motion—is a reversible process, there has been debate about whether diffusion—transport due to mixing—can be run backward in time. Batchelder (2006) discusses the complexity introduced by adding a random walk to trajectories in a backward-running simulation and

argues that the resulting collection of "source" locations determined from multiple backward trajectories from a single "destination" may be interpreted as a probability envelope of possible sources.

FITT and BITT approaches each have advantages. In FITT simulations, all relevant processes from a physical model can directly be included. However, a large number of potential source locations must be identified and seeded with particles, with the hope that some of the particles transition through the observed (or desired) destination in a specific time window. This is not computationally efficient. Conversely, when they can be applied, BITT simulations have the advantage that all of the particles seeded at the desired end point (destination) are useful for identifying potential sources. This works well for wholly passive particles, but when an individual behavior or sinking term is added, BITT may not be an appropriate modeling approach. As argued by Thygesen (2011), the addition of sinking or other behaviors within a bounded space can lead to flawed reverse vertical trajectories. Consider, for instance, sinking particles in the ocean; if a particle which is heavier than the surrounding water is released near the surface (with little or no vertical advection), it will immediately begin to sink, and continue to do so until it either hits the bottom boundary or reaches a depth where it is neutrally buoyant. If the simulation is run for a sufficiently long time, the particle will remain at the neutrally buoyant depth until the end (assuming no advection brings it to the surface again). Now suppose the same particle is released at either the bottom or the depth of neutral buoyancy, and the simulation is run backward. Because the particle is denser than the water directly above, it will begin to rise immediately (backwards sinking=positive buoyancy), and continue to rise backward in time until it reaches the surface. There it will remain, until the simulation ends. Because

of vertically sheared velocity fields, common in most places, the resulting trajectories are *not* symmetrical, and therefore represent a situation for which BITT is not appropriate. Therefore, when the buoyancy of eggs is important, FITT is the better approach, despite the less efficient use of particles in the computations.

Both backward and forward in time simulations were used in this study. Except in simulations where sinking was considered, eggs were advected as passive particles and a random vertical displacement model was used to approximate sub-grid scale vertical turbulent mixing. There were three simulation types: (a) BITT of passive particles, (b) FITT of passive particles, and (c) FITT with particles of variable buoyancy. Simulation type (c) was performed for two kinds of eggs, light and heavy, to explore the sensitivity of transports to a range of reasonable egg densities. For each of these cases and for each year (2000-2004), simulations were run in ensemble format, such that eggs were released every day for 152 days spanning a period just before and through the peak of a typical upwelling season: day 119 to 270 of each year (April 29-September 27).

BITT simulation setup: Eggs were initialized within 1km of station NH05 within the model, which was at 44.65°N, 124.16°W, where the model grid's 60-m isobath intersects with the NH-line at 44.65°N. (Note that this model location is about 1.9km inshore of the true NH05 location. The reason is discussed in more detail below.) Five thousand eggs were initialized at random depths from 5m below the surface to 5m above the bottom. At each release date, these eggs were released (5000 day^{-1}), each assumed to have completed 99% of the egg development (e.g., just about to hatch) were initialized and their locations tracked backward in time until they

corresponded to 0% completed development of egg stage (i.e. just spawned). Aging, using temperature-controlled development time is described below.

FITT simulation setup: Eggs were initialized throughout the water column (at 10m, 20m, 45m, 70m, 95m, 120m, 145m, and 170m) along the 180m isobath in the model from 44.5°N to 45.5°N every 0.025 degrees, totaling 328 locations (41 horizontal locations by 8 depths, Figure 3.1). At each location, 100 eggs (32,800 total) were initialized at 0% development completed (i.e. just spawned) and their development and trajectories were tracked forward in time until the eggs hatched.

Analysis: For BITT simulations, a successful shelf-break spawning site was identified as an egg whose trajectory went seaward of the 180m isobath, indicating a potential spawning location at or seaward of that isobath. For FITT simulations, two levels of "success" were considered: (1) a spawning site was identified if an egg from the release site transitioned within 1km of NH05 at any time before it hatched, or (2) a spawning site was identified if an egg was located at or shoreward of the 60m isobath before hatching, anywhere along the coast. Although the main aim of this study is to explore whether eggs observed at NH05 might have been spawned at the shelf break, it is instructive also to determine whether eggs from anywhere along the 180 m isobath are ever transported to the 60m isobath anywhere on the central Oregon shelf.

Environmental metrics based on the physical model fields were used to characterize environmental conditions that result in eggs being transported from the shelf break to the inner shelf. For each release date and at each release latitude, the longitude of the maximum alongshore velocity (v) velocity was used to determine the location of the coastal jet core. The coastal alongshore jet may be a barrier to cross-shelf flow, so knowing the

location of this feature relative to the particle informs cross-shelf transports. Eggs were released from the same locations each day and for FITT simulations, each egg's cross-shelf distance from the surface jet core was recorded.

In addition, the individual (trajectory) histories for each egg included *u*, *v*, and *w* velocities and most recent temperature so that conditions experienced could be compared on an egg-by-egg basis. Derived variables for each egg include the distance between the 180m and 60m isobaths at the initial location (shelf width), the mean temperature experienced, and the time to hatch (FITT; or time from spawn - BITT). Temperature, *u*- and *v*-velocities, and initial distance from surface coastal jet core were compared for successful and unsuccessful eggs using Welch's T-Test. This was done by randomly sampling the unsuccessful egg population (which greatly outnumbered successful eggs) at 200 eggs/day for all years of those that did not make it to the 60m isobath and comparing that group to the entire group of successes for all years.

3.4 Model Details:

a. Physical circulation model

The physical circulation model fields used in this study are from the Regional Ocean Modeling System (ROMS), originally developed by Song and Haidvogel (1994) and used widely for coastal models (e.g. Gruber *et al.* 2006, Di Lorenzo 2003, Di Lorenzo *et al.* 2005, and many others). Physical fields used to force the particle tracking (Lagrangian) models are daily-averaged and are described and discussed in Drake *et al.* (2011). The model domain spanned 134°W-116°W and 30°N to 48°N with a resolution that ranged from 2.5km to 3.2km in the zonal direction and 3.7km meridionally. Vertical structure was described by 42 terrain-following levels in an s-coordinate

scheme. Physical simulations were run with a spin-up year (1999). Horizontal (*u, v*) and vertical (*w*) velocities, vertical diffusivity (K_v), salinity (*s*), and temperature (*T*) fields were daily averaged and stored for 2000-2004. The specific interest here was the Oregon coast (Figure 3.1), where extensive data on *Euphausia pacifica* distributions are available from the U.S. GLOBEC sampling in 2000-2002.

The bottom bathymetry used in this grid was optimized for the Monterey Bay region, nearly 8 degrees south of the NH-Line, and the model bathymetry does not exactly match that of the central Oregon coast. The model has a slightly narrower shelf at the NH-Line than the real bathymetry. In order to account for this bathymetric difference, station NH05 with a bottom depth of about 60m was matched to the model grid location where the 60m isobath intersects the NH-Line, approximately 1.9km inshore of its true location. Similarly, the shelf break in the model was defined by the 180-m isobath within the model rather than by longitude. The overall result is a 3.1 km narrower shelf along the NH Line in the model than is observed in the real bathymetry. This approach was used because the model (and real ocean) dynamics are more strongly controlled by the bathymetry of the model (and ocean) geographical positions.

b. Particle tracking: Advection, diffusion, and sinking

In cases where advection and diffusion were the only processes transporting eggs, velocities (*u, v, w*) and vertical diffusivity (K_v) from the ROMS model were used to calculate the displacement of an egg. For each 360s time step, advection and diffusion were handled sequentially: advective velocities at an egg's location were determined using using bilinear horizontal interpolation on the vertical levels bracketing the current depth, which were linearly interpolated vertically to the current depth. This was

done for the two time snapshots that bracketed the current time, with the final velocities determined by temporal linear interpolation. All advective displacements were done using Runge-Kutta 4th-order interpolation over the time step. Vertical displacements (velocities) due to vertical mixing was done similar to that described in Batchelder *et al.* (2002) with additional steps to smooth vertical gradients based on methods described by North *et al.* (2008). The profile of vertical diffusivity (K_v) at the horizontal (x, y) location of a particle was obtained by bilinear spatial interpolation of each vertical level from the bracketing model time snapshots, which were linearly interpolated in time. The resolution of the K_v profile was increased 8-fold by linearly interpolating values between vertical grid points, which were smoothed with a running-average filter, and used to fit a tension spline, as discussed in North *et al.* (2008). Vertical displacement due to diffusion was calculated using the random-walk model presented by Hunter *et al.* (1993) and added to the advective displacement, such that the vertical location at time t is described by:

$$z_{adv} = z_{t-1} + w\Delta t$$

$$z_t = z_{adv} + K'(z_{adv})\Delta t + R\sqrt{2K(z_{adv} + \frac{1}{2}K'(z_{adv})\Delta t)\Delta t}\ ,$$

where z_{t-1} and z_t are the initial and final vertical locations of a particle, respectively; z_{adv} is the vertical location after advection only; w is vertical velocity (m s^{-1}); K and K' are the vertical diffusivity (m^2 s^{-1}) and the vertical gradient of diffusivity (m s^{-1}), respectively ; R is a random number (dimensionless) from a normal distribution with zero mean and unit variance; and Δt is the time step (seconds). Note that the $K'(z_{adv})$ and $K(z_{adv}$ +

$0.5K'(z_{adv})$) terms refer to depths at which K and K' values are estimated, not multiplicative terms. Horizontal diffusion was not considered here.

In cases where sinking was considered, Stokes' settling velocity (w_s; *cm* s^{-1}) was calculated:

$$w_s = \frac{2}{9}\left[g r_{egg}^2 \left(\frac{\rho_w - \rho_{egg}}{\mu} \right) \right],$$

where g is gravitational acceleration (cm s^{-2}), r_{egg} is the egg radius (cm), ρ_{egg} is egg density (g cm^{-3}), ρ_w is water density (g cm^{-3}), and μ is the dynamic viscosity of the surrounding water (g cm^{-1} s^{-1}). Egg radius was approximated for each individual as a function of development achieved, based on egg size data in Gómez-Gutiérrez *et al.* (2010). Egg density was assumed to also vary with egg development, based on densities given by Ju *et al.* (2006). To avoid further complexity that would be introduced by compression of the egg with depth, density of seawater at atmospheric pressure was used. Seawater density was calculated from model values of temperature (°C) and salinity (psu) at the location of the egg using the UNESCO (1983) Equation of State for seawater density at atmospheric pressure. Dynamic viscosity was a function of water temperature and salinity according to equations (22) and (23) in Sharqawy *et al.* (2010).

c. Development Model (egg hatching time)

Development was described with a Belehrádek formulation that depends solely on temperature:

$$D_i = a_i(T + b)^c,$$

where D_i is the number of days from egg to stage i, a_i (day $°C^{-1}$) is an empirically-determined, stage-specific constant that defines initial functional slope; b (°C) is a stage-independent temperature shift specific to the species; and c (dimensionless) is an empirically-derived constant that determines

curvature, and is often assumed (for copepods) to be –2.05, based on numerous crustacean zooplankton development experiments carried out by a number of independent workers (e.g. Harris *et al.* 2000, McLaren 1969, Mauchline 1998). Estimates for a_i (1217 day °C^{-1}) and b (15.052°C) were based on *Euphausia pacifica* stage duration measurements at several temperatures provided in Feinberg *et al.* (2006) and Iguchi and Ikeda (1994) (see Chapter 4 for more discussion on *E. pacifica* development). This development model is used more extensively in Chapter 4; here only the transition from stage 1 (egg) to stage 2 (first nauplius, or hatching) is relevant.

d. Egg biometry and sinking

Two types of forward simulations with sinking were run: one with "low density" eggs and one with "mean density" eggs. The changing density of developing eggs was roughly based on the approximations used in the model by Ju *et al.* (2006), which estimated sinking rates of *E. pacifica* eggs based on a prescribed stepwise density schedule dependent on development. This schedule was in turn based on information about lipid composition and metabolism throughout egg development. Ju *et al.* (2006) only calculated egg sinking rates (and therefore estimated density) through the late limb-bud stage (LLB, about 67% of the way to hatching, assuming a 40 hour hatch time in the laboratory), so here, density was estimated as a cubic function of cumulative development was fit to the stepwise density schedule and allowed to decline beyond what was reported in Ju *et al.* (2006):

$$\rho = \rho_{init}(-0.018f_m^2 + 0.006f_m + 1),$$

where ρ is the current density (g cm^{-3}), ρ_{init} is initial density, and f_m is the cumulative fraction of the egg duration completed (0-1). Egg density at each stage of development was calculated as a fraction of ρ_{init} , ρ_{init}(mean) being

1.050 g cm^{-3} and ρ_{init}(low) being 1.040 g cm^{-3}, based on the means and low end of density ranges reported for *E. pacifica* egg stages in Gómez-Gutiérrez (2010, his Table I). While the egg density declined during embryonic development, egg radius was assumed to remain constant at 0.0195 cm. From the sinking velocity equation, it is clear that a constant sphere size and declining density will result in a decreasing sinking velocity (all else remaining equal). Therefore, the net effect of egg development in this model is a reduction in its sinking velocity.

3.5 Results

ROMS fields and metrics:

Monthly mean sea surface temperature (SST) fields from the ROMS output for 2000-2004 show interannual differences (e.g. May 2000-2004, Figure 3.2). First of all, the interannual differences between years 2000-2002 and years 2003-2004 are apparent in the warmer SSTs in the latter years, particularly 2004, which in May is up to 4°C warmer along the coast than in 2000-2002. Comparisons of June SSTs show a greater degree of early upwelling (as seen in extent offshore of cold water near the coast) in both 2000 and 2002 than in 2001, 2003, or 2004. June 2000 was overall cooler than the other years through the upwelling season (Figure 3.3).

Success rates:

Overall, very few eggs, even in the absence of mortality, successfully transitioned from the presumed shelf-break *E. pacifica* spawning site to the near-shore site (NH05) where eggs are commonly sampled (Table 3.1). Overall, when considering the total number of successes over the duration of all 152 days for each upwelling period modeled, fewer than 3 of 1000 eggs, and more commonly fewer than 1 of 1000 eggs, successfully connected

presumed shelf-break spawning sites and inshore observed egg locations over the duration of each upwelling period considered here.

Only in 2001 were any passively transported eggs backtracked to beyond the shelf break; the rest of the simulated years (2000, 2002-2004) no eggs were able to backtrack to the shelf-break within the temperature-controlled duration from spawn to hatch. BITT simulations show that eggs may have originated at or seaward of the shelf break on only 6 of 152 days from May to October of 2001 (Figure 3.4), and that even on those days, less than 7% of the total eggs released "connected" the two regions. These eggs were all released within the top 30m of the water column and tended to be seeded over deeper bottom depths, or the westernmost portion of the 1km-radius region surrounding NH05 (Figure 3.5). Comparisons of temperature and cross-shelf velocity (Figure 3.6) show that successful eggs generally experienced higher temperatures than the unsuccessful eggs, reflecting the fact that they largely remained in the upper portion of the water column. Successful eggs in 2001 had average cross-shelf velocities in excess of 0.1 m s^{-1}, whereas velocities of unsuccessful eggs were either slower toward shore, averaged about 0 m s^{-1}, or were offshore.

Results from FITT simulations were similarly unsuccessful in getting eggs to within 1km of NH05. Regardless of passive or sinking drift behavior, no eggs originating from the shelf break spawning locations drifted to within 1km of NH05 during the upwelling period of any year. However, eggs released at the shelf break were occasionally transported to or shoreward of the 60m isobath (just not at the latitude of NH05) and the remainder of these results concerns these "successes."

Connection of the offshore region to the nearshore region depends on several factors: distance to travel, duration of drift, speed and direction of

drift, and obstacles encountered. The effect of these factors can be examined through comparisons of successful and unsuccessful groups of eggs and their corresponding histories including latitudes of origin, temperature, hatch rate, *u*- and *v*-velocities, and proximity to a coastal surface jet.

Passively drifting eggs provided the greatest connectivity between the shelf break and the inner shelf (shallower than 60m isobath). Successful eggs were all released North of the Newport Hydrographic Line (Figure 3.7), where the continental shelf is narrower. Vertically, eggs that successfully transitioned to the 60m isobaths were initiated near the surface or at the deepest depth (170m, Figure 3.8). Very few mid-depth spawners (45-145 m) were able to connect the shelf break and inner shelf. In contrast, sinking eggs released near the surface almost never successfully connected the two regions; instead, the majority of successful sinking eggs came from deeper than 45m, most commonly from 70m and deeper. Like passive eggs, all successful sinking eggs originated from North of the NH line, mostly from 45.1-45.3^{o}N, where the shelf is narrowest between 60-180m (steepest bathymetry)

Drift duration is temperature-dependent, as the study followed eggs from spawn to hatch with a temperature-dependent egg hatching time. Successful passively drifting eggs released in the upper 20m of the water column experienced significantly higher temperatures than unsuccessful eggs released from the same depths (Figure 3.9; 11.77°C versus 10.85°C across all years, $p<0.001$). In contrast, successful passive eggs released near the bottom (at 145 and 170m) experienced cooler mean temperatures than those unable to reach the 60m isobath (6.49°C and 6.88°C, respectively, $p<0.001$). Similarly, all successful sinking eggs had cooler mean temperature histories than their unsuccessful counterparts: mean density sinking eggs

released between the surface and 45m had mean temperatures of 7.08°C when successful and 7.29°C otherwise ($p<0.001$), and low density sinking eggs released in the same part of the water column experienced a mean of 7.77°C when successful and 7.91°C when not ($p=0.005$, Figures 3.10 and 3.11). At deep release sites (145-170m), successful eggs again encountered cooler temperatures than unsuccessful eggs: mean density sinking eggs had mean temperatures of 6.52°C when successful and 6.79°C when not ($p<0.001$). (Deep-release low density eggs had the same temperature differences between successful and unsuccessful groups as mean-density eggs, since both groups had nearly identical trajectories from these release locations.)

Interannual differences in sea surface temperatures were apparent in the interannual differences in hatching time for FITT simulations (Figure 3.12). Hatching times in 2004 were shorter than other years, particularly in surface-spawned eggs, though faster development is evident even at depth in 2004.

In all cases (behaviors and depths), successful eggs experienced significantly more positive (that is, faster onshore) *u*-velocities than unsuccessful eggs (Figures 3.13-3.15, all comparisons were significant with $p<0.001$). Passive shallow-release eggs averaged 0.13 m s^{-1} when successful and -0.07 m s^{-1} when not; passive deep-release eggs averaged 0.07 m s^{-1} when successful and 0.0 otherwise. Mean-density sinking eggs released within the upper 45m averaged 0.072 m s^{-1} when successful and -0.03 m s^{-1} otherwise, whereas eggs released near the bottom (145 to 170m) averaged 0.08 m s^{-1} when successful and 0.01 m s^{-1} otherwise. Likewise, low-density sinking eggs released near the bottom averaged the same velocities as mean-

density sinking eggs, but at the surface averaged only 0.05 m s^{-1} when successful and -0.03 m s^{-1} otherwise.

There were also significant differences (all with $p<0.001$) between the *v*-velocities encountered by successful and unsuccessful eggs, but the patterns differed between passive simulations and sinking simulations (Figures 3.16-3.18). Passive eggs released near the surface were more successful when they were only weakly advected southward, averaging -0.05 m s^{-1} when successful and -0.13 m s^{-1} otherwise. At depths near the bottom, passive eggs that were successful averaged -0.12 m s^{-1} while unsuccessful eggs were transported northward at an average rate of 0.03 m s^{-1}. In contrast, successful sinking eggs released near the surface behaved like deep-released passive eggs, with mean velocities of -0.15 m s^{-1} for mean-density eggs and -0.16 m s^{-1} for low-density eggs. Unsuccessful sinking eggs were, on average, transported only weakly to the south, at rates of -0.004 m s^{-1} and -0.03 m s^{-1} (mean- and low-density eggs, respectively). At the near-bottom release depths, *v* transport rates were similar to those of the deep-released passive eggs: -0.10 m s^{-1} when eggs were successful, and 0.023 m s^{-1} when not (for both mean- and low-density eggs).

Finally, the along-shore coastal jet may be an obstacle to cross-shelf transport of an egg from the shelf break to the inner-shelf region. Here, the maximum southward velocity near the coast was used to approximate the center of a coastal jet. Because the potential "obstacle" is a surface feature, only successful and unsuccessful eggs released in the upper 45m of the water column are compared. Passive eggs were significantly more inshore of the surface jet core when successful, averaging 1.37km inshore (east of the jet) at the time and location of release, than when they weren't successful, being released 7.75km offshore of the jet core ($p<0.001$).

3.6 Discussion

The purpose of this study was to test the hypothesis that *Euphausia pacifica* eggs spawned at the shelf break are transported onshore to a nearshore station (NH05) five nautical miles from the coast, where eggs are commonly found in plankton samples. Because the exact depths and timing of *E. pacifica* spawning are not established, simulations considered a range of potential spawning depths throughout the upwelling season. Another unknown for these eggs is precisely what motions they undergo after release. Depth-stratified net sampling of the depth distributions of *E. pacifica* eggs indicate that while a large portion of them remain in the surface layer near the shelf break, a sizeable number are found as deep as 200 meters or more (Keister *et al.* 2001). It is unknown whether these eggs are in deep waters because they were released there or because they sank to that depth following spawning at shallower depth, as has been suggested and measured in the laboratory by Gomez-Gutierrez *et al.* (2005). Simulations in this study included both passive and sinking eggs to test the hypothesis under a range of egg release depths and sinking rates.

Only the backward-in-time trajectory simulations (BITT) connected eggs from within 1km of NH05 to the shelf break, indicating a potential spawning location at or seaward of the shelf break. That this outcome occurred only six times (all in 2001) and for fewer than 7% of the released eggs on even those days, coupled with the fact that no forward-in-time trajectory (FITT) simulation, either with passive or sinking eggs, resulted in a single egg being advected to within 1km of NH05, lends confidence to a conclusion that eggs sampled at NH05 during the upwelling season are highly unlikely to have come from egg release near the shelf break.

The BITT simulations suggest that most eggs that reach the NH05 station come from potential spawning sites much nearer to NH05 than the shelf break, and that many potential spawning locations are inshore of the station. Adult ripe (spawning) females of *E. pacifica* are rarely found in these regions (Gómez-Gutiérrez et al 2010). Passive eggs released in the upper water column were more likely to move farther inshore across the shelf or from the North, whereas passive eggs at deeper depths (≥ 40m) traveled less distance. Trajectory length depended on temperature (which controls the rate of development and therefore travel duration), and velocity. Surface velocities can be an order of magnitude faster than deeper velocities, and will more than compensate for the longer transport durations at depth. Even large temperature differences will change drift duration of an egg by about a factor of 2 before it hatches (e.g., 56.6 hours at a constant 6°C versus 29.2 hours at a constant 14°C), thus it is reasonable to expect greater transport distances for eggs that remain in surface waters. BITT spawning regions from 2003 and 2004 simulations differ notably from the potential spawning regions of the previous 3 years. The combination of anomalously high sea surface temperatures and weaker upwelling indicate a spatially reduced potential spawning region in 2004 for surface oriented eggs. Whereas surface-released eggs in 2000-2002 have broader regions of potential origin than eggs that remained near the bottom, eggs which remained near the bottom of the water column in 2003 and 2004 have more expansive potential regions of origin than surface-released eggs.

While BITT simulations are useful for identifying the widest envelope of potential spawning locations by backtracking passive eggs from an observed location, *E. pacifica* eggs probably do not behave passively. Gómez-Gutiérrez (2003) observed that off Oregon, eggs are released near the surface

at night and probably sink quickly. Subsequently lab measurements show a mean sinking rate of 128m d^{-1} (Gómez-Gutiérrez *et al.* 2010). Because sinking could not be satisfactorily included in a BITT simulation, FITT simulations were required to examine whether sinking made clear potential spawning areas. Passive FITT simulations, the null model that would be expected to include the broadest range of eventual hatch locations from eggs released at the shelf break (180m isobath) because some particles seeded in the surface would remain in the surface rather than sinking and traveling near the bottom like deep-seeded eggs, failed to produce a single egg that hatched within 1km of NH05 during upwelling periods of five years. Therefore, we conclude that no presumed spawning depth between 10-170m along the 180m isobath between 44.5°N and 45.5°N is likely to provide eggs sampled at NH05.

Several factors, including distance to travel, duration of drift, speed and direction of drift, that determine connectivity between the shelf break and inner shelf were examined through comparisons of successful and unsuccessful groups of eggs and their corresponding histories including latitudes of origin, temperature, hatch rate, *u*- and *v*-velocities.

Along the seeding region from 44.5°N to 45.5°N, the shelf width ranges from a minimum of about 13.3km to about 33km (Figure 3.19). But the zonal distance between 180m- and 60m isobaths is not always the shortest; between about 44.95°N and 45.25°N, the shortest distance between isobaths requires a slight southeast trajectory. This range not only includes the narrowest parts of the shelf, but also the originating latitudes of most of the successful eggs in all simulations, providing a good estimate for the maximum extent of transport likely to be experienced by successful eggs, about 27km from passive eggs released at 44.7°N, which only occurred on 1

day of all years. More commonly, the maximum extent of transport occurred with passive surface eggs released from 44.85°N, or about 20km. Both of these maximum extents are shy of the minimum (i.e. directly across the shelf) 28km distance required to reach NH05 from the 180m isobath. As expected, the sinking eggs had far less range, as they sank into lower-velocity waters and were not retained in the surface layer where flows are swifter. The region of potential spawning for these eggs (45.1°N to 45.3°N) was very reduced compared with the region of potential spawning for passive surface eggs (44.7°N to 45.4°N).

Using constant temperatures to determine transport duration, the mean velocities required to transit directly across the shelf to NH05 from the 180m isobath are estimated (Figure 3.20). Even at 11.5°C (the 25th percentile of mean temperatures experienced by all successful passive eggs released at 10m), a sustained cross-shelf velocity >0.2 m s^{-1} is required, in the absence of any alongshore velocity (to ensure shortest trajectory) to reach NH05. This cross-shelf velocity was rarely encountered, even by passive surface eggs. At 14°C, the 75th percentile of mean temperatures experienced by all successful passive eggs, the reduced drift duration requires mean cross-shelf velocities that were never observed. From these estimates, it is clear why neither passive nor sinking eggs arrived at NH05 from shelf break spawners. Eggs sampled at NH05 are unlikely to have originated at the shelf break. The minimum distance required to bridge the gap between the 180m isobath and the 60m isobath requires significantly slower velocities at the same temperatures, shown in red in Figure 3.20.

Unsurprisingly, eggs in all simulations required some positive (onshore) *u*-velocity to reach the nearshore region. Between 44.5°N and 45.5°N, the easternmost point along the 180m isobath is still west of the

westernmost point along the 60m isobath, thus successful transitions from 180m to 60m require net eastward flow.

Meanwhile, *v*-velocities were not quite very informative for passive surface eggs, which averaged weakly southward *v*-velocities when successful, but experienced a narrow range of velocities which sometimes included northward transport. otherwise On the other hand, successful sinking eggs were almost always transported somewhat southward, with more negative *v*-velocities the shallower they were released. With the slower deep currents into which all of these eggs sink being their primary means of transport, they would not be expected to travel very far from their spawning locations, and those able to travel at least the minimum distance between isobaths might be the only successful eggs recorded. The southward transport would be necessary to carry them in the southeastern direction required to reach the 60m isobath by the shortest distance possible. The sinking eggs that were released shallower would have less time to travel since they had a "head start" in their development when they were spawned in warmer waters. The near-bottom eggs, having the longest development time in the coldest waters, would have the luxury of being able to travel north while moving inshore and still encountering the 60m isobath before hatching.

Interannual Differences

Large-scale climate processes such as El Niño and the Pacific Decadal Oscillation (PDO) contribute significantly to interannual differences in the oceanographic conditions and biological productivity off Oregon. The PDO is defined as the first principal component of North Pacific monthly SST anomalies (Mantua *et al.* 1997), and is driven by changes in the strength of the Aleutian Low pressure system centered over the Gulf of Alaska. During a positive PDO, the Aleutian Low is strong and the North Pacific Gyre is weak,

leading to stronger winds from the southwest and anomalously high sea surface height along the coast. These conditions favor weakened upwelling and the northward and onshore transport of warmer surface waters, hence the term "warm" PDO for positive-phase years. During positive PDOs, biological productivity is often reduced at the Oregon coast (e.g. Hare *et al.* 1999). During a negative PDO phase, the opposite pattern is evident: increased upwelling, cooler SSTs, and enhanced productivity at the Oregon coast (e.g. Peterson and Schwing 2003).

Off Oregon from 1999 to 2002, cold ocean conditions and strong upwelling prevailed, with high productivity (Peterson and Schwing 2003, Durazo *et al.* 2001, Schwing *et al.* 2002), and negative summertime PDO indices (http://jisao.washington.edu/pdo/PDO.latest). By 2003, summertime PDO indices were positive, and warm conditions prevailed, with reduced upwelling and SSTs along the NH Line one standard deviation higher than average (Goericke *et al.* 2005*a*). Positive PDO conditions persisted into 2004, with weaker upwelling and warm SSTs along the NH Line that were up to 4 standard deviations above historical averages in May (Goericke *et al.* 2005*b*). The Regional Ocean Modeling System (ROMS) faithfully reproduced these SST trends for simulation years 2000-2004, providing a good modeling laboratory for exploring the impacts of these climatic phases on egg transport between shelf break and the inner shelf.

In this study, we found that both passive surface eggs and deep eggs sometimes transitioned from the shelf break to 60m. In order to get to the 60m isobath from the 180m shelf break, a surface passive egg requires (1) swift onshore transport, (2) low enough average temperature to remain an egg in transit, (3) generally downwelling conditions, and (4) no obstacles (e.g. jet or eddies) in the way. In contrast, passive eggs released near the

bottom require onshore transport and strong upwelling conditions in order to successfully reach the nearshore region before hatching.

Sinking eggs released near the surface, like mid-depth passive eggs, are unlikely to reach the 60m isobath because they begin in waters that are warm enough for enhanced development, but rapidly sink into waters that are not swift enough to transport them to the inner shelf region before the egg hatches. They also move offshore initially when upwelling is strong before sinking into onshore flowing waters. For shelf break spawned sinking eggs to be successful, they must quickly sink into the coldest bottom waters (or begin there) to ensure the longest possible transit time, and they must be released when upwelling is strong, with deep onshore transport velocities relatively high and sustained.

While relatively few eggs from the shelf break were successfully transported to the inner shelf, there was a significant interannual variation of success linked to SST. Egg transport duration (time from spawn to egg hatch) is temperature-dependent. Interannual differences in sea surface temperatures affect transport duration, and therefore the number of eggs transported into the nearshore region, mostly for the passive surface-released eggs, which largely remained in surface waters. A higher number of passive surface eggs were transported from the shelf break to the inner shelf during negative PDO years (2000-2002) than during positive PDO years (2003-2004). In fact, *no* eggs were transported to the inner shelf region in 2004, most likely because SSTs were very high (short egg durations). The largest number of passive surface eggs transported inshore occurred in 2001, when SSTs were cool and upwelling was strong.

Deep-released passive eggs were transported to the nearshore region about as often in 2003 as in years 2000-2002, but none were transported as

far in 2004. To understand these differences, we can again look to the PDO sign for these years. The PDO values for 2003 were not as strongly positive as in 2004, suggesting that there were more upwelling events in 2003 than in 2004. This would be consistent with several recent studies examining biological indicators of PDO phase and connectivity between nearshore and offshore stations in this region. Bi *et al.* (2011) found that during cool PDO years, cold-water neritic copepod species were dominant across the shelf and concluded that the shelf station (NH05) and slope station (NH25, just offshore of the shelf break) are connected by the strong upwelling during this phase. Keister *et al.* (2011) used a ROMS physical circulation model and passive tracer experiments to explain the mechanism behind the hypothesis that the relative dominance of warm or cold-water copepod species at local scales is controlled by climate-driven basin-scale circulation and found that surface water advection varied with the phase of the PDO such that shelf and slope waters are connected by strong upwelling during the negative phase and strong downwelling during the positive phase.

Simulation results and field observations

In their collection of euphausiid eggs at NH05 and NH15 (10 nautical miles offshore of the inner shelf station, 80m bottom depth) from 1999-2001, Feinberg and Peterson (2003) found variable relationships between egg abundances and SST. In particular, they found that while low egg abundances at NH05 could occur at any time, high abundances of euphausiid eggs at the inshore station only occurred *during* upwelling events. This relationship did not hold at the shelf station farther offshore, where peaks in egg abundance were sometimes preceded by cold-water events, sometimes followed them, and sometimes were associated with warm water. Assuming that *E. pacifica* eggs contributed significantly to the increased abundances at NH05 (the eggs

were not speciated between the two main euphausiids in the area, *E. pacifica* and *T. spinifera*), the clearer response of egg abundances to SST changes at NH05 than NH15 suggests increased abundance at the inner shelf station is the result of transport of eggs farther from their source than at NH15. In other words, the results of the current study indicate that eggs found at NH05 are not from the shelf break but from closer to the inner shelf region; if adult females are instead continuously spawning near NH15, transport of these eggs to NH05 would be more clearly related to SST at NH05, while egg peaks would not necessarily have a strong relationship at NH15, their source. (As long as transport is the primary relating factor to SST, and not another spawning cue.)

Furthermore, the finding by Feinberg and Peterson (2003) that highest abundances of euphausiid eggs at NH05 coincided with upwelling events, and that egg abundances were greater overall at the inner shelf station when PDO was more negative is more consistent with the results of the deep passive and sinking egg simulations than the passive surface simulations summarized here. If eggs are released in surface waters, as observed by Gómez-Gutiérrez (2003), the most likely behavior/depth candidate from these simulations to match field observations is surface-released sinking eggs that are spawned much nearer to NH05 than the shelf break. Feinberg and Peterson (2003) hypothesize that egg abundance at the inner shelf station varies with onshore transport of adult females to a more inshore spawning location, which would be consistent with the findings of this study, with the additional requirements of egg sinking and upwelling *after* egg release to complete the transfer.

The distributions of *E. pacifica* eggs and gravid females in collections from 1970-1972 also show high abundances of eggs as far inshore as NH01,

while gravid females were collected primarily at stations offshore of NH15 prior to egg appearance (Gómez-Gutiérrez *et al.* 2010). The years 1970-1972 occurred during a cool PDO phase so the sampling season might reasonably be expected to have strong upwelling events, which would favor onshore transport of deep passive eggs or sinking eggs if released nearer the surface.

This numerical model study, supported by well founded experimental observations of temperature controlled egg hatching time and density controlled sinking rates, found that the shelf break cannot be the primary source of eggs to an inner shelf station (NH05) where *E. pacifica* eggs are commonly observed. However, transport of eggs from regions inshore of the shelf break to the inner shelf region is possible and, depending on sinking behavior and release depth, is strongly connected to upwelling events. Regardless of sinking behavior or release depth, strongly positive PDO years are not likely to be years with large fluxes of *E. pacifica* eggs to the nearshore region from farther offshore on the shelf.

Table 3.1. Number (% of total eggs released) of *E. pacifica* eggs that successfully transitioned from presumed shelf-break spawning sites and inner-shelf egg collection sites in BITT and FITT simulations. There were no successful eggs in 2004 for any simulation.

	2000	**2001**	**2002**	**2003**
BITT	0 (0)	2066 (0.270)	0 (0)	0 (0)
FITT – Passive	1146 (0.023)	5553 (0.111)	3833 (0.077)	681 (0.014)
FITT – Sinking (mean density)	763 (0.015)	1375 (0.028)	2084 (0.042)	853 (0.017)
FITT – Sinking (low density)	611 (0.012)	1009 (0.020)	1399 (0.028)	662 (0.013)

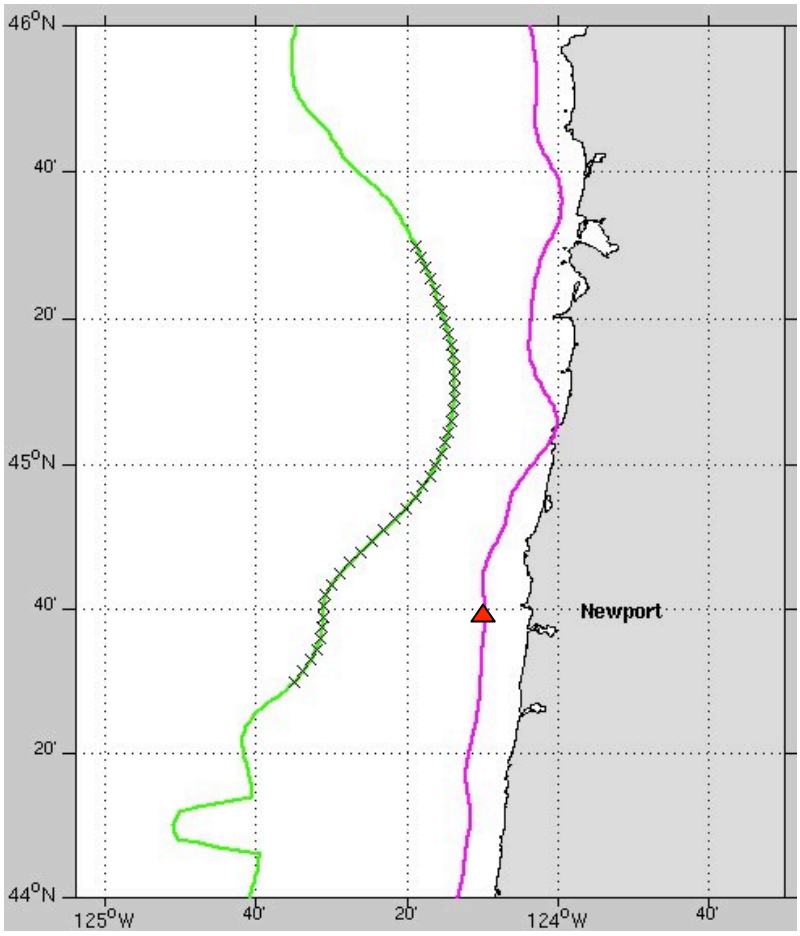

Figure 3.1. Initial positions of FITT simulation eggs. The ROMS grid's 180-m isobath is shown in green, the 60-m isobath in magenta. NH05 location in the model is denoted by a red triangle.

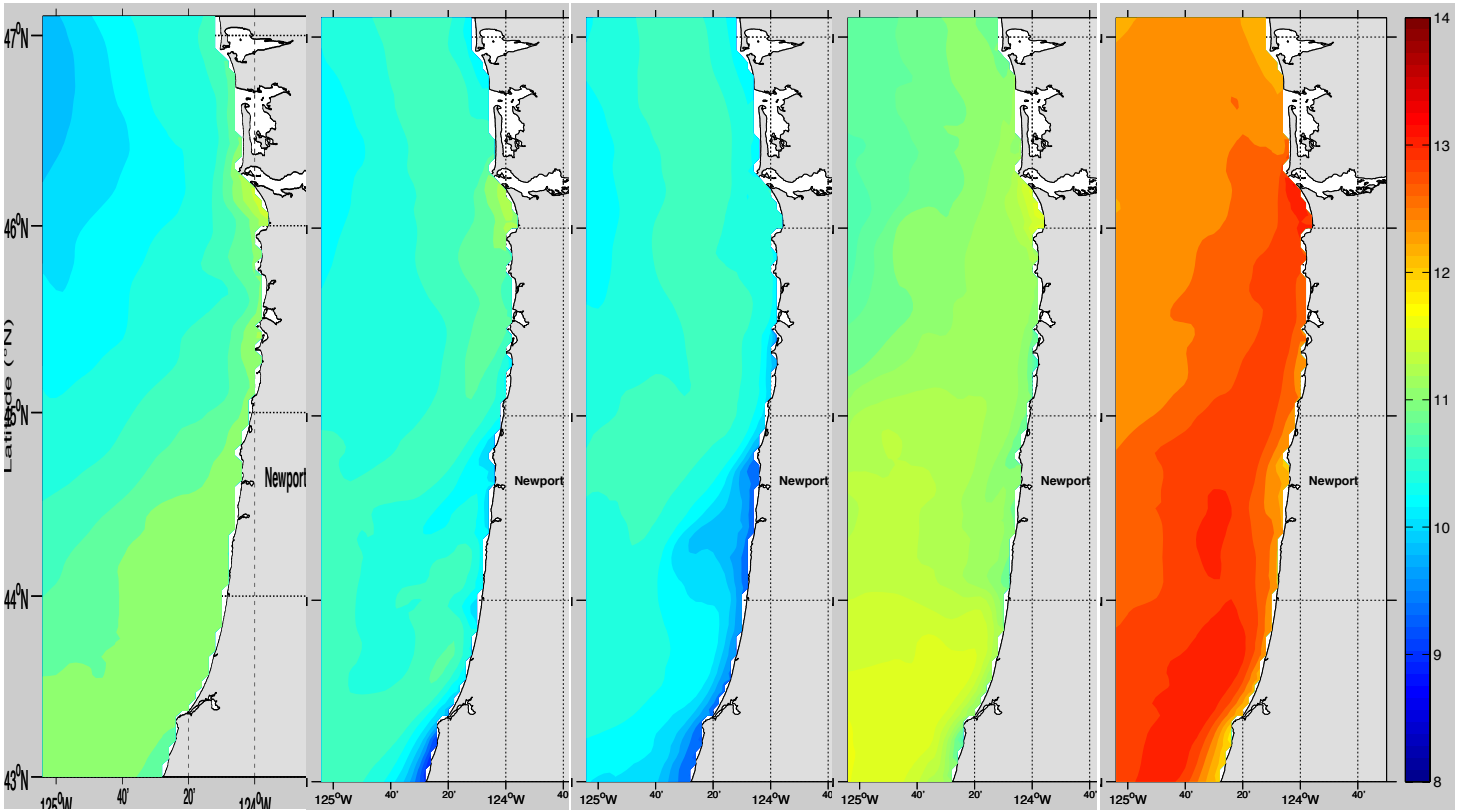

Figure 3.2. Mean Sea Surface Temperature (°C) for May from ROMS for 2000-2004.

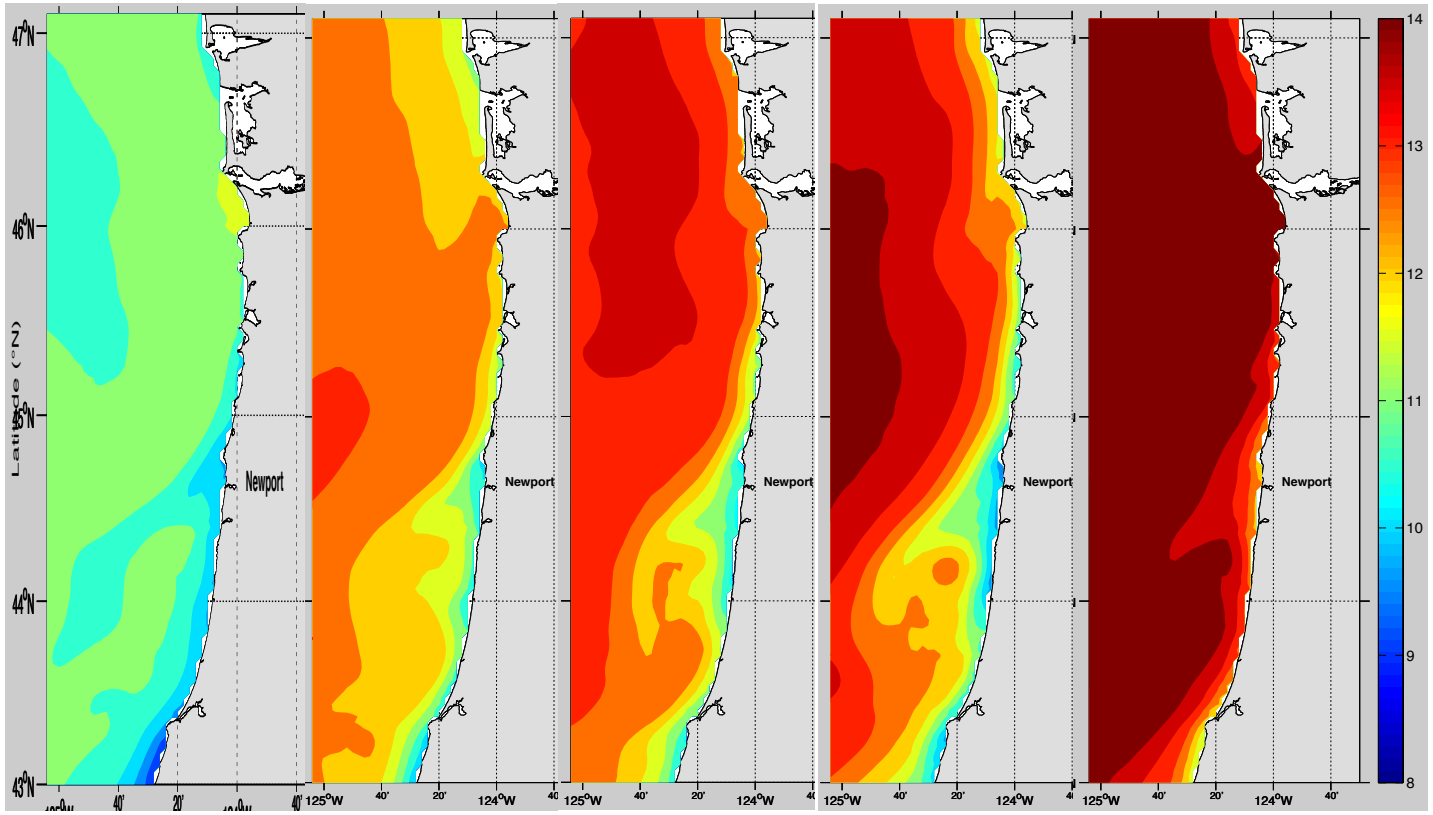

Figure 3.3. Mean Sea Surface Temperature (°C) for June from ROMS 2000-2004.

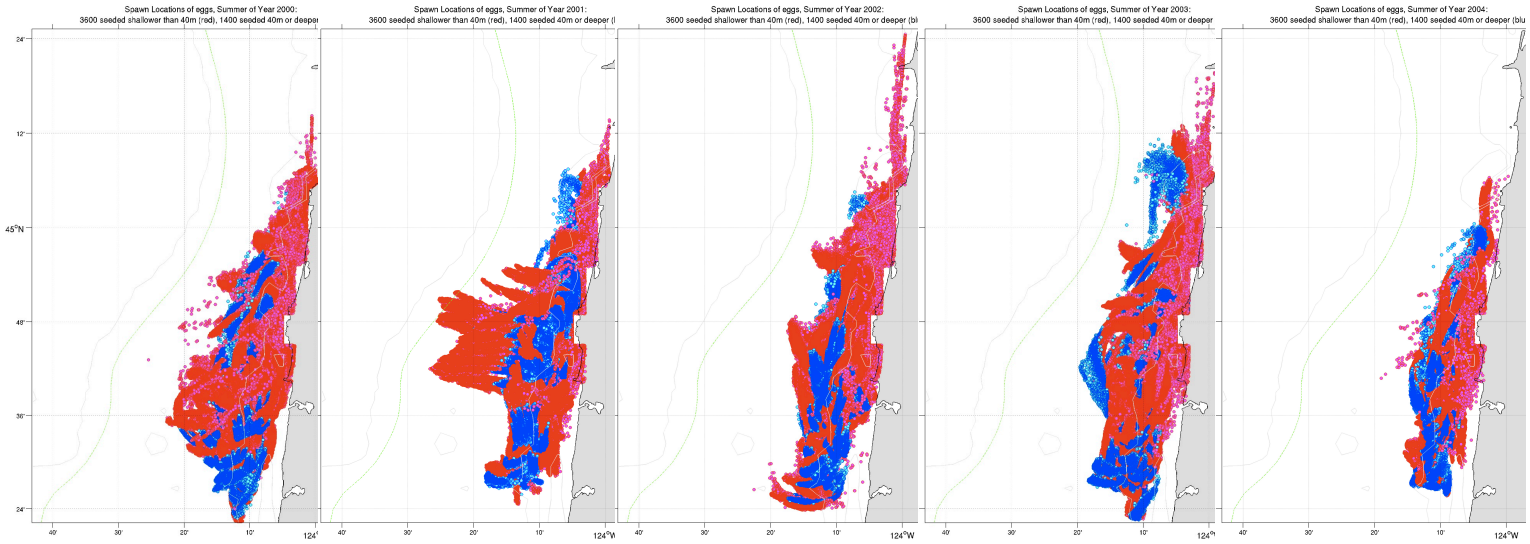

Figure 3.4. BITT simulation spawn locations**.** 2000–2004, left to right. Red markers indicate spawn locations of eggs released shallower than 40m, blue markers are spawn locations of eggs released between 40 and 55m. The 180m isobath is denoted by a dashed green line. Successful eggs were only found in summer of year 2001, and were all released from shallower than 40m.

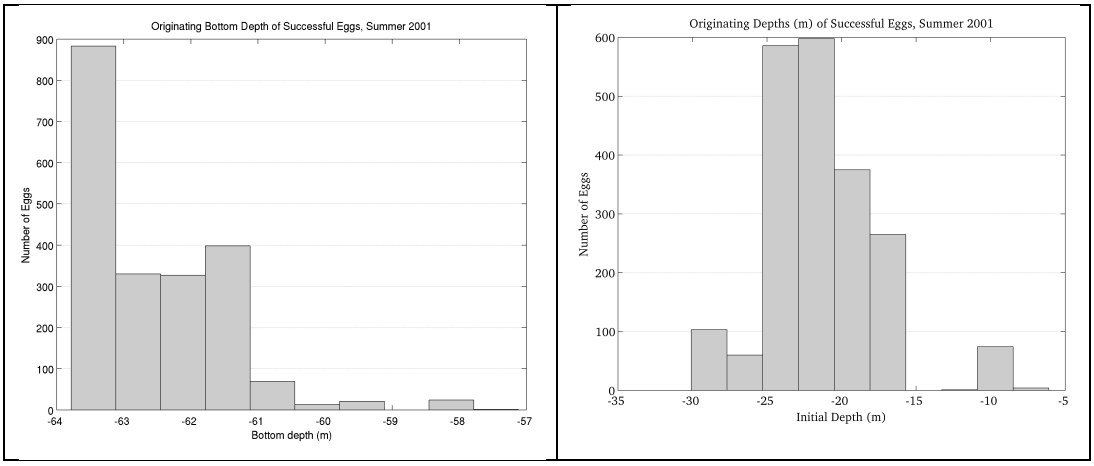

Figure 3.5. BITT simulations, 2001: seed locations and depths of successful eggs. Eggs that backtracked to the shelf break were primarily those that were seeded in the offshore portion of the 1-km region surrounding station NH05, as shown by the deeper-than-60m depths (left panel). Successful eggs were typically in the upper half of the water column.

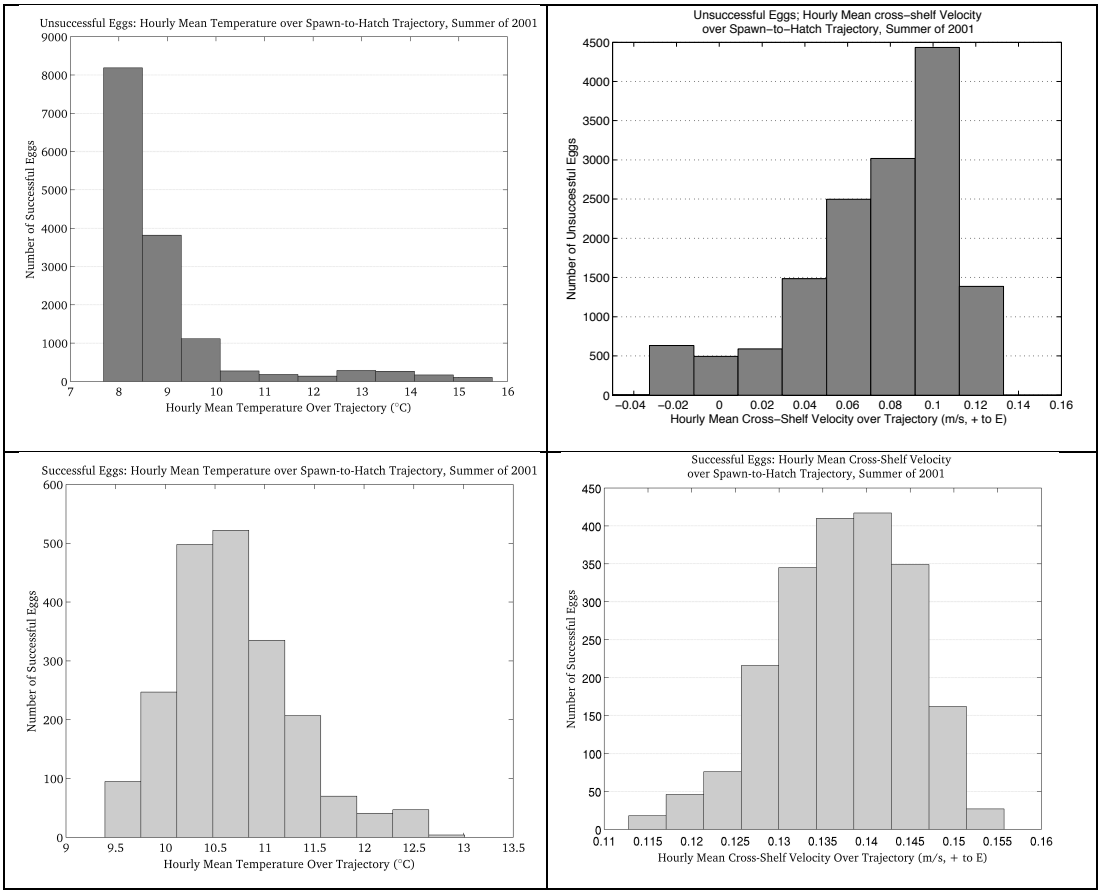

Figure 3.6. BITT simulations, from 6 successful days in 2001: temperature and velocity. Histograms of unsuccessful (top row) and successful (bottom row) eggs' mean temperature over trajectory (left column) and mean cross-shelf velocity over trajectory (right column, positive is onshore) are shown.

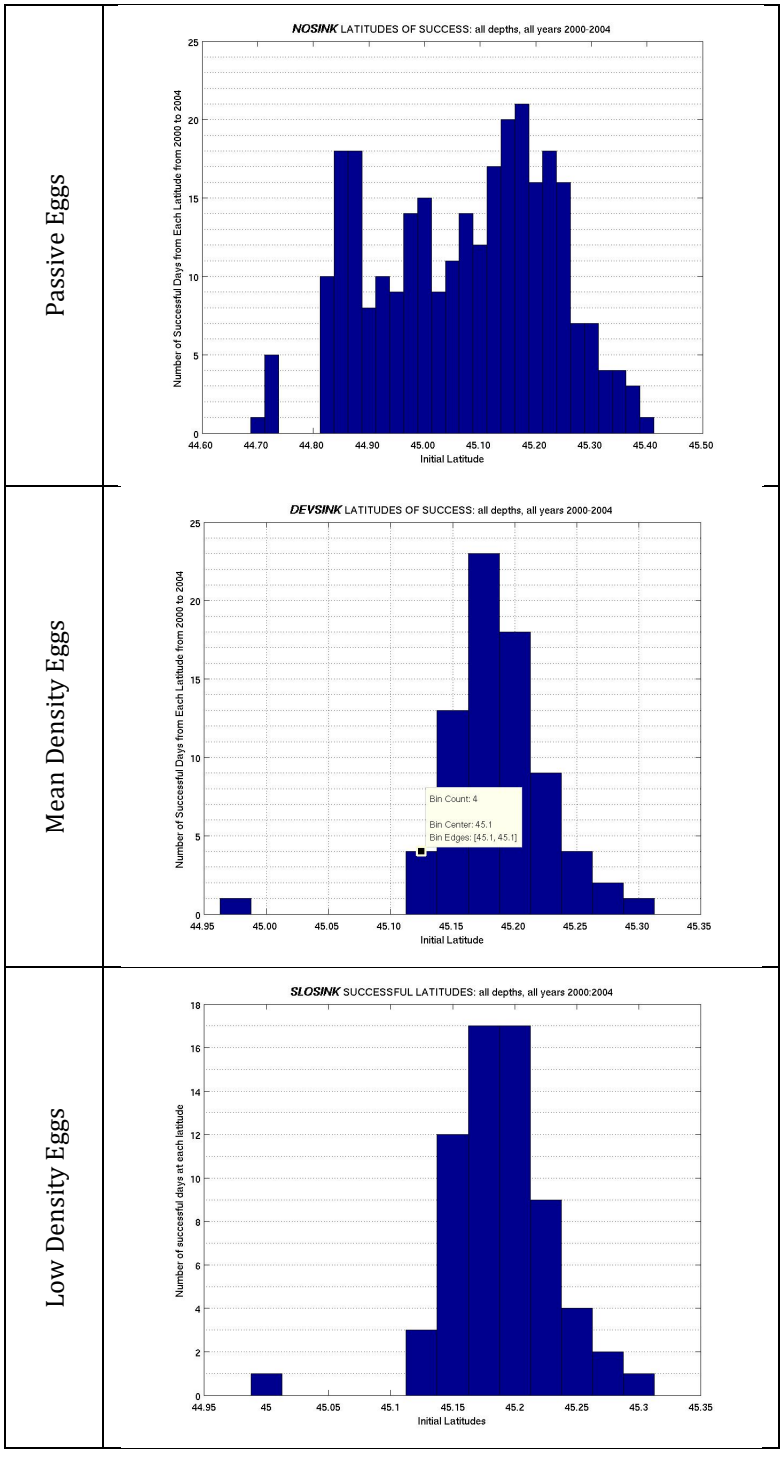

Figure 3.7. Summary of Successful FITT Latitudes.

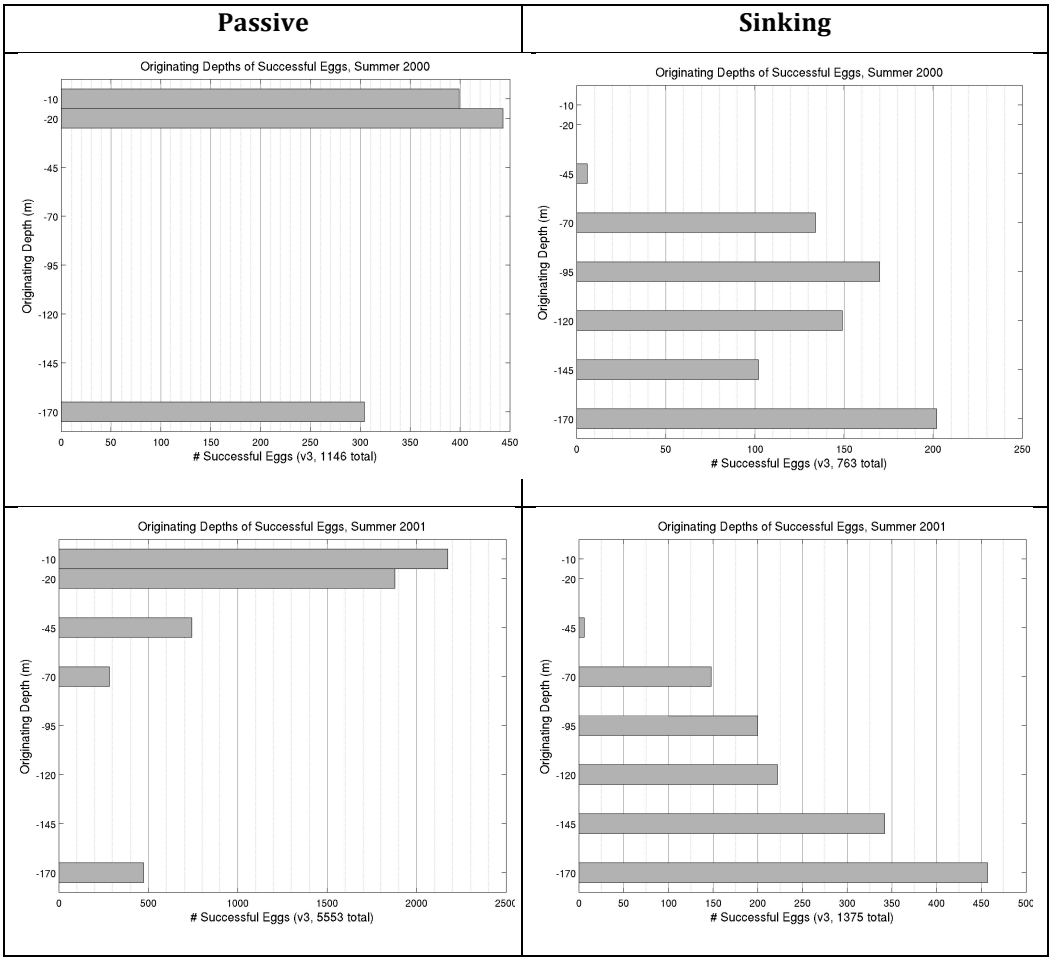

Figure 3.8. Summary of successful FITT spawning depths. Histograms of originating depths for all successful eggs, those hatching at or shoreward of the 60m isobath) from 2000 (top panels) to 2003 (bottom panels, next page) are shown. (No eggs were successful in 2004.) "Sinking eggs" in these figures are eggs that started with mean density. Low-density sinking eggs had nearly identical patterns and are not shown. Note that the *x*-axis scale changes from panel to panel.

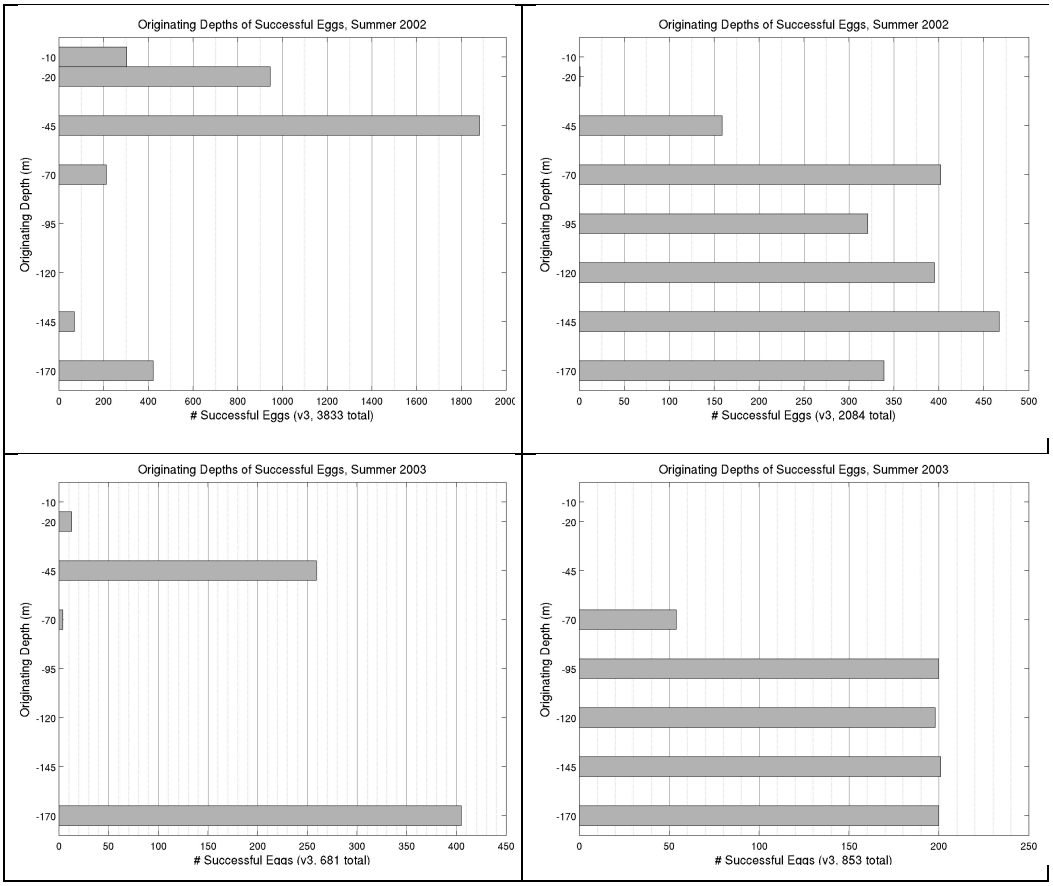

Figure 3.8. Summary of successful FITT spawning depths. (Continued)

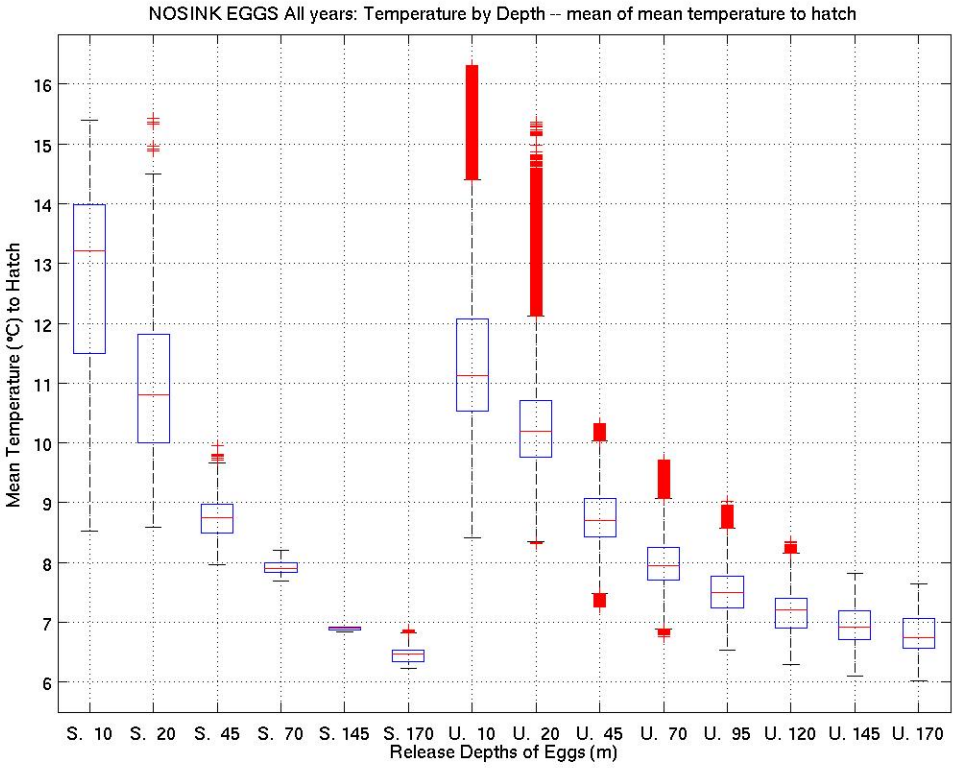

Figure 3.9. Mean temperature from spawn to hatch of passive eggs by release depth, all years pooled. Successful eggs are plotted on the left (e.g. The "S. 10" box plot shows eggs that were successful from the 10m release depth), and unsuccessful eggs are plotted on the right (e.g. The "U. 45" box plot shows eggs that were unsuccessful from the 45m release depth.) The central line of each box plot is the median, the upper (lower) edge of the box is the 75th (25th) percentile, and red crosses are outliers.

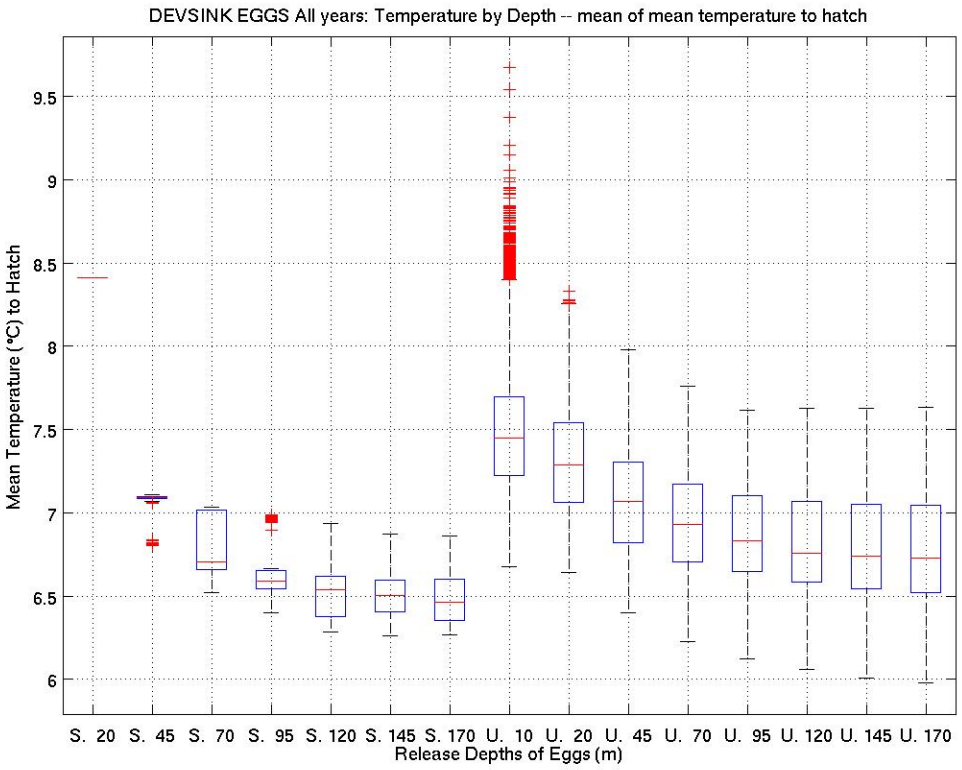

Figure 3.10. Mean temperature from spawn to hatch of mean-density eggs by release depth, all years pooled. Successful eggs are plotted on the left (e.g. The "S. 70" box plot shows eggs that were successful from the 70m release depth), and unsuccessful eggs are plotted on the right (e.g. The "U. 45" box plot shows eggs that were unsuccessful from the 45m release depth). The central line of each box plot is the median, the upper (lower) edge of the box is the 75th (25th) percentile, and red crosses are outliers.

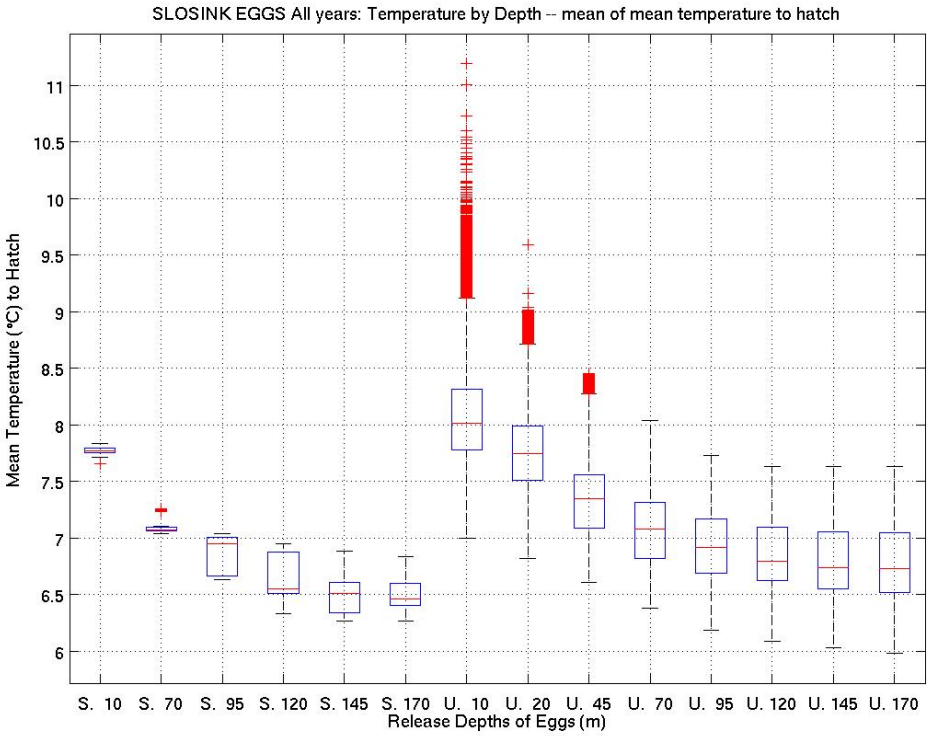

Figure 3.11. Mean temperature from spawn to hatch of low-density eggs by release depth, all years pooled. Successful eggs are plotted on the left (e.g. The "S. 10" box plot shows eggs that were successful from the 10m release depth), and unsuccessful eggs are plotted on the right (e.g. The "U. 45" box plot shows eggs that were unsuccessful from the 45m release depth). The central line of each box plot is the median, the upper (lower) edge of the box is the 75th (25th) percentile, and red crosses are outliers.

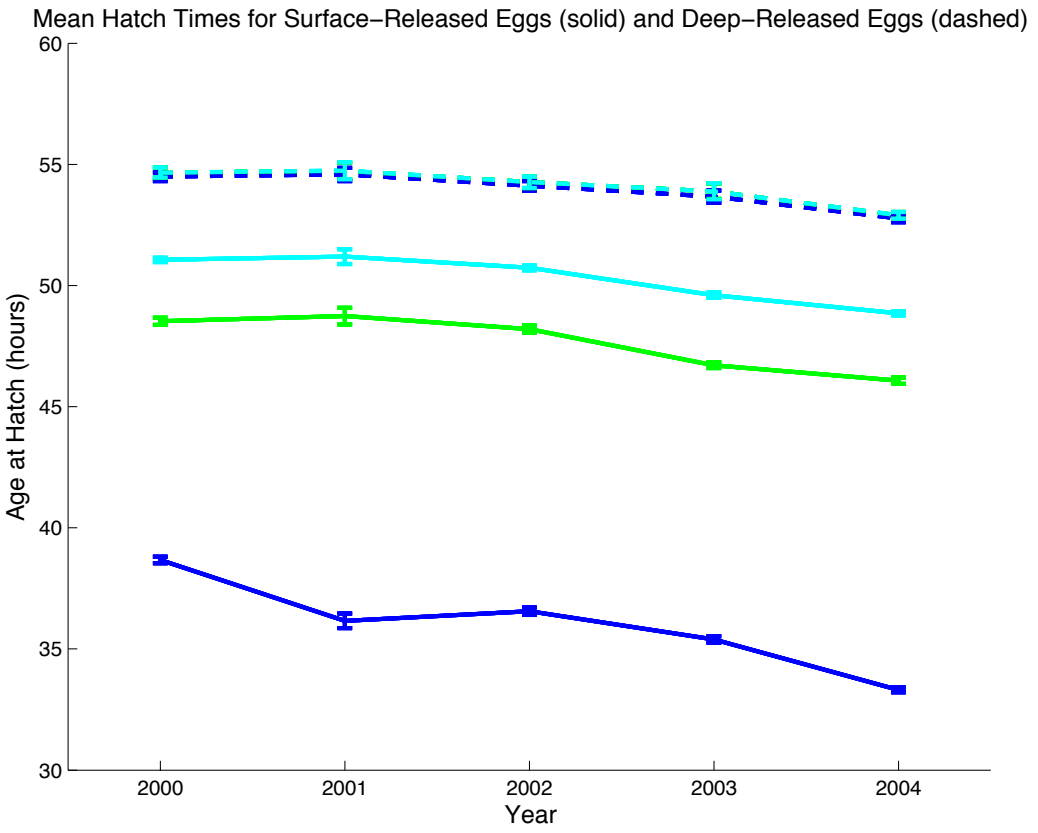

Figure 3.12. Mean Hatch Ages for Eggs during different simulation years, all behavior types. Solid lines show hatch ages for eggs released within the top 20m of the water column, dashed lines are eggs released near the bottom, 145-170m. Dark blue lines show mean (± standard deviation) hatch ages for passive eggs, green lines show mean (± standard deviation) hatch ages for low density sinking eggs, and light blue lines show mean (± standard deviation) hatch ages for mean density sinking eggs. The dashed light blue line almost exactly covers the dashed green line (i.e. the hatch ages for all sinking eggs released near the bottom are nearly identical between behaviors).

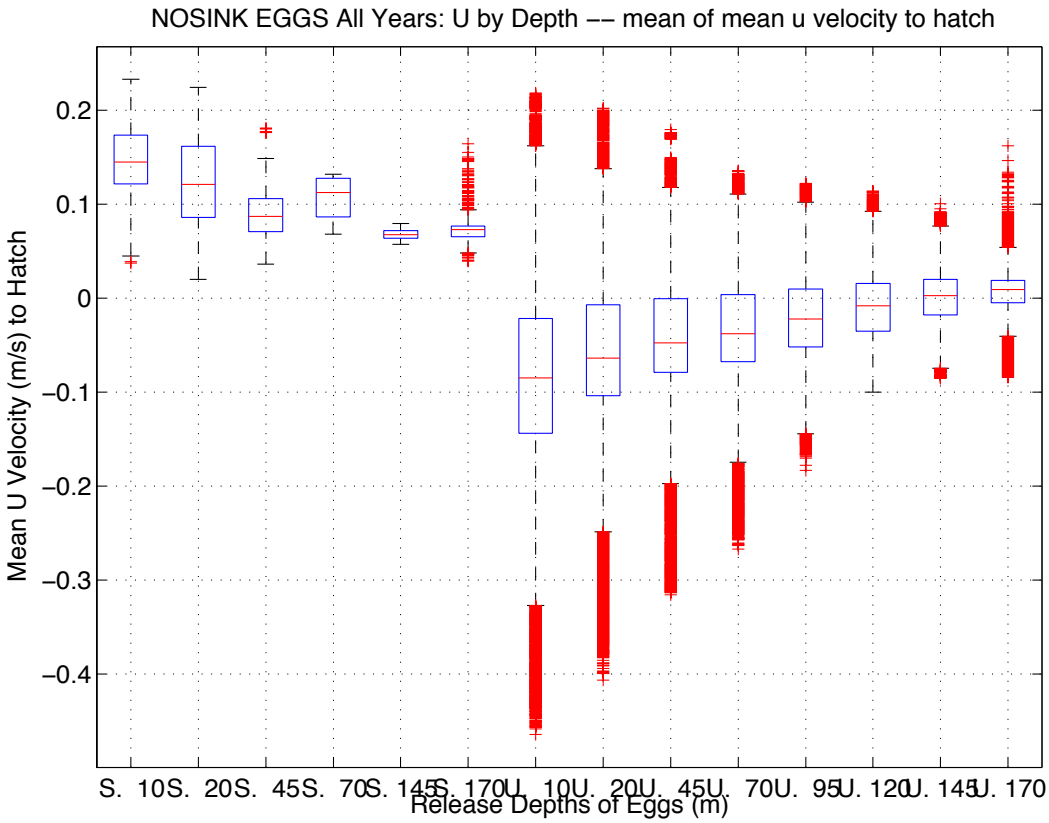

Figure 3.13. Mean U-velocity from spawn to hatch of passive eggs by release depth, all years pooled.

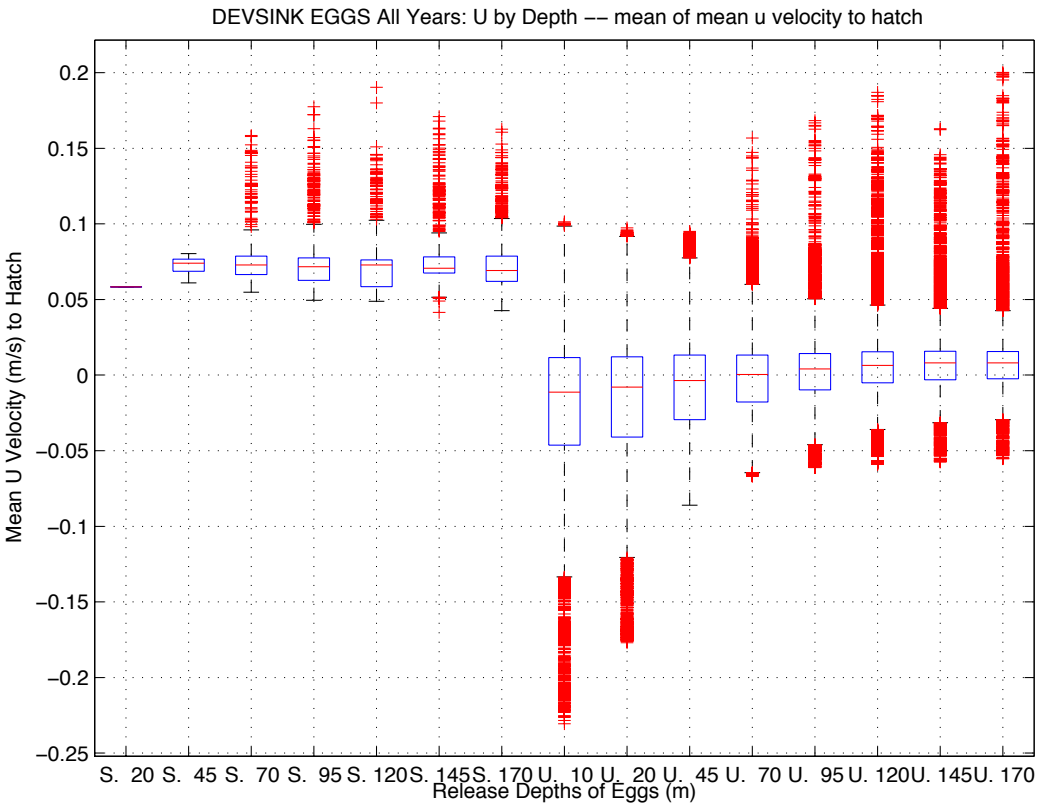

Figure 3.14. Mean U-velocity from spawn to hatch of mean-density sinking eggs by release depth, all years pooled.

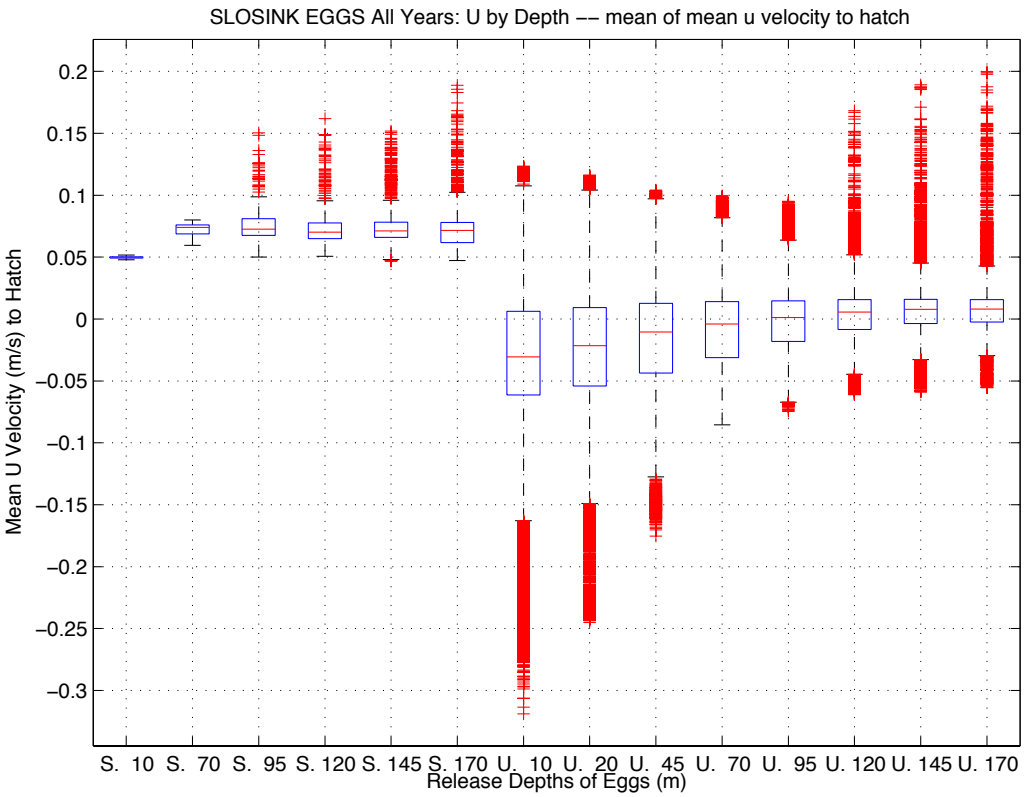

Figure 3.15. Mean U-velocity from spawn to hatch of low-density sinking eggs by release depth, all years pooled.

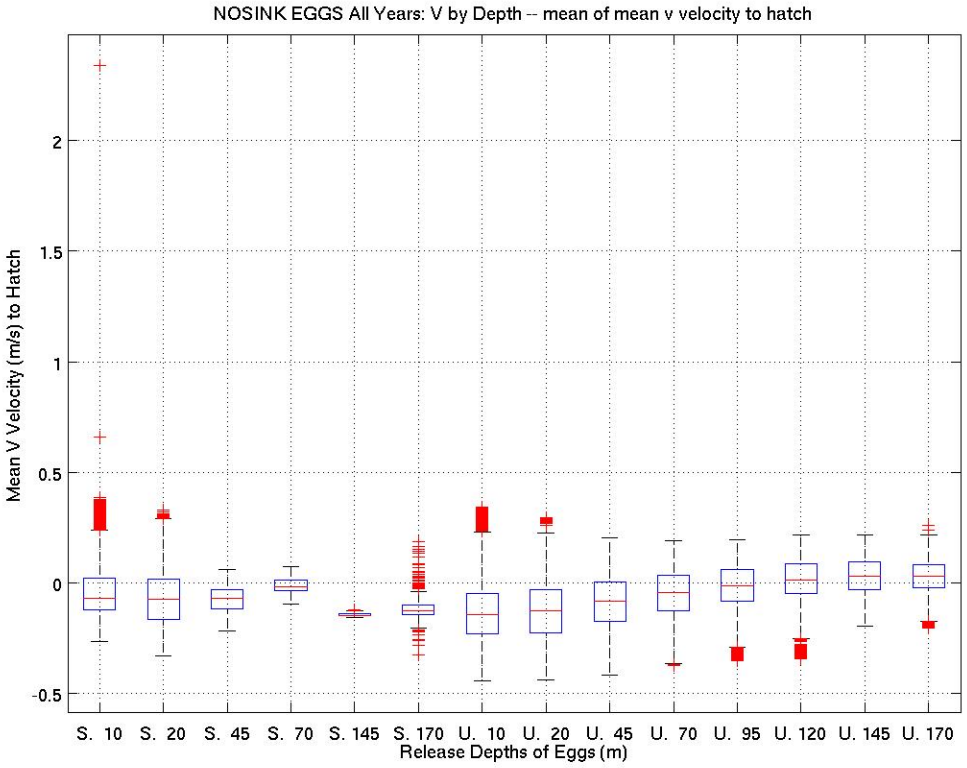

Figure 3.16. Mean V-velocity from spawn to hatch of passive eggs by release depth, all years pooled.

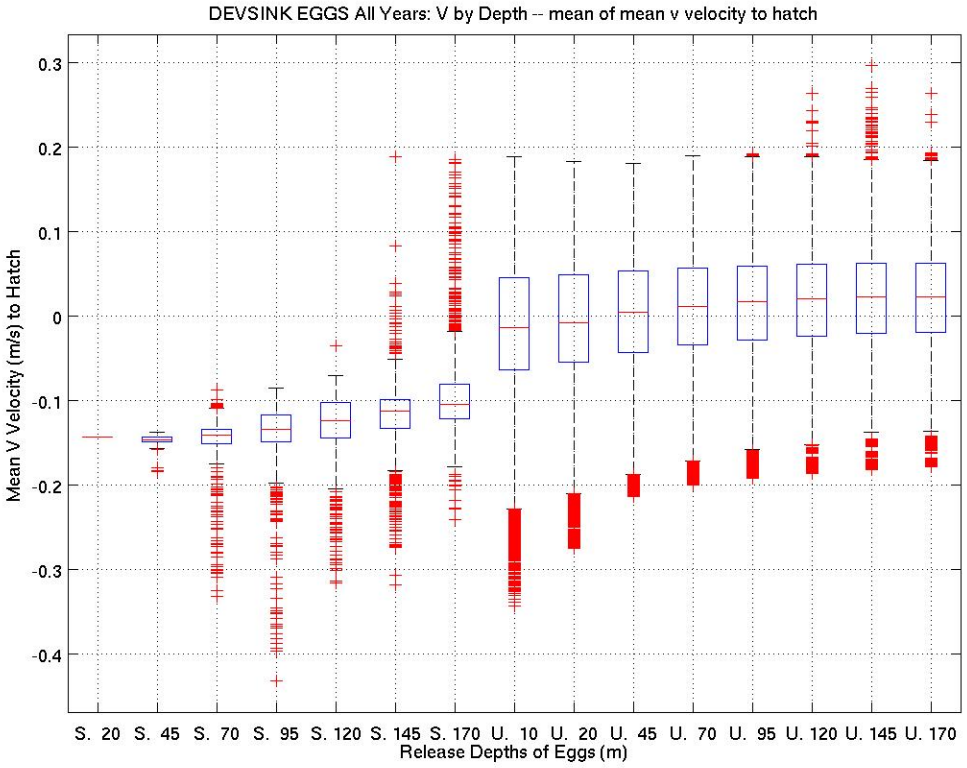

Figure 3.17. Mean V-velocity from spawn to hatch of mean-density sinking eggs by release depth, all years pooled.

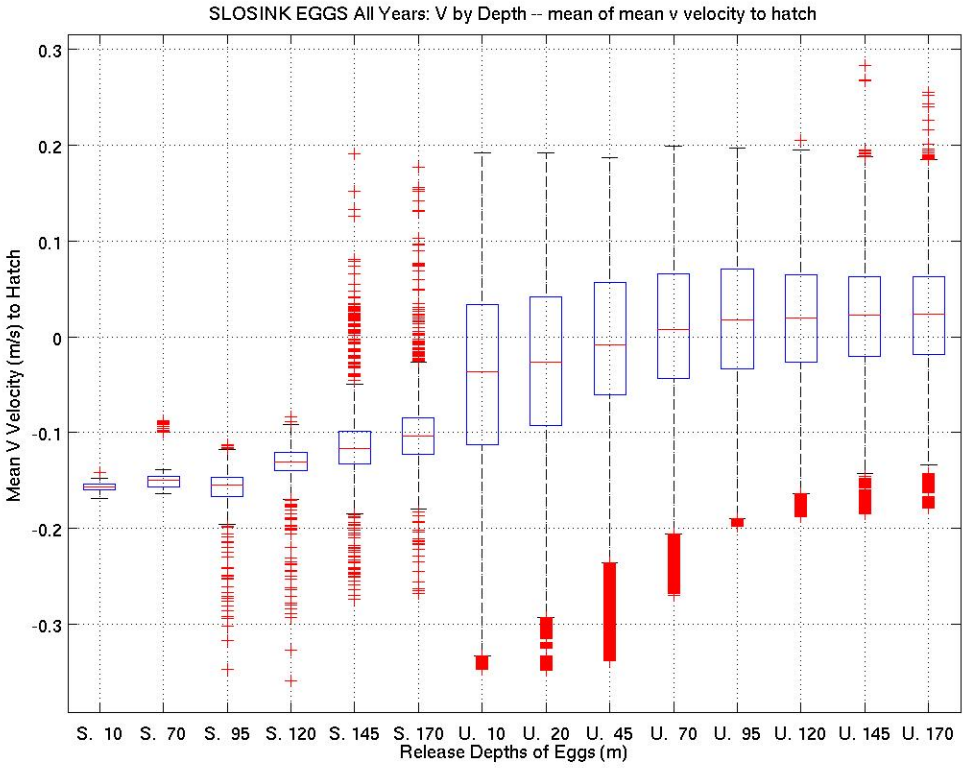

Figure 3.18. Mean V-velocity from spawn to hatch of low-density sinking eggs by release depth, all years pooled.

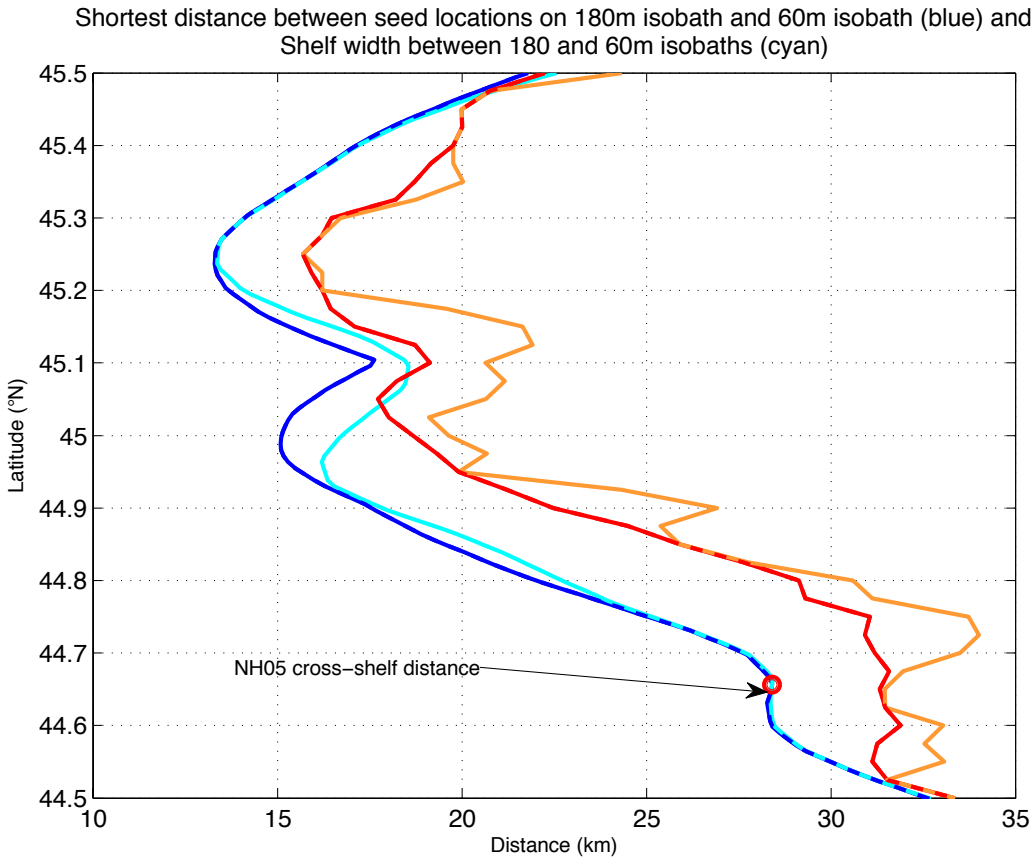

Figure 3.19. Shelf width and shortest distance between isobaths. The light blue line represents the cross-shelf distance between the 60- and 180m isobaths in the model, and the dark blue line represents the shortest distance possible from each seeding latitude along the model's 180m isobath and the 60m isobath. Red and orange lines represent the same metrics for real-world bathymetry (from Smith and Sandwell, 1997): orange is the shortest distance between the real 60- and 180m isobaths and red is the shortest distance possible from each seeding latitude along the real-world 180m isobath and the real-world 60m isobath. The model's NH05 cross-shelf distance (same as the shortest possible distance in the model) is marked for reference.

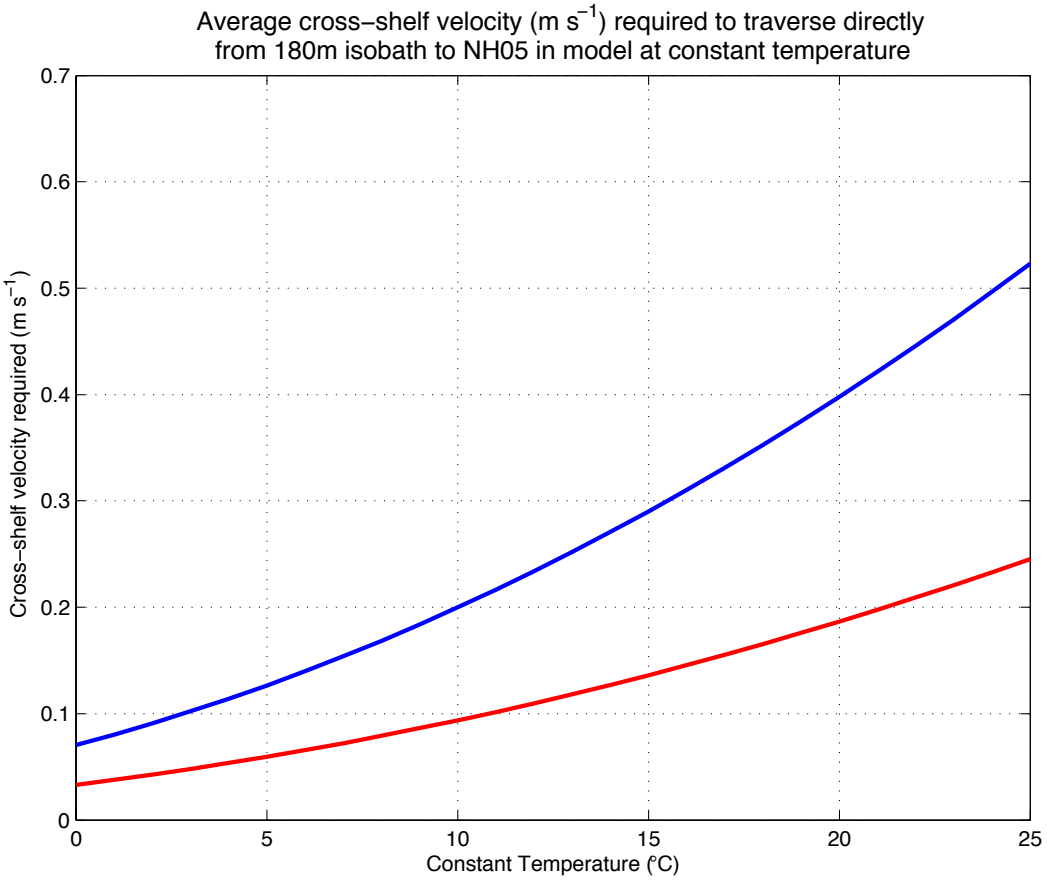

Figure 3.20. Cross-shelf speed required to traverse directly across shelf. Blue line denotes speeds required to move directly East across the shelf from the 180m isobath to NH05. Red line is the speed to the East required to move the shortest cross-shelf distance within the seeding region (13.3km).

4.0 *Euphausia pacifica* bioenergetics and retention in the Northern California Current

4.1 Introduction

Euphausia pacifica has been identified as a key grazer and prey item in the northern California Current system and therefore an important trophic link between phytoplankton and top predators ranging from sea birds (Ainley *et al.* 1996) and salmon (Emmett *et al.* 2006) to blue whales (Croll *et al.* 2005). As an essential secondary producer in the Oregon upwelling region, there is a great deal of interest in understanding the growth rates of this species and how that rate varies in time and space.

Growth rates of euphausiids are often estimated by one of two techniques: the instantaneous growth rate (IGR) method, a direct measurement of length changes between molts of live animals in the laboratory, or the cohort method, where populations are followed in a region over time to estimate the population's mean growth rate from length distributions in samples. Both methods have advantages and their own set of assumptions.

Direct measurement of growth between molts in the laboratory provides information on individual variability and growth rates that reflect most recent *in situ* conditions (Shaw *et al.* 2010). Therefore, the growth rates determined from IGR are short-period, highly variable, and not necessarily representative of the mean growth of a population or a season. Furthermore, growth rates of euphausiids reared in laboratory incubations have been estimated to be as low as half the rate found in the same species in the field and therefore IGR estimates may be biased (Harvey *et al.* 2010).

On the other hand, the cohort analysis estimates growth rates over periods of several weeks to several months and therefore integrates longer

time periods and individual variability. This rate may more accurately reflect the mean population over a season or longer, and has been used to estimate *E. pacifica* growth rates in several studies in the northern California Current (Brinton 1976, Smiles and Pearcy 1971, Bollens *et al.* 1992). However, a central assumption to this type of analysis is that the same population is sampled repeatedly.

This assumption may not be valid for the upwelling region off Oregon and Washington, in the northern California Current. The California Current System is a dynamic region with circulation features driven by strong wind stress, continental shelf features and bottom topography. Within the region spanning the inner continental shelf to a region extending far beyond the shelf break, there are strong alongshore flows both southward and northward throughout the year. Vertical shear is strong where southward-flowing California Current waters near the surface overlay northward-flowing California Undercurrent waters. Upwelling season brings with it offshore surface transport and a coastal jet that generates offshore-flowing filaments and eddies. Therefore, there is substantial opportunity for populations of plankton to exchange over short time periods. It is not difficult to imagine that a group of krill sampled one month may have been transported outside a study region by the next month, and repeated sampling in one location might yield estimates based on a far broader krill distribution than assumed, or for krill that have experienced different growth and stage development schedules.

Several retention mechanisms have been suggested in order to consider *Euphausia pacifica* (and other zooplankton) at the Oregon coast as belonging to a somewhat self-sustaining population. Diel-vertical migration (DVM) has been hypothesized to interact with both upwelling circulation

(Peterson 1998, Batchelder *et al.* 2002, Lamb and Peterson 2005), and larger-scale currents, such as the Davidson Current, outside of upwelling seasons (Carr *et al.* 2008) to retain zooplankton close to the coast. If *Euphausia pacifica* are retained within the sample region, then the assumption of repeatedly sampling the same population holds. If it leaves the sample region but returns to release eggs in the sample region, it can be considered self-seeding. While a self-seeding population with long-term (several month) excursions outside of the region of interest may be capable of maintaining its position over successive generations, it might not be sufficiently retained for cohort analysis to accurately reflect average growth rates of krill in a population.

In order to explore the potential for self-seeding, however, one must first consider the stage durations leading to a reproductive adult. While the durations of *E. pacifica* larval stages have been reported in a number of laboratory studies (e.g. Feinberg *et al.* 2006, Pinchuck and Hopcroft 2006, Ross 1981), there are no direct measurements of the duration of juveniles prior to reaching reproductive maturity. Survivorship curves from field samples suggest that the juvenile stage may be as long as six months (T. Shaw, L. Feinberg, H. Bi, and W. Peterson, unpublished). Harvey *et al.* (2010) used a biochemical marker to estimate age in *E. pacifica* collected in the field and calibrated to laboratory-reared individuals of known age and found that reproducing females that had been collected in the field were as young as three to four months, suggesting a far shorter duration of the larval and immature stages combined.

A species as long-lived and widely distributed as *E. pacifica* presents several challenges to understanding nuances of its life history, and studies are often limited to exploring only portions of its life cycle. Field sampling

over expansive regions and long time periods, typical of their distribution and generation times is expensive. Laboratory studies designed to observe its physiology over its full life cycle must overcome difficulties inherent in rearing animals in captive environments for extended periods of time. Modelers are confronted with difficulties in developing models that capture adequately both the physical environment and the ecosystem upon which *E. pacifica* depends with realistic temporal and spatial evolution.

While progress has been made toward realistic circulation models for the Northern California Current, ecosystem models coupled to these fields often do not produce realistic fields over the length of time required to run simulations for a full life cycle of *E. pacifica*. For instance, the ecosystem model used later in this chapter produces phytoplankton patterns that resemble temporal patterns of surface chlorophyll observations sometimes, but at other times has extremely low phytoplankton abundances when satellite observations indicate a period of high chlorophyll. Ideally, a highly-resolved circulation model coupled to an ecosystem model that faithfully reproduced observed food distributions and abundances would be a good foundation upon which to answer questions involving the full life cycle of *E. pacifica*. As model fields with the degree of realism required to evaluate questions of this scale were not available, we use simplified frameworks to make explorations of these scales.

This chapter considers the large-scale questions of retention and self-seeding potential by looking at the full life cycle of *E. pacifica* in two ways. First, a Lagrangian individual-based model (IBM) of bioenergetics and development is forced by static food and temperature fields from a 3-dimensional Eulerian model of the circulation and lower trophic level ecosystem. This setup provides a simplistic framework to estimate a range of

juvenile stage durations as a result of biotic and abiotic conditions likely to be found in the upwelling zone. This method also affords a clear view of impact of spatially-variable fields that drive differences in the bioenergetics of the individual krill. Second, the potential for self-seeding by, or resampling of, the same population of *E. pacifica* in the region is explored with a particle tracking simulation run with krill capable of DVM that evolves as a function of development that is controlled exclusively by temperature and does not rely on accurately-modeled food resources.

4.2 Methods

The IBM is driven by velocity (u, v, w), temperature, salinity, light, and food fields. These external forcing fields are provided by a Regional Ocean Modeling System (ROMS, Song and Haidvogel 1994) configured for the 3-dimensional representation of the California Current and coupled with the North Pacific Ecosystem Model for Understanding Regional Oceanography (NEMURO, Kishi *et al.* 2007).

Circulation model

The ROMS model domain spanned 134-116°W and 30-48°N with a horizontal resolution that ranged from 2.5 km to 3.2 km in the zonal direction and 3.7 km meridionally. A spatial subset of this grid, spanning from 34°N to 48°N and 132.5°W to 120°W, was used in these simulations due to storage and computation costs. Vertical structure was described by 42 terrain-following levels in an s-coordinate scheme. Physical simulations were run with a spin-up year (1999). Horizontal (u, v) and vertical (w) velocities, salinity (s), and temperature (T) fields were averaged daily and stored for 2000-2001. Further details of the model bathymetry construction are discussed in Drake *et al.* (2011). The coupled ecosystem ROMS model was

initially developed and run by Chris Edwards and Jerome Fiecheter (University of California, Santa Cruz) for studies in the Monterey, CA region where the bathymetry was tuned to closely match central CA bathymetry. On the Oregon shelf, the model bathymetry is more smoothed, with narrower shelves and less spatial accuracy than in central California.

The ROMS model was forced on all open boundaries by monthly-averaged fields from the Simple Ocean Data Assimilation (SODA; Carton *et al.,* 2000) reanalysis to guarantee realistic transport values and temperature and salinity profiles. For consistency, initial conditions are also based on SODA. Surface forcing is derived from the Coupled Ocean-Atmosphere Mesoscale Prediction System (COAMPS; Hodur *et al*., 2002), and consists of daily-averaged winds, air temperature, sea level pressure, specific humidity, precipitation, and short-wave and downwelling long-wave radiation.

NEMURO Ecosystem model

The multiple food fields used to drive the bioenergetics model are outputs of the NEMURO model. NEMURO is an Eulerian ecosystem model representing what are thought to be the essential components of North Pacific ecosystems. It consists of 11 state variables: nitrate, ammonium, small and large phytoplankton biomass, small, large and predatory zooplankton biomass, particulate and dissolved organic nitrogen, particulate silica, and silicic acid concentration. Specifically, the ROMS-NEMURO coupled model (hereafter RN) is parameterized such that large phytoplankton represent diatoms, small phytoplankton represent nanophytoplankton, small zooplankton represent microzooplankton, and large zooplankton represent mesozooplankton (primarily copepods). Here, a single snapshot of these fields is used to demonstrate the functioning of the IBM (introduced below).

The initial and boundary conditions for nitrate and silicic acid are based on monthly climatological values from the World Ocean Atlas 2001 (Conkright and Boyer, 2002). For lack of better information, the initial and boundary conditions for the other biological variables are set to a small value. Several modifications were made to the NEMURO functions of Kishi *et al.* (2007): (1) light limitation includes photoinhibition (Platt et al., 1981); (2) Holling Type 2 grazing for zooplankton (instead of Ivlev); (3) added microzooplankton grazing on large phytoplankton; and (4) Phytoplankton Michaelis-Menten term for silicic acid adapted to match Yamanaka *et al.* (2004). Details of these modifications are described in Fiechter and Moore (2009). Note that the iron limitation in Fiechter and Moore (2009) is not implemented in the NEMURO model used here. A variable chlorophyll:carbon ratio was added to NEMURO by J. Fiechter as a function of light, temperature, and nutrients based on the empirical relationship described by Cloern *et al*. (1995). A molar conversion from N to C was used when converting biomass of prey fields from units of N to C, assuming a Redfield C:N ratio (106:16), and using molar mass of 12 for C.

Individual-based model

The IBM for North Pacific krill, *Euphausia pacifica*, is a modification of an earlier 1-D (vertical dimension) IBM developed for copepods of the genus *Metridia* (Batchelder and Miller, 1989; Batchelder and Williams, 1995), and subsequently used with multi-dimensional particle tracking in the Oregon upwelling system by Batchelder *et al*. (2002). In this chapter, growth, development and reproduction are calculated for each individual at hourly time steps (recorded every six hours). The IBM is run offline using previously stored daily-averaged fields (temperature; salinity; *u*-, *v*-, and *w*-velocities; diatoms; nanophytoplankton; microzooplankton; and mesozooplankton)

from the RN simulation. For each time step of the IBM, the two RN snapshots that bracket the current time are retrieved (if not already in memory) and interpolated tri-linearly in space and then linearly in time to obtain the values needed to model each individual's dynamics.

Euphausia pacifica Bioenergetics:

Stage Development

Euphausia pacifica develops through a series of life stages from egg to adult, with significant morphological changes at some stages, such as the addition of feeding appendages in the first calyptopis stage, the fifth stage in this model (Mauchline and Fisher, 1969). Other morphological enhancements, such as the division of the body into distinct segments beginning with the metanauplius, development of compound eyes and addition of swimming appendages in the furcilia stages, continue until the larvae molt into the juvenile stage. At this point, the euphausiid resembles an adult but is not yet reproductively mature. Adults are strong swimmers capable of large diel-vertical migrations (Brinton 1962) and vision good enough to potentially avoid net capture, especially during the day (Brinton 1967).

Development (life-stage progression) in bioenergetics models is often implemented using body weight thresholds that must be achieved in order to progress to the next stage (e.g. Carlotti and Wolff 1998, Batchelder and Miller 1989, Miller *et al.* 1998). In this model, development is driven by temperature, which allows for shrinkage within a stage when food is scarce, as has been noted for this species in laboratory estimations of growth rates (Shaw *et al.* 2010). As discussed in chapter 3, the development from one stage to the next is determined by the Belehrádek function,

$$D_i = a_i(T + b)^c, \qquad \text{(A)}$$

where D_i, the number of days from egg to stage i, a_i (day °C^{-1}) is an empirically-determined, stage-specific constant which defines initial functional slope; b (°C) is a stage-independent temperature shift specific to the species; and c (dimensionless) is an empirically-derived constant that determines curvature, and is often assumed (for copepods) to be –2.05, based on numerous crustacean zooplankton development experiments carried out by a number of independent workers (e.g. Harris *et al.* 2000). Estimates for a_i (Table 4.1) and b (15.052°C) were based on measurements of *Euphausia pacifica* egg and larval stage durations at several temperatures reported in Feinberg *et al.* (2006), Ross (1981), and Iguchi and Ikeda (1993), Pinchuck and Hopcroft (2006). The advantage of using a development model that is temperature-dependent only is that the evolution of stage-based behavior, which is expected to have an impact on emerging distributions of krill, can be explored in the absence of realistic food fields.

As mentioned, the juvenile stage duration of *E. pacifica* is uncertain, but current estimates derived from cohort and survivorship analyses in the Oregon upwelling region suggest that the juvenile stage may last as long as six months in the field (T. Shaw, unpublished). During periods of limited food availability, krill can not only shrink in length between molts (Marinovic and Mangel 1999), but female euphausiids may resorb their gonads when conditions do not favor reproductive surplus (Gómez-Gutiérrez *et al.* 2010). If juveniles resemble adults in all but size and reproductive maturity, it is reasonable to expect that some adults in the field may actually be misidentified as juveniles, thus lengthening the duration of the stage in unfavorable food or temperature conditions. The low end of the range of juvenile stage durations is provided by estimates of spawning female age, found to be as young as three months (Harvey *et al.*, 2010), suggesting a

juvenile stage duration significantly shorter than that estimated by cohort analysis. In the model described here, the juvenile is considered to be a reproductively capable adult only when it has attained a mass of 950 μgC, or about 12mm total length; this is larger than the largest juvenile (11.6mm) observed in samples from the Oyashio region during 2007 (Kim *et al*. 2010), and equal to the length of the smallest spawning female captured off Oregon (Feinberg *et al*., 2007).

Growth

Initial egg weight is 3.2 μgC, the mean carbon weight according to Gómez-Gutiérrez (2003). Eggs and non-feeding naupliar and metanauplius stages lose weight at a rate described by a temperature-influenced weight-specific basal metabolism rate (R_B) until reaching the first feeding stage, calyptopis I. From calyptopis I through juvenile, growth was calculated as the balance between assimilated food and metabolism, or

$$G = AE * I - R, \quad (1)$$

where G is growth rate (μgC d^{-1}), AE is assimilation efficiency (unitless), I is ingestion rate (μgC d^{-1}), and R is respiration rate (μgC d^{-1}). For adults, growth was the balance of these terms and reproductive costs, or

$$G = AE * (1 - \omega)I - R, \quad (2)$$

where ω is a fraction of ingested food reserved for reproduction and not used for somatic growth. R is the sum of active (R_A) and basal (R_B) respiration rates. R_A is a fraction of ingested food, lower for older stages than for larvae (Equations 3 and 4; these and subsequent equations are listed in Table 4.2. Parameter values are listed in Table 4.3).

Ross (1982*a,* 1982*b*) presented a full energetic budget of *E. pacifica*, including experimentally measured assimilation, growth and respiration for a range of stages. From these measurements she derived several weight-

specific (allometric) equations for these processes and found that weight-specific growth rates declined as an animal grew. Her direct measurements of growth did not equal the balance of the component processes, assimilation and metabolism (Ross 1982*b*), which she attributed to measurement errors. In order to build a mechanistic IBM rather than scale growth directly, R_B is the allometric function (Equation 5, Table 4.2) that fit the difference between her growth function and assimilation, accounting for the assumed R_A, and her function for assimilation informed the maximum daily ingestion rate. The measured Q_{10} by Ross for ingestion (3.36) and respiration (2.0 for larvae, 1.9 for juveniles and adults) was also used. Assimilation efficiency was constant at 81.3%, as Ross found no temperature effect in her experiments.

Ingestion rate was a function of food density, temperature, and individual weight. While diatoms are likely the main component of its diet (Ross 1982*a*; Ohman 1984), *E. pacifica* is an opportunistic feeder that exploits varied food resources (Mauchline 1967; Endo 1981; Nakagawa *et al.* 2001; Pinchuk and Hopcroft 2007) including copepods (Ohman 1984), marine snow (Passow and Alldredge 1999; Dilling *et al.* 1998), and even small prey such as naked ciliates (Nakagawa *et al.* 2002, Nakagawa *et al.* 2004). In the model, all feeding life stages consume diatoms if present. Various stages consume different combinations of additional phytoplankton and zooplankton from the NEMURO model: calyptopis I through furcilia III eat diatoms and a portion of the nanophytoplankton field; furcilia IV/V through furcilia VII eat diatoms, a fraction of the nanophytoplankton, and microzooplankton; and juvenile and adult *E. pacifica* eat all of these but also consume mesozooplankton. The fraction of nanophytoplankton biomass assumed to be available to euphausiids was estimated to decline linearly from 50 to 20% with increasing nanophytoplankton biomass because it was

assumed higher biomasses were associated with smaller (and unavailable) nanophytoplankton cell sizes (Equation 6, Table 4.2).

Because several prey types are likely consumed concurrently, we used a multiple prey resource consumption model to estimate ingestion (see Gentleman *et al.* 2010 for discussion of various formulations). Ohman (1984) used a Holling Type 2 curve to fit measured ingestion rates of *Pseudocalanus* copepods and a sigmoidal curve fit to measured diatom ingestion rates of diatoms. Gentleman and Neuheimer (2003) recommended using a satiating response with increasing food density. Therefore, ingestion (I_{TOT}) of all accessible prey combined was modeled as a sigmoidal, passive switching model of multiple prey resources (i) ("filtered" or "captured"):

$$I_{TOT} = \sum \frac{c_i N_i^2}{1+\sum b_i N_i^2}, \quad (7)$$

where c_i and b_i are resource-specific constants and N_i is the concentration of resource i.

For the purposes of the multiple resource model, relatively small prey (e.g. diatoms, nanophytoplankton, and microzooplankton), if accessible to an individual were summed into a single food resource (captured by filtering) and mesozooplankton (raptorially captured) were considered a separate food resource for Equation 7. Therefore, for stages that did not consume mesozooplankton (all larvae), the ingestion relationship simplified to a single-resource sigmoidal function. A close sigmoidal approximation of Ohman's (1984) Holling Type 2 curve for *E. pacifica* ingestion rates of *Pseudocalanus* copepod was used to represent the mesozooplankton food choice in the multiple resource model. Ohman's function describing diatom ingestion was scaled so that the maximum ingestion rate matched Ross's (1982*a*) predicted ingestion rate for an adult of the same weight and at the same temperature (4.7 mgC at 8°C) as the mean adult used in Ohman's study,

then normalized by that maximum ingestion rate such that the food-dependent function scaled from 0 to 1. Ingestion rate was further modified by the allometric relationship (Equation 8, Table 4.2) found by Ross (1982*a*) at full food rations and by temperature, with a Q_{10} of 3.36, as reported by Ross (1982*a*).

Reproduction

Adults were considered reproductively capable when they surpassed 950μgC. This weight roughly corresponds to 12mm *E. pacifica*, the smallest reproductive female size reported by Gómez-Gutiérrez *et al.* (2006) and Feinberg et al. (2007; 2013), according to the total length to dry weight relationship reported by Feinberg *et al.* (2007) and assuming 40% of dry weight is carbon (Equation 9, Table 4.2). Egg production is a function of female body size, recent food, and last interbrood period. The IBM of Batchelder *et al.* (2002) used a dynamic egg production scheme, where a fraction of positive net growth in a time step was allocated to reproductive weight. The proportion allocated to reproduction increased with individual female body mass. A clutch of eggs was spawned when a minimum amount of reproductive weight had accumulated. Thus, interbrood period was variable depending on the ability of the female to accumulate reproductive stores.

A slightly different scheme is employed here for *E. pacifica*: instead of a fraction of positive growth, a variable fraction (0.2 to about 0.26) of ingested food is allocated to a separate reproductive material store rather than to somatic growth (and is not counted toward the weight of the individual; Equation 10, Table 4.2). When enough reproductive weight is accumulated, a brood of eggs is released. In taking a fraction of ingestion (rather than positive growth), a female may shrink over an interbrood period

but still produce eggs (as has been observed in the field and laboratory, e.g. Shaw *et al.*, 2010). A further modification to the reproduction model is that brood size is a function of female size and her recent feeding history. Feinberg *et al.* (2007) reported a linear relationship between *E. pacifica* female total length and brood size, which was used here to set the base brood size expected for each female once it reached reproductive size (Equation 11, Table 4.2). The linear relationship between female length and brood size, while significant, did not explain very much of the variability in brood sizes (Feinberg *et al*., 2007), and the authors suggested that recent feeding history might be an important factor both at the individual level and in determining the intensity of spawning for the population at an event scale (Feinberg *et al.* 2003). Thus, the base brood size was modified using a logarithmic function of the female's integrated food consumption over the previous interbrood period (ranging from a minimum of 0.5 for recent low consumption to a maximum of 1.3 for recent high consumption: Equation 12, Table 4.2). When the female accumulated enough reproductive material to support the expected brood size, that number of eggs was released, provided she was within 45m of the surface. If 10 days passed with the female accumulating less than 2.5% of the expected brood size, she was considered unfit to reproduce and all stored reproductive weight was converted into somatic weight and a new expected brood size was recalculated on the next time step. If >22 days elapsed since the expected brood size was calculated and eggs had not been released (but at least 2.5% of the expected brood size was accumulated), half of the stored reproductive weight was released as eggs, half was put toward body weight, and a new expected brood size was calculated in the next time step.

Behaviors

Diel-vertical migration (DVM) was implemented as a stage-dependent behavior based on day length and preferred depth according to distributions documented using vertically-stratified MOCNESS nets off Oregon (Keister *et al.* 2001). Krill occupied surface waters (10m +/- a random depth offset to introduce individual and daily variability) during darkness, otherwise they remained at their preferred daytime depth (Table 4.4) or 5m above the ocean floor, whichever was shallower. Adult preferred daytime depth in the model is 350m, which is deeper than the MOCNESS samples used to inform these depths. This depth was chosen to capture the ability of adult *E. pacifica* to migrate far deeper than the 200m lower bound of MOCNESS samples, as deep as 600m, according to Brinton (1967). Early larval stages (nauplius I, nauplius II, and metanauplius) use their antennae to swim weakly upward at a rate of 37.4 m d^{-1} (=0.4 mm s^{-1}). This is fast enough to allow larvae hatching from sinking eggs to reach the surface mixed layer by the time they develop to calyptopis I, which is consistent with the vertical distributions of this stage from MOCNESS samples off Oregon (Keister *et al.* 2001) and in the Western Pacific (Liu and Sun 2010). Egg sinking is implemented as described in Chapter 3.

Starvation

A generous starvation mortality scheme was employed (after the simulations were run) to kill off extremely small or slow growing individuals. No starvation occurred until the second calyptopis stage, after which any individual in stage *i* that did not achieve the mean individual body weight of the prior stage *i*-1 was considered to have starved and was removed from the population. Juveniles also needed to maintain a higher weight than at the midpoint through the previous stage, but also needed to exceed 20μgC. An

individual that made it to the juvenile stage would die from starvation if its weight fell below 50% of the maximum weight attained at any point in the past. No other mortality (predation or natural) was implemented here.

Particle Tracking

Details of the particle tracking model were discussed in Chapter 3. For the simulations of this chapter, vertical diffusion was not considered, so a longer time step of 3600 seconds (1 hour) was used. Empirical tests indicated that hourly time steps provided accurate transport trajectories when using daily averaged ROMS fields and a 4^{th} order Runge-Kutta integration of 3-dimensional velocity fields. Reflection routines were used near surface, bottom and land boundaries to prevent particles from non-physical exits from the ocean domain. Particles that encountered the open ocean boundaries had their "grounded" status changed to true so that they would not be tracked beyond the first open boundary encounter (i.e. they could not return to the domain later with a current reversal).

Simulations

The bioenergetics model was forced by temporally and spatially static food and temperature fields from day 200 from year 2001. That field had strong food gradients (in all four food types) spatially and a broad range of food concentrations. Five thousand krill eggs were randomly positioned 5 – 45m depth in the region defined by the 45m isobath to 80km offshore of the 45m isobath, and from Cape Blanco (42.8°N) to 47.5°N. For 250 days, each individual grew and developed in its *x*, *y* location; no advection was allowed in the *x* or *y* directions. Motion in the *z* direction was allowed; eggs sank, early larval stages swam weakly upward, and once individuals had developed into older stages capable of migration, they were allowed to migrate vertically according to day length and stage.

To explore the potential for self-seeding and retention, 5,000 identical krill were released from the same locations described for the IBM simulations at the beginning of June, August, and September 2000 and 2001. Each individual was tracked for 250 days, which was enough time to develop from egg to reproductive adult and release eggs. Three behaviors were considered to explore the effect of DVM on retention within the region and potential self-seeding: (1) passive krill, (2) sinking eggs that developed into older stages having stage-specific patterns of diel-vertical migration, and (3) adult krill already fully capable of diel-vertical migrations to their preferred depth of 350m. The passive krill serve as the null model for comparison to the simulations that have DVM behavior on dispersal, while the two simulation types with DVM behavior show the difference between following a cohort (1) from sinking egg to juvenile versus (2) the duration of its adulthood.

4.3 Results

Part 1. Bioenergetics model

A goal of this chapter was to estimate *Euphausia pacifica* juvenile stage duration for the range of food and temperature conditions that might be found along the Oregon and southern Washington coasts and extending offshore 80km of the 45m isobath. This region includes transect line that was sampled several times a month by researchers interested in learning the mean growth rate of juveniles and adults in the local *Euphausia pacifica* population.

Static Ocean Laboratory

The biomass concentrations of surface diatom, mesozooplankton, microzooplankton, nanophytoplankton, and sea-surface temperature are

shown in Figures 4.3-4.7. Diatom concentration, the most important prey item controlling for krill growth in this model, ranged from 0 to above 16 mmolN m^{-3}, and is most concentrated very close to the coast. Mesozooplankton, with a max of ~1 mmolN m^{-3}, is highest in concentration just offshore of the maximum concentration of diatoms. Microzooplankton distribution roughly overlaps that of the mesozooplankton but with maximum concentration (up to 0.85 mmolN m^{-3}) north of the maximal mesozooplankton concentration. Nanophytoplankton are scarce with the main distribution offshore of the maximum diatom regions and providing less than 0.3 mmolN m^{-3} of food to krill in most of the seeding region. Sea-surface temperature near the coast is as low as ~8°C and warms up to more than 12°C in the offshore portion of the seeding region.

Larval development rates

Figure 4.8 shows development times required for newly spawned eggs to advance to all of the larval krill stages from laboratory rearing experiments. Days to attain larval stages metanauplius through juvenile determined from temperature histories in the static ocean environment are presented in Figure 4.9. Mean development time from egg laying to juvenile stage for krill that retained at least 20 μgC was 62.1 ± 3.9 days (range: 53.5 to 75.25 days; data not included in Figure 4.9 so earlier larval data is easier to see). These static environment model-based development rates compare favorably with published data (same figure: median days to stage at 10.5°C from Feinberg *et al*. 2006; median days to stage at 8°C and 12°C from Ross 1981). Mean average temperature (the mean of each individual's trajectory average) experienced by all individuals was 9.0 ± 0.59°C (range of 7.4 – 10.3°C), within the range of published laboratory temperature conditions used to estimate development rates. Mean development time in the model

was slower for the earlier stages (metanauplius through the first furcilia stage) than the lowest published median time, but were within the range of published estimates by the second furcilia stage. The range of days to stage increases with each stage, reflecting the integrated differences in temperature histories among the individuals in the model. At the end of the 250-day model run, 2717 of the 2915 surviving individuals were adults and 198 were juveniles.

Juvenile and adult growth rate

Growth rate is a measure of food attained in excess of an organism's reproductive and metabolic needs. In this model, active and basal respiration were assumed to be the only loss of body carbon after assimilation (though see Ross 1982*a* for estimates of carbon loss during molts). For adult female krill, the additional carbon needed to produce eggs was taken from assimilated food, not from accumulated positive growth. However, both respiration and reproduction must be accounted for in the ingestion rate required to maintain weight. Minimum ingestion rates required to maintain various body masses of juveniles (no reproductive losses) and adults at temperatures spanning 6 to 16°C are shown in Figures 4.10 and 4.11, respectively. Because the krill in this model eat only at night when near the surface, these ingestion rates would need to be roughly doubled during the period the krill is eating to attain sufficient food for weight maintenance.

Mean growth rate for juveniles and adults that survived to the end of the 250d simulation (59% of total particles) was 0.06 ± 0.009mm d^{-1}, or a weight-specific growth rate of 0.02 ± 0.001 d^{-1}. Considering adults only, the mean growth rate was 0.04 ± 0.01 mm d^{-1}, or a weight-specific growth rate of 0.008 ± 0.002 d^{-1}. At the end of the 250-day simulation, surviving individuals had weights from 342 μgC to 4579 μgC, with a mean adult weight of 2460 ±

773 μgC. Weight-specific mean growth rate of the surviving individuals is plotted in Figure 4.12. The allometric growth rate determined by Ross (1982*a,b*) is plotted also for comparison. When the mean individual weight is below about 1500 μgC, growth rate is higher than that predicted by Ross, but is much closer to the rates of Ross for larger individuals.

Mean juvenile stage duration, the period of time between molting into the juvenile stage and becoming large enough to reproduce, was 110.8d ± 30.8d, with a minimum of 78d (Figure 4.13). 41% of the initial eggs failed to survive the simulation and an additional 198 (7% of survivors) were juveniles that had not reached reproductive weight within the 250 days.

Interbrood period (the interval between the release of two successive broods of eggs by a female) ranged from 2 to 7.8 d, with a mean of 5.9 d (Figure 4.14). Brood size had a wide range, from 4 to 128 eggs brood^{-1}, with a mean of 61.35±24.2 eggs brood^{-1} for all females (Figure 4.15). Minimum days from egg to reproductive size (which is not identical to days to first reproduction, as adults needed to amass reproductive stores after reaching this weight) was 140.3 days, with a mean of 168.8d ± 19.3d (Figure 4.16). Total number of eggs released by individuals during the simulation was often <800 eggs female^{-1}, but in a few hot spots exceeded 1600 eggs female^{-1} (Figure 4.17).

Part 2. Particle Tracking Simulations

To assess whether *Euphausia pacifica* are able to sustain populations in the dynamic Northern California Current without relying on continuous or frequent influx of *E. pacifica* from other regions (we term this self seeding) we conducted a series of 250-day simulations using 5,000 initial krill. For each release date, three types of krill were considered: those with no

behavior (passive), eggs that developed into diel-vertically migrating larvae (larvae+DVM), and diel-vertically migrating adults (Ad+DVM). The proportion of particles within the seeding region each day was recorded (Figures 4.18 and 4.19) and movies of particle movements and locations were made to clarify the dynamics (snapshots are shown from every 30 days in Figures 4.20 through 4.37).

Up to 20% of the original seeded population was represented in the seeding region at the end of the simulations. Passively transported krill had the least retention, and adults with fully-expressed DVM had the highest retention. Initially, however, the best-retained krill were from the larvae+DVM simulation, at first leaving the seeding region more slowly than either Ad+DVM or passive krill, but then leaving at a higher rate within the first ~25 days.

June and August simulations in both years feature swift shallow offshore transport through the western boundary as well as swift transport through the southern boundary in a narrow band along the coast. September simulations in both years are characterized by comparatively sluggish alongshore coastal transport and many large persistent eddies (particularly evident in 2000). These eddies aid in the retention of krill within the seeding region for a longer period than observed in other simulations. In addition, the krill are present in the seeding region closer to the time of the fall transition, when transport is less consistently offshore. This is true for all three behaviors but retention is highest for the Ad+DVM behavior as the vertical migration inhibits their offshore transport.

Notable Features

Passive krill in the June 2000 simulation were advected at a nearly constant rate out of the seeding region. Larvae+DVM and Ad+DVM were

advected at slower rates, with a slight return to the region of both (increase in the number within the seeding region).

In the June 2000 larvae+DVM simulation, a small number of larvae along the coast and slope move southward through the southern boundary of the seeding region until day 5, but then return to the region due to flow associated with a small eddy. By day 11 the majority of the larvae had developed into calyptopis stages that remain near the sea surface (upper 10m) and are rapidly transported offshore in the surface Ekman layer over the next 20 days.

In the June 2001 larvae+DVM and Ad+DVM simulations, krill are advected back into the seeding region around day 155 from offshore and from the south near the coast by a two-week long slumping of water towards the coast. The same event sweeps both larvae and adults back into the region. Passive krill are similarly affected, however there are too few left in the simulation near the western boundary to see a signal of the same magnitude.

4.4 Discussion

Development

Development rates in the model compared favorably with rates measured under constant temperature and unlimited food conditions in the laboratory (Feinberg *et al*. 2006, Ross 1981). Mean development in the model was slower for the earlier stages (metanauplius through the first furcilia stage) than the lowest published median rates, but by the second furcilia stage were within published estimates. The variation among individuals in the time to achieve a specific life-stage transition was greater for older life stages than younger life stages, reflecting the integrated differences in temperature histories among the individuals in the model.

Though the mean of the trajectory average temperature was higher (9°C) than the lowest published laboratory conditions (8°C), the temperature history of an individual is very dynamic, changing throughout the day with diel migration and throughout the individual's life, with ontogenetic shifts in daytime depth. All trajectories start with eggs in the upper 45 m that sink into the deepest, coldest waters (~ 5°C for some individuals) experienced along their histories before ascending to the surface by the first calyptopis stage and beginning vertical migrations. (An example temperature history for a single krill is shown in Figure 4.39.) The cold environment at the beginning of each individual's history explains why development is slower in the early life stages in the model than those observed in the lab at constant conditions. Both Ross (1981) and Feinberg *et al.* (2006) found substantial variability in individual development rates, even within cohorts, and even under constant temperature conditions. The variability reported in both studies increased as animals progressed through the life stages, and small differences in developmental rates summed up over many days. By the time krill molt into juveniles, the individual variability in development rate is apparent, reflecting the integrated differences in temperature histories among all individuals in the model, though the individuals are themselves modeled identically (i.e. without additional fitness factors that vary from individual to individual).

Growth

Because the model did not depend on surpassing weight thresholds for development, weight is not necessarily related to stage, but reflects instead how well an individual is growing when it is time to molt according to the temperature-dependent development rate, and is therefore a reflection of food resources (since development depends only on

temperature). The low weights at stage for larvae in the simulations are not consistent with published length and weight ranges for early larval stages (Boden 1950, Ross 1979, Suh 1993) and unpublished weights of furcilia collected off Oregon (a mean of 7 μgC for furcilia I up to a mean of 72 μgC for furcilia VII, L. Feinberg unpublished), and reflect a growth that is outpaced by development. Because the food fields did not vary with time for this IBM simulation, it is clear that, at least in some locations, there is sustained sufficient food in the model for growth; therefore mismatch indicates that the allometric formulation used here may need to be adjusted for early larval growth.

Nevertheless, juvenile and adult growth of the survivors were well within the bounds of published measurements of growth from the field. Using the total length to dry weight ratio (Feinberg et al 2007), and assuming dry weight was 40% carbon, modeled growth rates in mm d^{-1} from the model could be compared directly with published estimates from length frequency analysis and direct experimental measurements of *E. pacifica* growth rates. Individual adult *E. pacifica* growth rates estimated from the instantaneous growth rate (IGR) method by Shaw *et al.* (2010) ranged from -0.05 to +0.08mm total length per day, with a seasonal pattern indicating a mean positive growth rate of 0.02mm d^{-1} during summer upwelling conditions and 0.011mm d^{-1} during winter downwelling. Field estimates of *E. pacifica* growth rates from cohort length analyses suggested growth estimates as high as 0.06 mm d^{-1} (Smiles and Pearcy 1971). More recent cohort analyses from the Oregon coast show long-term growth rates of 0.015 – 0.034 mm d^{-1} (L. Feinberg, T. Shaw, W. Peterson, and H. Bi, unpublished), which are close to the IGR results. The model's mean growth rate of 0.06 mm d^{-1} for juveniles and adults more closely resembles the rate estimated by Smiles and Pearcy

(1971) than the mean individual rate measured by IGR (Shaw *et al.* 2010), but the fact that adult growth rate (0.04mm total length per day) is less than juvenile growth rate agrees with the findings of the latter study. Also, Harvey et al. (2010) noted that field krill seemed to grow at about twice the rate of lab-reared krill, and Ross (1982*a*) also suggested a possible container effect in the growth estimates of laboratory-reared krill.

Beyond the Oregon upwelling zone, these modeled growth rates are intermediate between rates estimated from more northern populations (generally lower than modeled) and more southern populations (higher than modeled). The modeled growth rates for juveniles+adults are close to those measured for *E. pacifica* in the Gulf of Alaska, which ranged from 0.03 – 0.07mm d^{-1} for krill shorter than 16.3mm, and slightly higher than those for krill longer than 16.3mm (about 0 to 0.03mm d^{-1}; Pinchuk and Hopcroft 2007). Estimates of growth from cohorts off Southern California were as high as 0.1 to 0.12 mm d^{-1} for juveniles 5-8mm length (3-3.5 mm $month^{-1}$), though for larger juveniles, growth slowed to about 0.067mm d^{-1} (3mm in 1.5 months).

Weight-specific growth rates from the model, 0.02 d^{-1} for juveniles + adults, and 0.008 d^{-1} for adults only, were comparable to the average positive weight-specific growth rates reported by Shaw *et al.* (2010), 0.0135 and 0.0089 d^{-1} during upwelling and downwelling periods, respectively. (These rates ranged from -0.028 to 0.13 d^{-1} during upwelling and -0.031 and 0.03 d^{-1} during downwelling.) The growth rates of this model easily fit within this range and also exhibit similar patterns to the allometric growth rates estimated by Ross (1982a). The mean weight-specific growth rate of surviving individuals from the model was about double what Ross predicted for mean individuals smaller than 1500 μgC, but was similar to rates

reported by Ross for larger individuals. In Figure 4.12, the sudden declines in growth rate at ~1500 and again at ~2200μgC are artifacts of a change in day length; as the population grows, day length in the model is increasing and therefore krill are spending more time away from the surface and not eating. This is evident in the synchronized shift in slope of weight trajectories for all individuals, and sudden (but minor) change in all individuals' "hunger" value (not shown). A finer time step would make this transition less abrupt, but this behavior warrants additional consideration.

Modelled juvenile stage duration was as short as 78 days and perhaps longer than 210 days, with the shortest time to adulthood being 140.3 days. This is far shorter than the ~180-day estimates from survivorship curves based on multi-year sampling at the Oregon coast (T. Shaw, L. Feinberg, H. Bi, and W. Peterson, unpublished). Harvey *et al.* (2010), using biochemical aging, found that the youngest spawners collected from the field in July 2004 appeared to be only 3-4 months old. Assuming an average time to juvenile of ~60d (Feinberg et al 2006), the juvenile stage duration for these early spawners would be 30-60d, shorter than what was modeled here. It seems unlikely that spawners this young would be common, but it is important to note the extremely wide range of characteristics individual krill might express as a function of their environment and intrinsic variability. Comparing the juvenile stage duration map (Figure 4.13) to the surface diatom concentration (Figure 4.3) and the sea surface temperatures (Figure 4.7) of the static ocean fields, it is clear that the modeled individuals with the shortest juvenile stage duration were those that were the best fed and that experienced relatively warm temperatures. This results from several model nuances: (1) juvenile stage ends when the individual achieves 950μgC; (2) faster growth is a result of higher ingestion rates relative to respiration rates;

and (3) though both respiration and ingestion rates have a temperature dependence, their Q_{10} values differ (2.0 and 3.36, respectively; Ross 1982*a*). The result is greater positive growth at higher temperatures, as ingestion outpaces respiration when suitable food (diatoms) is abundant. In the field, the combination of high food and relatively warm water might occur during or immediately following an upwelling event leading to a diatom bloom – particularly at the leading edge of the upwelling front, where there would be a high concentration of chlorophyll and warmer waters than closer to shore, where the coldest waters were upwelled. One might expect to find the earliest spawners to have spent substantial time in regions of relatively warmer waters and rich food resources.

Particle Tracking

Some seasonal differences were evident in the particle tracking simulations. Notably, simulations started in September began with sluggish flow near the coast compared with the June and August starts. In addition, September featured more energetic and persistent mesoscale features, such as eddies, than the other months. A significant feature in June- and August-start simulations was a southward coastal jet, which often transported large numbers of krill (all behaviors) out of the seeding region within weeks. Transport along the shelf in this feature often peeled away from the coast as it followed the topography of Cape Blanco, transporting krill far offshore. This offshore meander of the coastal upwelling jet is commonly observed in the northern California Current System (e.g. Barth et al 2005). Away from the coast, surface waters moved offshore in large events that carried large numbers of krill from the seeding region. The early weeks of all runs featured upwelling filaments which carried large numbers of krill from the nearshore to the offshore region, with earlier dates having smaller filaments that

transported krill more directly westward and later simulations having filaments with large meanders that shed cyclonic eddies.

Eddies were an important feature in krill retention within the seeding region for all three behaviors. This was especially apparent in September runs, which began with krill being entrained in several eddies that persisted for weeks, effectively retaining krill within the seeding region despite offshore transport of the majority of krill outside of these eddies.

A strong coastal current from the south that switches on during late fall and early winter in all simulations acts as a return conduit near the coast for both larval and adult krill. Krill that are advected from offshore toward the coast south of the seeding region are then swiftly transported northward in a narrow band along the coastline. Passive krill did not enjoy such consistent returns to the region, as they were advected too far offshore early in the simulations to be returned to shelf regions.

One of the most striking differences between behaviors in the particle tracking simulations is the distribution of krill within the seeding region at the coast. Passive simulations ended with all krill being fairly uniformly dispersed, no greater concentration of krill near the coast than offshore. However, in all larvae+DVM and Ad+DVM simulations, krill are more concentrated near the coast than offshore even toward the end of the simulations.

Even with significant loss of krill from the seeding region, some krill are retained in the source region for 250 days, especially those that exhibit strong diel-vertical migration behavior. For cohort analysis assumptions to be met for a population of *Euphausia pacifica* off Oregon, the population should remain more or less in place at the location of repeated sampling. While that does not appear to be the case here, as the vast majority of the

krill are advected out of the seeding region, and the few that are retained in the seeding region are still very far offshore, there is evidence that some individuals are able to return to sites close to their origin through large-scale circulation and current reversals throughout the year.

Model considerations

The ROMS-NEMURO model used in these simulations generally did a good job of reproducing the temporal patterns in temperature (Figure 4.40) and *u*- and *v*-velocities (Figures 4.41 and 4.42) on the shelf, though temperatures were often slightly lower in the model than observations recorded by a mooring at NH10. However, food fields in the model were not sufficiently realistic for the long simulations needed to show the full development of krill egg to reproductive adult. Though the model represented well some temporal patterns in some places, producing peaks in surface chlorophyll at roughly the same time as peaks in chlorophyll were observed by the Sea-viewing Wide Field-of-view Scanner (SeaWiFS), it nearly always underestimated the concentration (Figure 4.43). In both locations shown, the mismatch between RN and SeaWiFS chlorophyll is greatest in June, August, and September/October, when it is at or near 0 mg Chl m^{-3} in the RN, but ranges up to 12 mg Chl m^{-3} in observations. With more realistic food fields, the IBM presented here would be a useful tool for estimating how important retention near the coast is for a population, as stronger statements about survival nearshore versus offshore could be made.

4.5 Conclusions

We demonstrated that an individual-based bioenergetic model of North Pacific krill, *Euphausia pacifica*, is capable of producing realistic juvenile and adult growth trajectories and reproduction when food resources

are sufficient and temperature is realistic. Furthermore, the impact of food resources and abiotic influences such as temperature are sufficient to introduce substantial variability among individual krill in a dynamic region such as the Northern California Current.

A goal of this chapter was to estimate the duration of the juvenile stage of *E. pacifica* before they become capable of reproduction for a range of food concentrations and temperatures that might occur along the Oregon and southern Washington coasts and extending offshore 80km beyond the 45m isobath. The model showed juvenile stage durations varied from very short (order of two months) to much longer (order of six months or more), even though individuals in the model did not have intrinsic differences in fitness, and were seeded in a relatively small region.

Another goal of the modeling was to explore the potential for self-seeding and resampling of a population of *E. pacifica* in the northern California Current. If the shortest juvenile stage estimated by the bioenergetics model (78 days) is applied to the particle tracking results, it would seem that there is some potential for self-seeding by a population in the region of study, as krill with behavior were either still present in the seeding region or had been re-circulated back into it (often along the coast) at 140 days through 250 days after simulations began, when they might be reproductively capable. These results provide the most optimistic potential retentions and self-seeding, because in these simulations there was no mortality applied to advecting krill, except that krill that encountered the model edges (mostly the southern or offshore border) were considered lost to the population. Moreover, during the particle tracking simulations, growth was not simulated, and many of the krill were transported far offshore where diatoms were not abundant and foraging conditions for krill

less suitable. It is unclear whether krill transported to food-poor and warmer regions offshore would be able to survive in the real ocean; they surely would decline in weight, develop physiological stress and be more vulnerable to predation-based mortality, which was not implemented here. Even if they survived the offshore period and returned to favorable conditions nearshore, the reduced individual body mass would require substantial time to recover if high food conditions were encountered before maturation and reproduction could occur.

Results from the particle tracking of individuals suggest that cohort analysis of adult krill could be useful for estimating in situ growth at certain times of the year, such as in the fall, for short durations, which might not have been expected in a highly advective eastern boundary current upwelling system like that of the Northern California Current. This would be the case because larger life stages of krill are able to express behaviors, such as diel and ontogenetic vertical migration, that were shown here to reduce alongshore transports and advective losses to offshore regions. Since much of the cohort sampling and analysis currently being done out of Newport, Oregon includes juveniles and adults, these conditions are generally met. But if the duration of a cohort analysis extends beyond a few months, or if the samples are collected outside of the fall season when transport out of the region was slowest, the assumption of a population being resampled is not likely to be met. Caution should be exercised, too, in attempting to follow a cohort from egg (or early nauplius) to adulthood in the field, as particle tracking simulations show that the younger, more surface-resident life stages have far lower regional retention than older stages.

Finally, it is interesting that, while fully-expressed DVM (i.e. that of the adults-only simulation) was able to retain a portion of the population in the

region for slightly longer than other simulations, it was still not enough to retain the full (or even half of the) population for the full simulation. This suggests that DVM alone is not sufficient for long term nearshore retention of a population of euphausiids without supplementation from outside the region, whether the loss is offshore or alongshore. The "outside" supplementation of euphausiids (mostly from the north) into an area of repeated sampling must be considered when interpreting results of cohort analyses. For the resulting growth rate estimates to be accurate for the region, that rate must apply roughly uniformly to the much broader area from which the outsiders come to join the population of interest. If a coherent growth rate in the region and points north is not the case, growth rates estimated by this method are likely to be underestimated (if growth of the northern euphausiids is slower, as is often assumed, or reproduction in the north is later). Furthermore, interannual variability of growth rates estimated in this manner may reveal more about the scale of krill transport from year to year than biologically-mediated differences in growth between years.

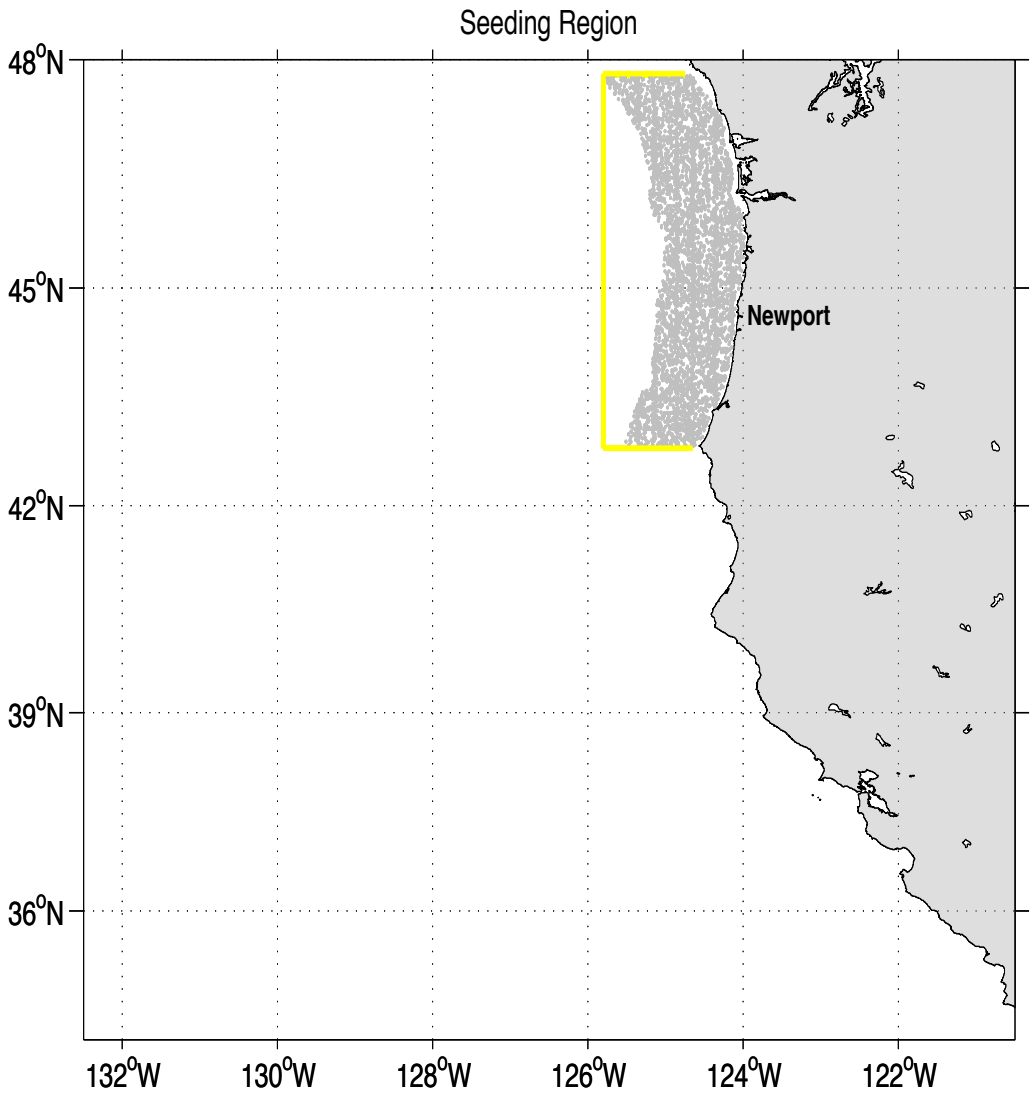

Figure 4.1. Simulation seeding region and initial krill locations. The subset domain of the ROMS model is shown above. Grey markers indicate positions of all 5,000 individuals in the IBM and from which they were released for each particle tracking simulation. The yellow box is the seeding region inside which krill are deemed "retained," or in which they would self-seed.

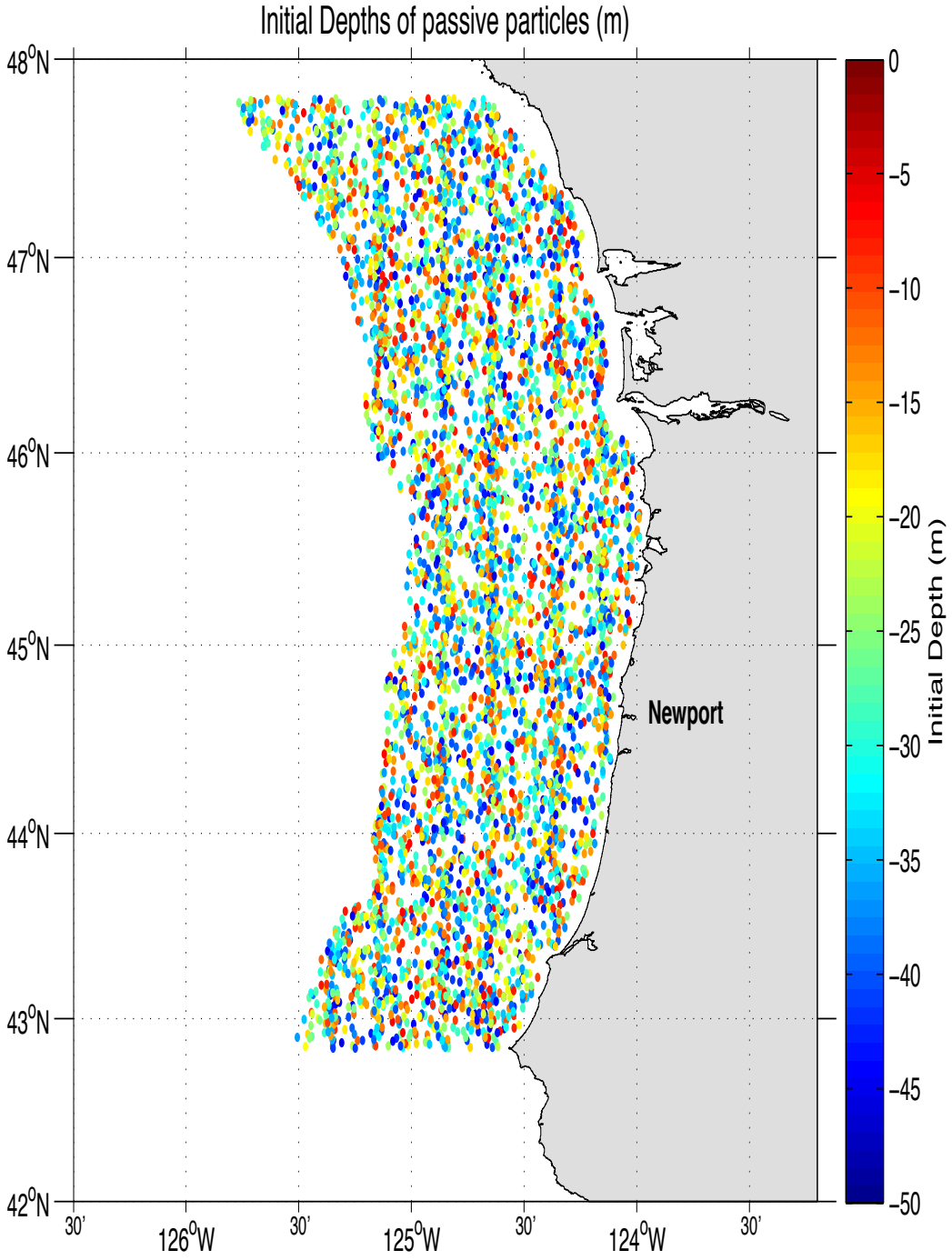

Figure 4.2. Initial particle depths for all simulations.

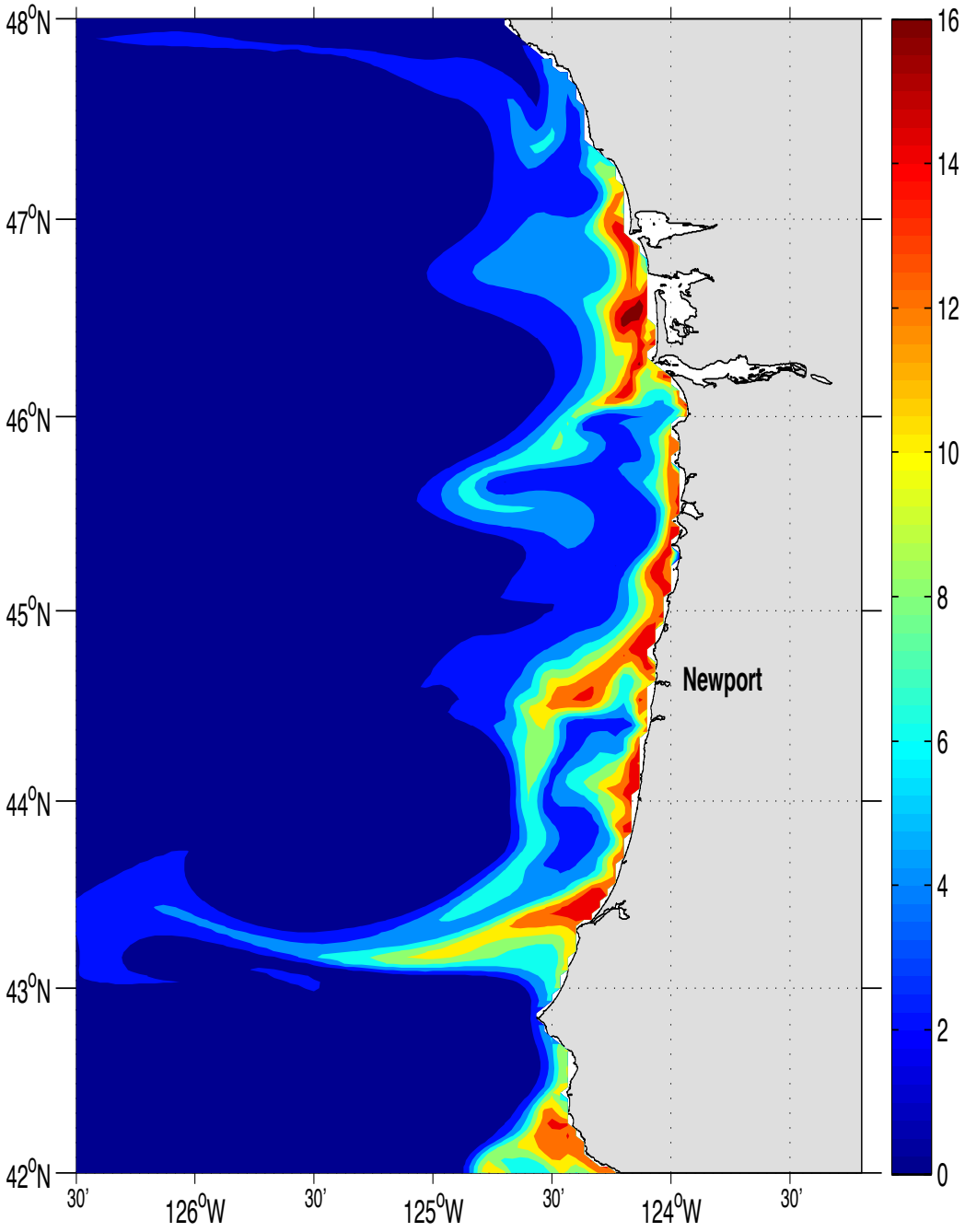

Figure 4.3. Surface Diatom Concentration (mmolN m^{-3}).

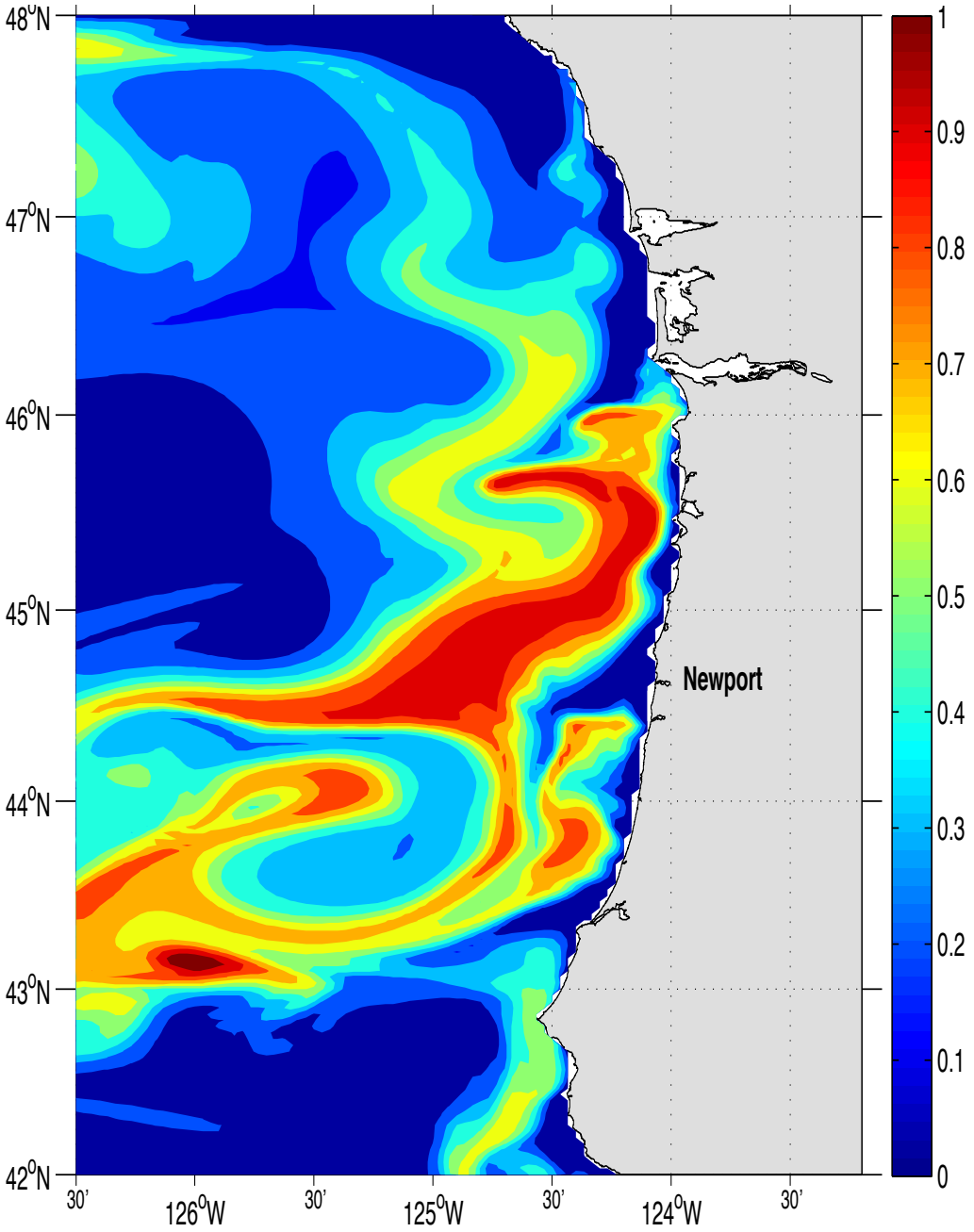

Figure 4.4. Surface Mesozooplankton Concentration (mmolN m^{-3}).

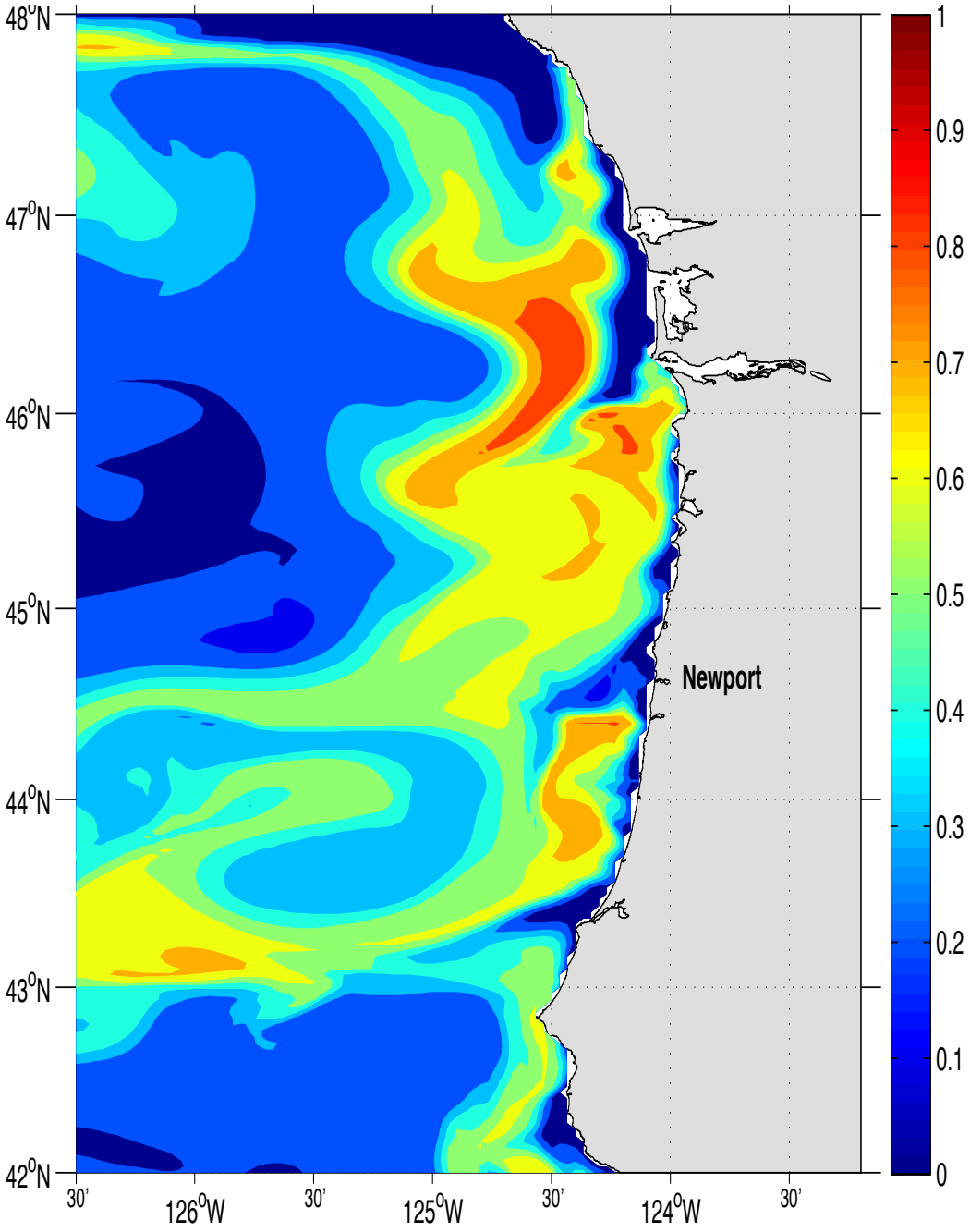

Figure 4.5. Surface Microzooplankton Concentration (mmolN m^{-3}).

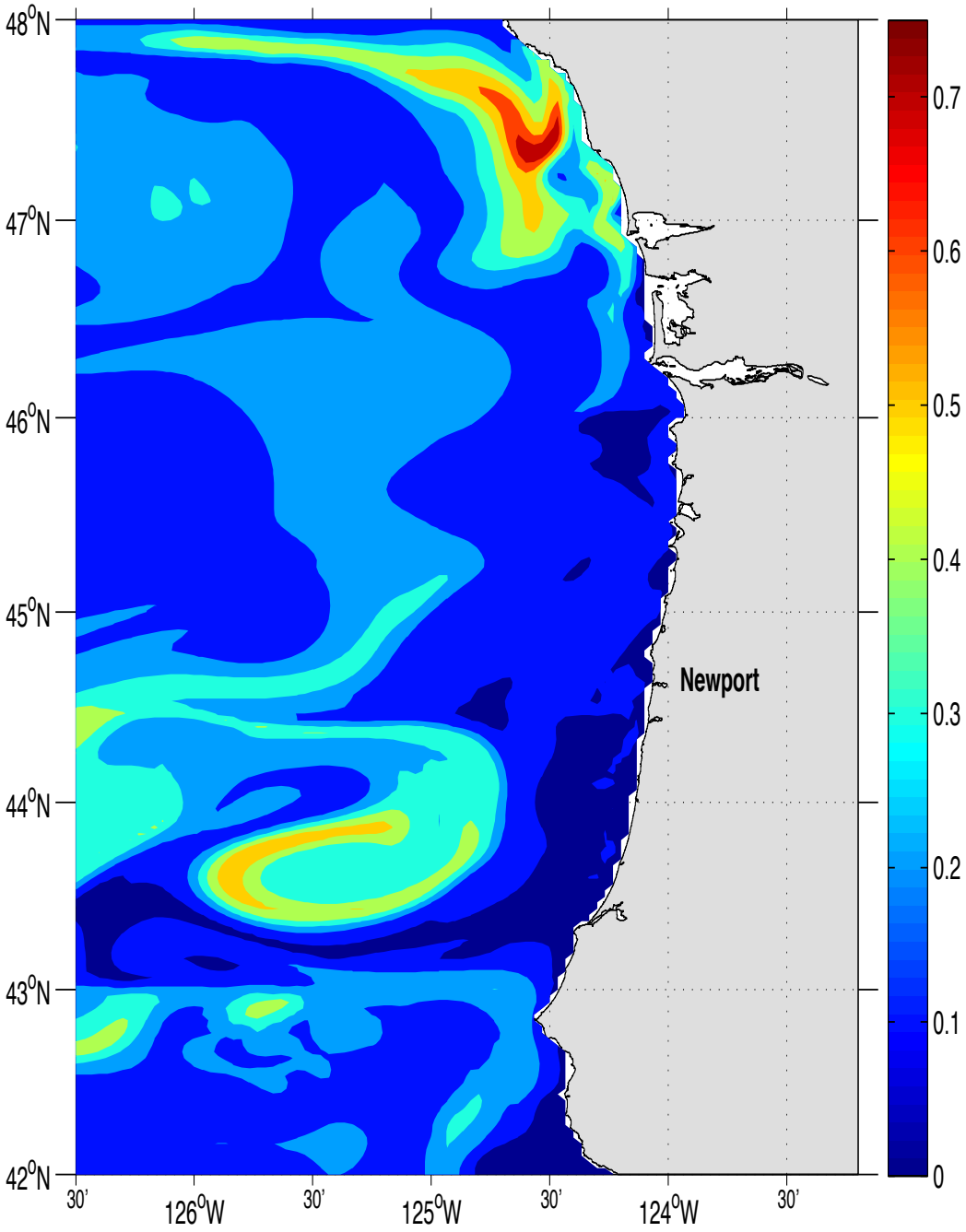

Figure 4.6. Surface Nanophytoplankton Concentration (mmolN m^{-3}).

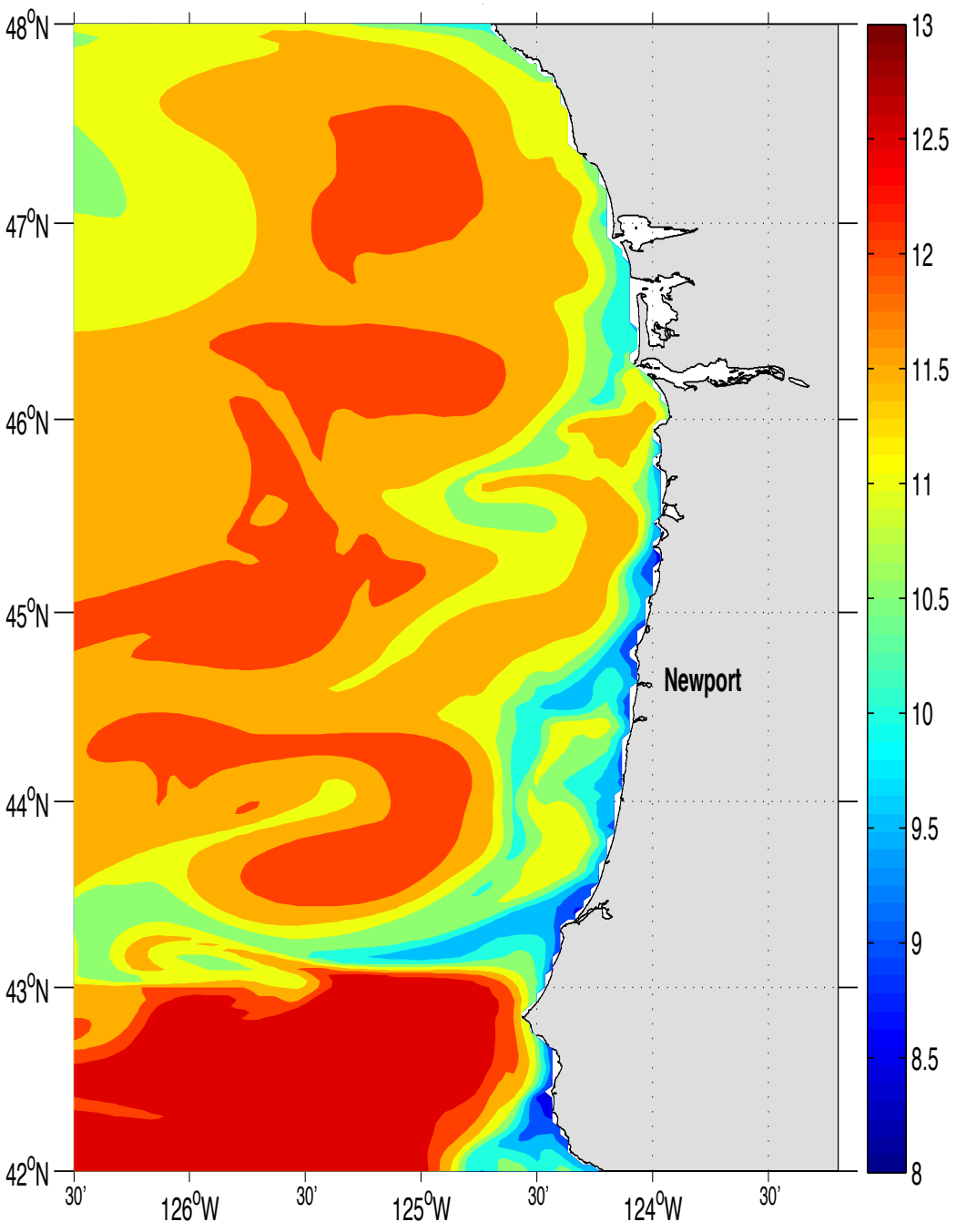

Figure 4.7. Sea Surface Temperature (°C).

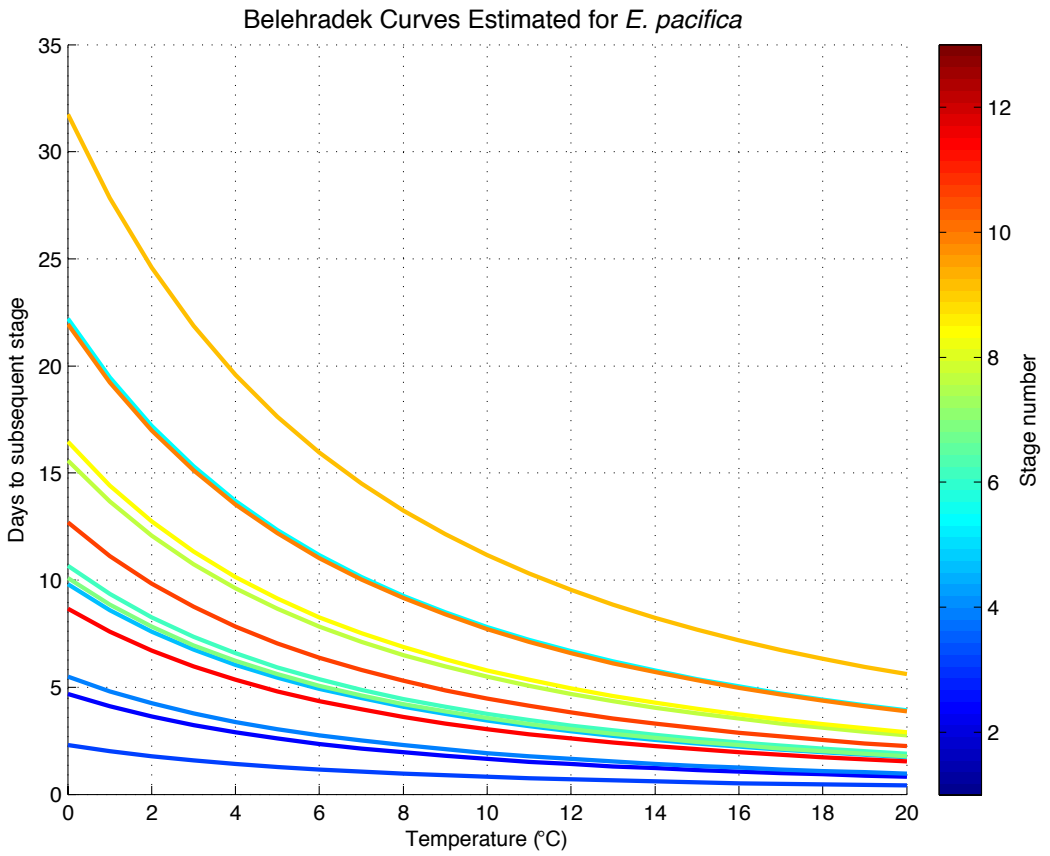

Figure 4.8. Belehrádek curves estimated for *E. pacifica.*

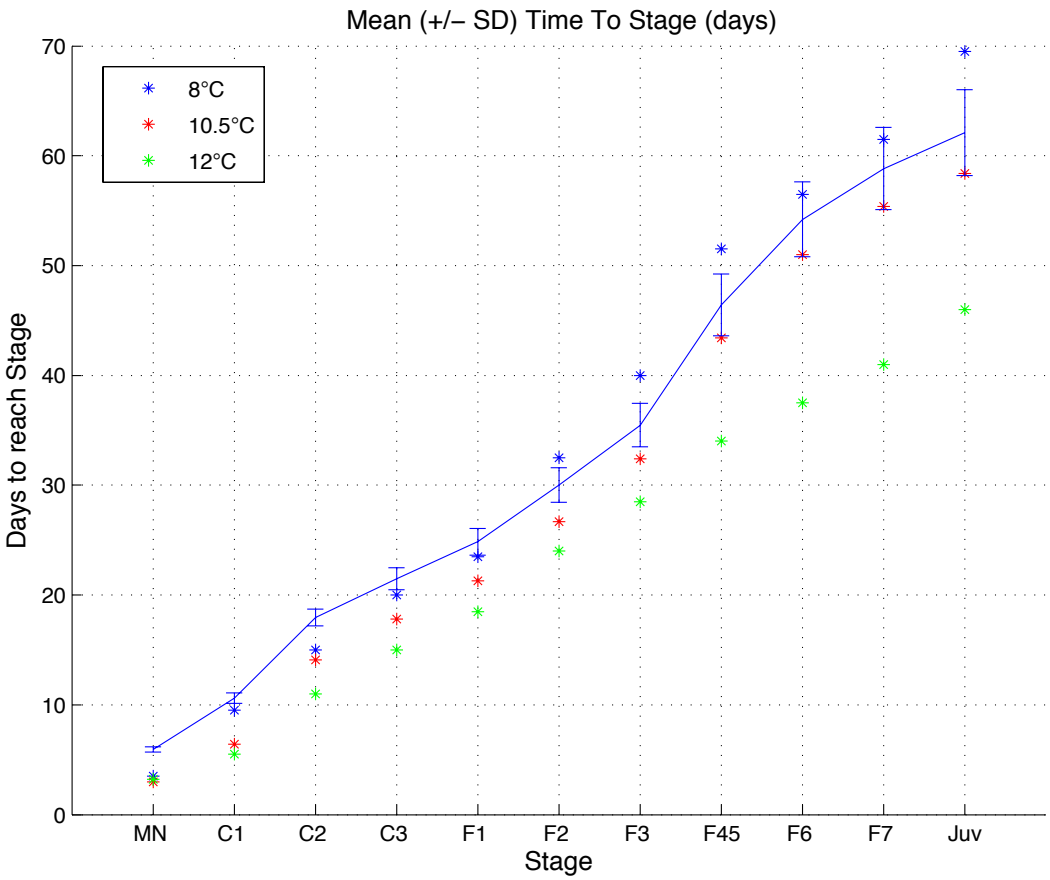

Figure 4.9. Mean (+/- SD) Time to Stage (days). Blue line and standard deviation bars show modeled days to each life stage from egg. Stars mark mean days to stage reported for laboratory-reared *E. pacifica* at 8, 10.5, and 12°C (blue, red, and green, respectively), as discussed in the text.

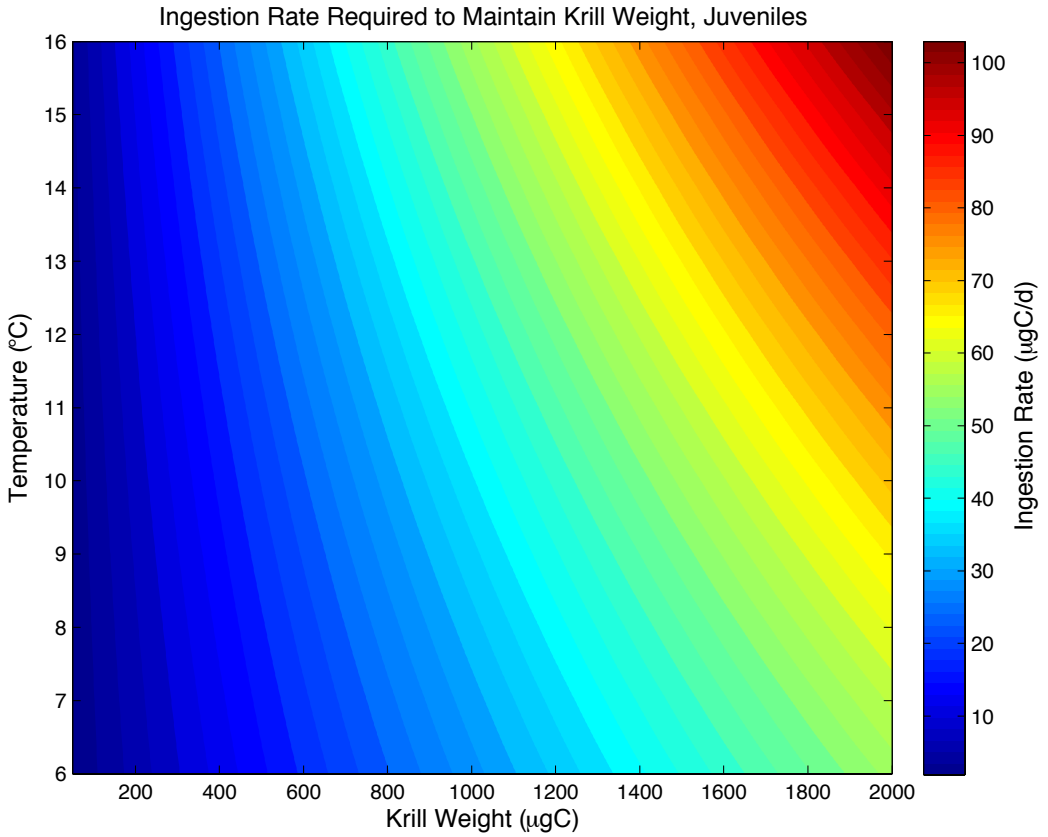

Figure 4.10. Ingestion rate required to maintain krill weight, juveniles.

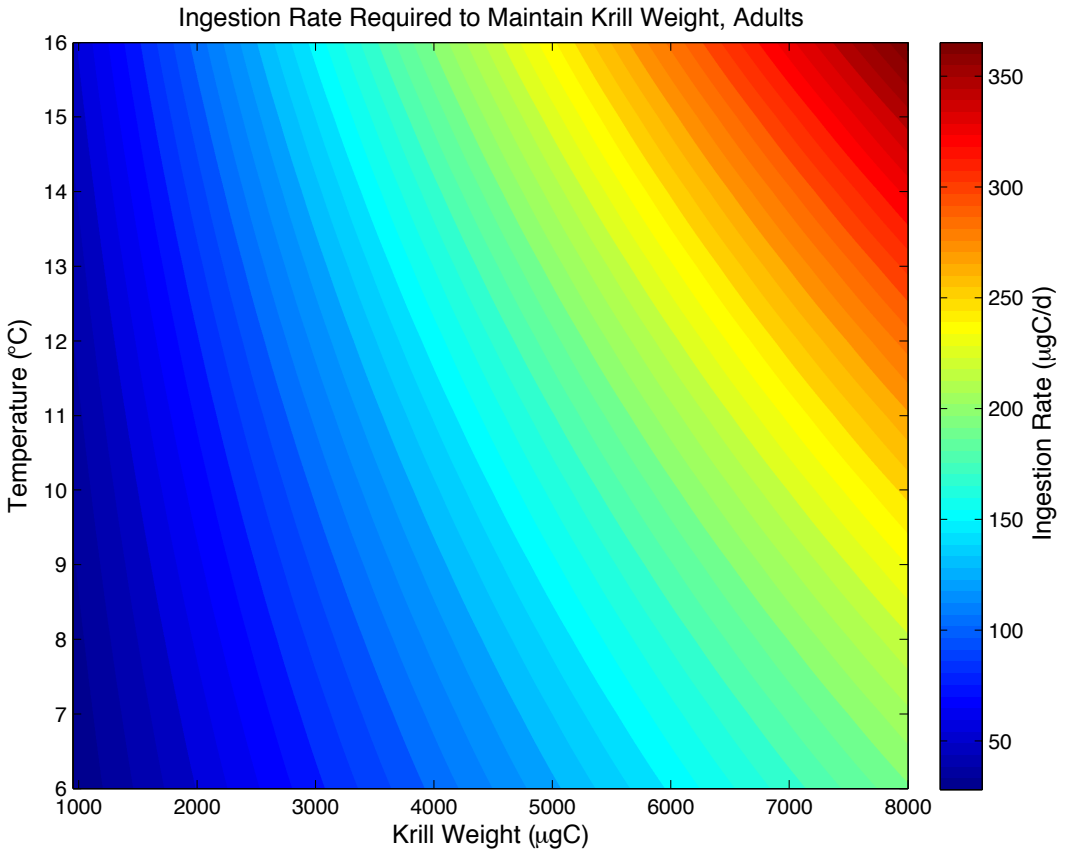

Figure 4.11. Ingestion rate required to maintain krill weight, adults.

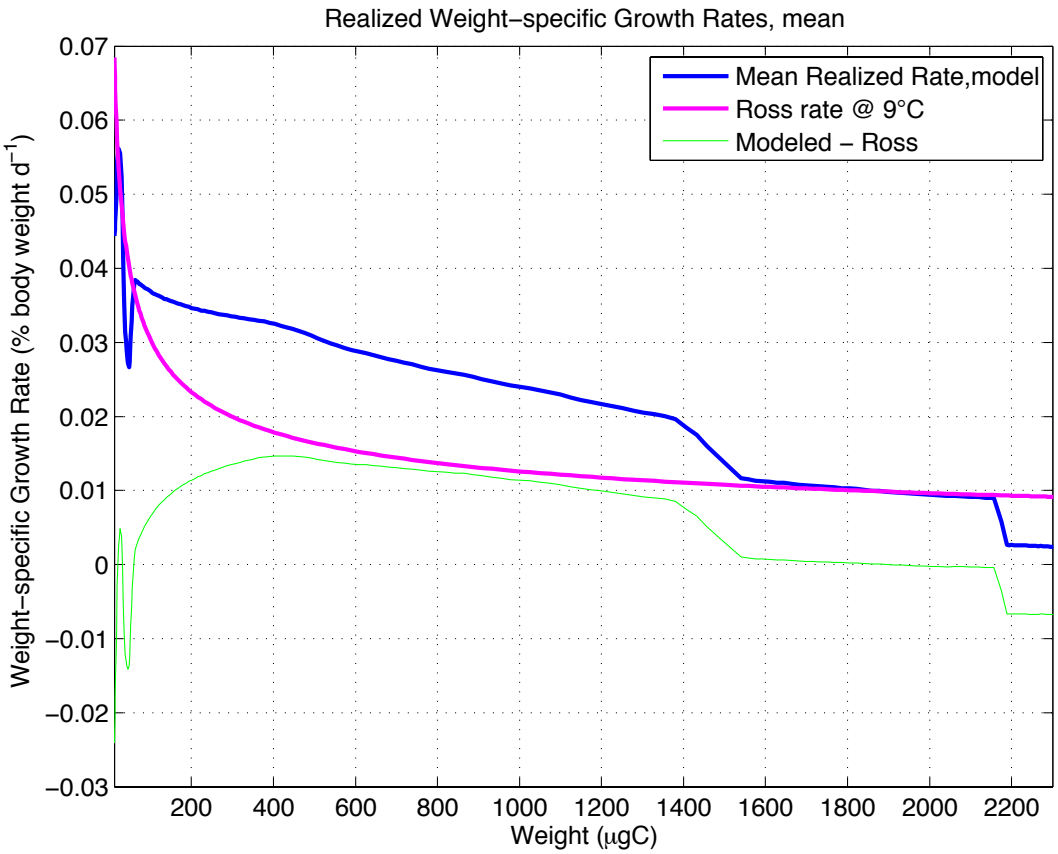

Figure 4.12. Realized weight-specific growth rates, surviving population mean. Surviving population mean weight-specific growth rate plotted (blue) plotted with weight-specific growth rate calculated from Ross (1982*a*) for constant laboratory conditions at 9°C (magenta). The green line shows the difference between the two.

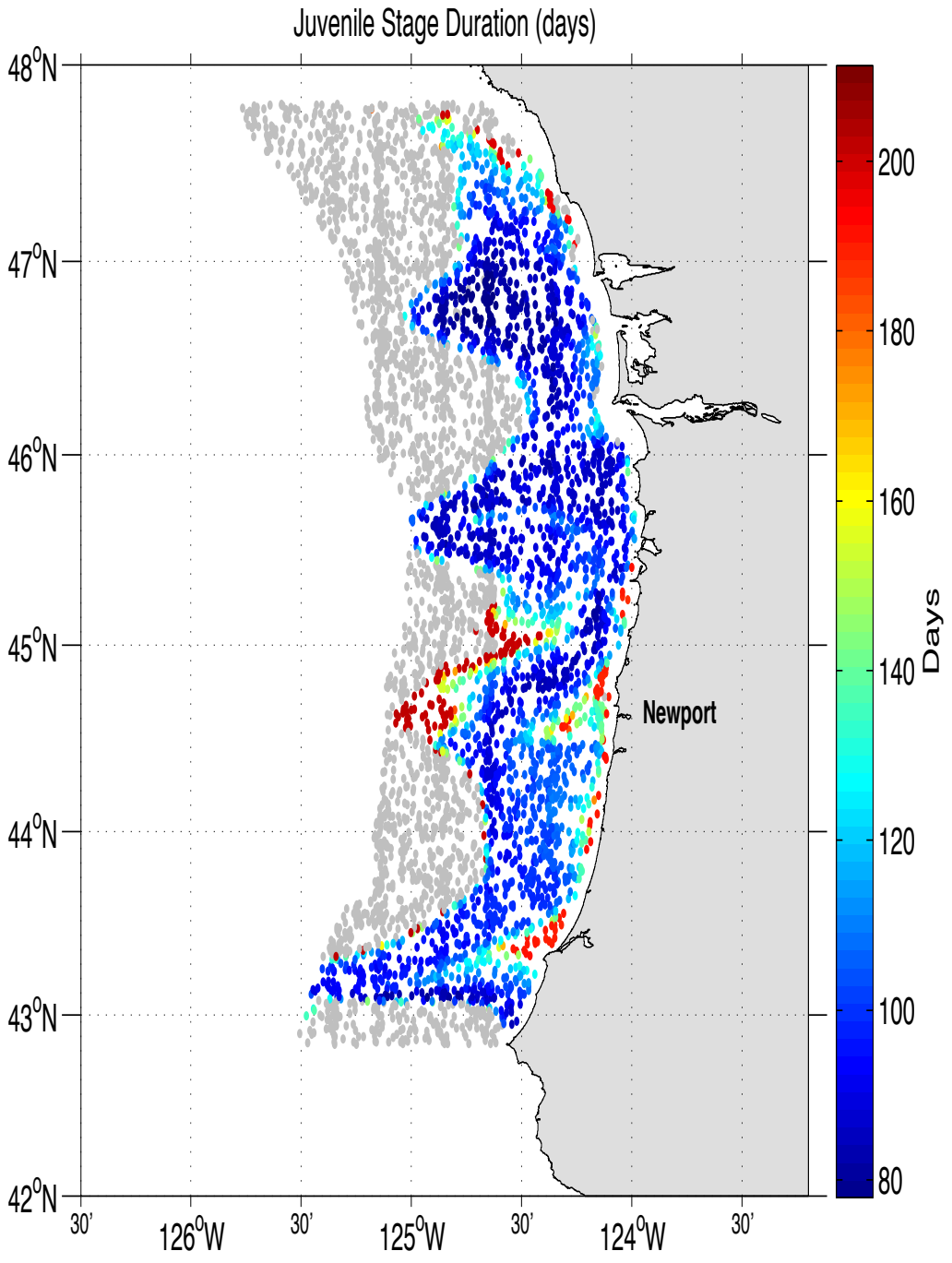

Figure 4.13. Juvenile stage duration (days). Grey markers denote krill that did not survive to juvenile stage.

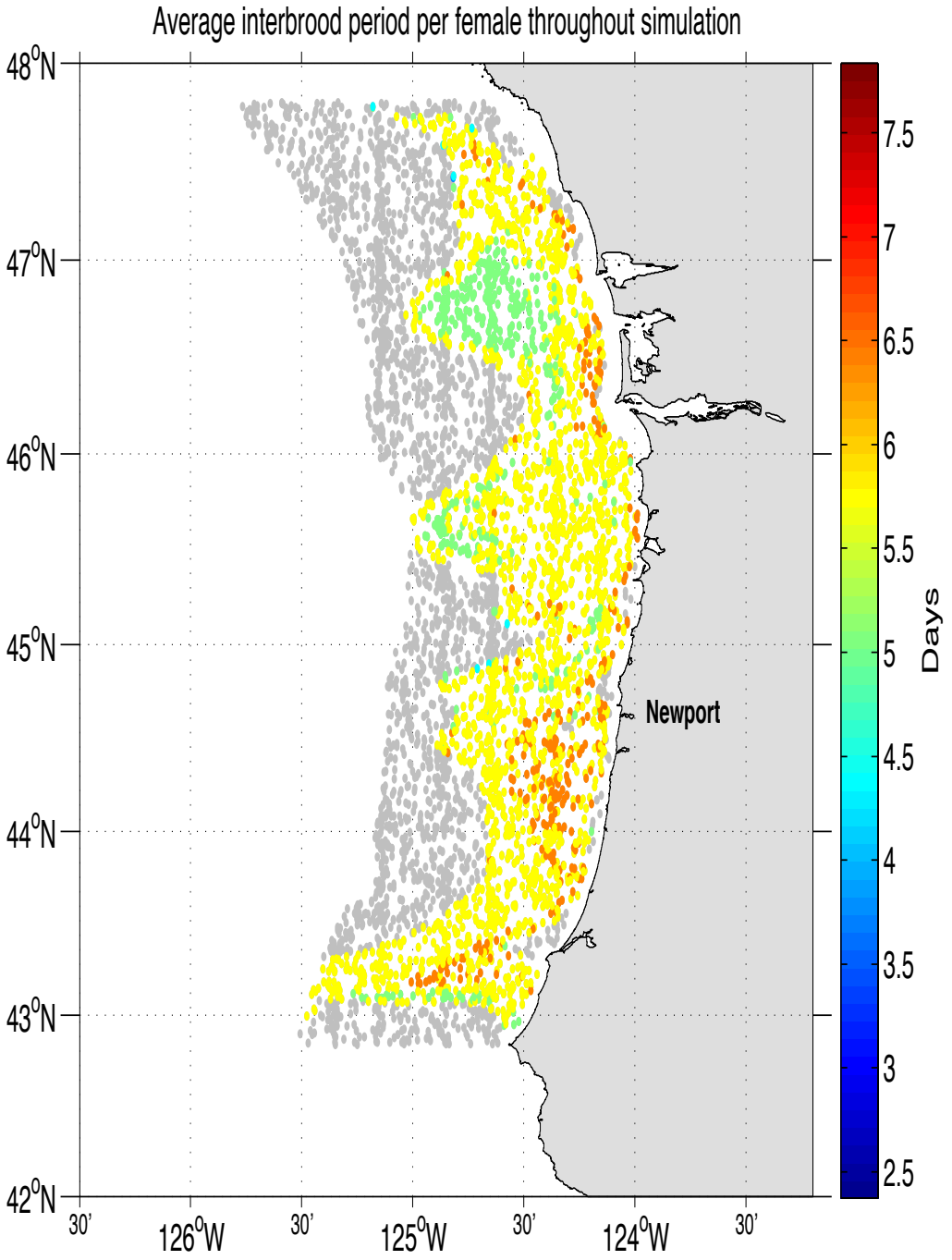

Figure 4.14. Average interbrood period per female throughout simulation. Grey markers denote krill that did not survive to reproduce, or that did not produce more than one brood (and therefore had no interbrood period).

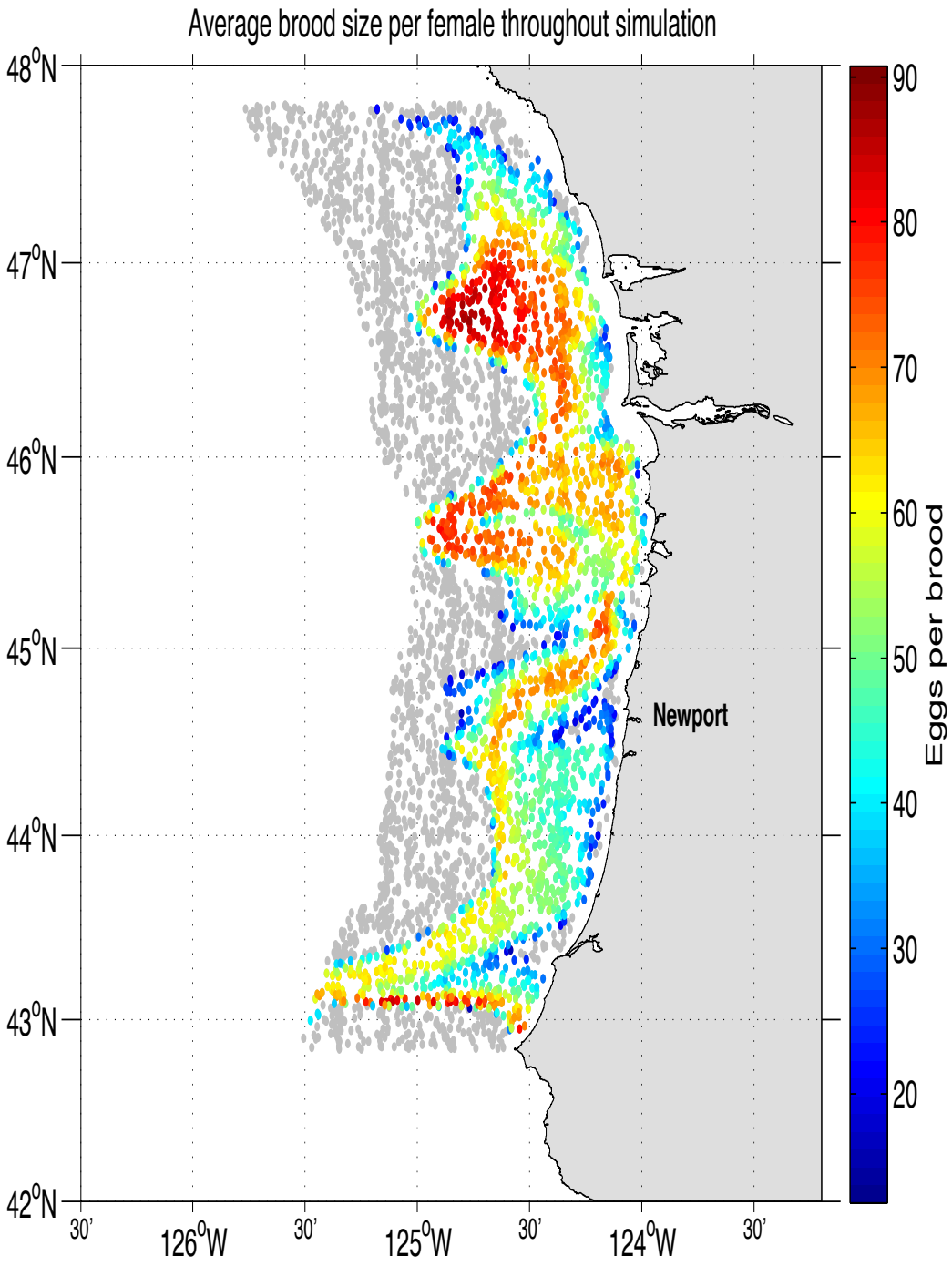

Figure 4.15. Average brood size per female throughout simulation. Grey markers denote krill that did not survive to adulthood or never reproduced.

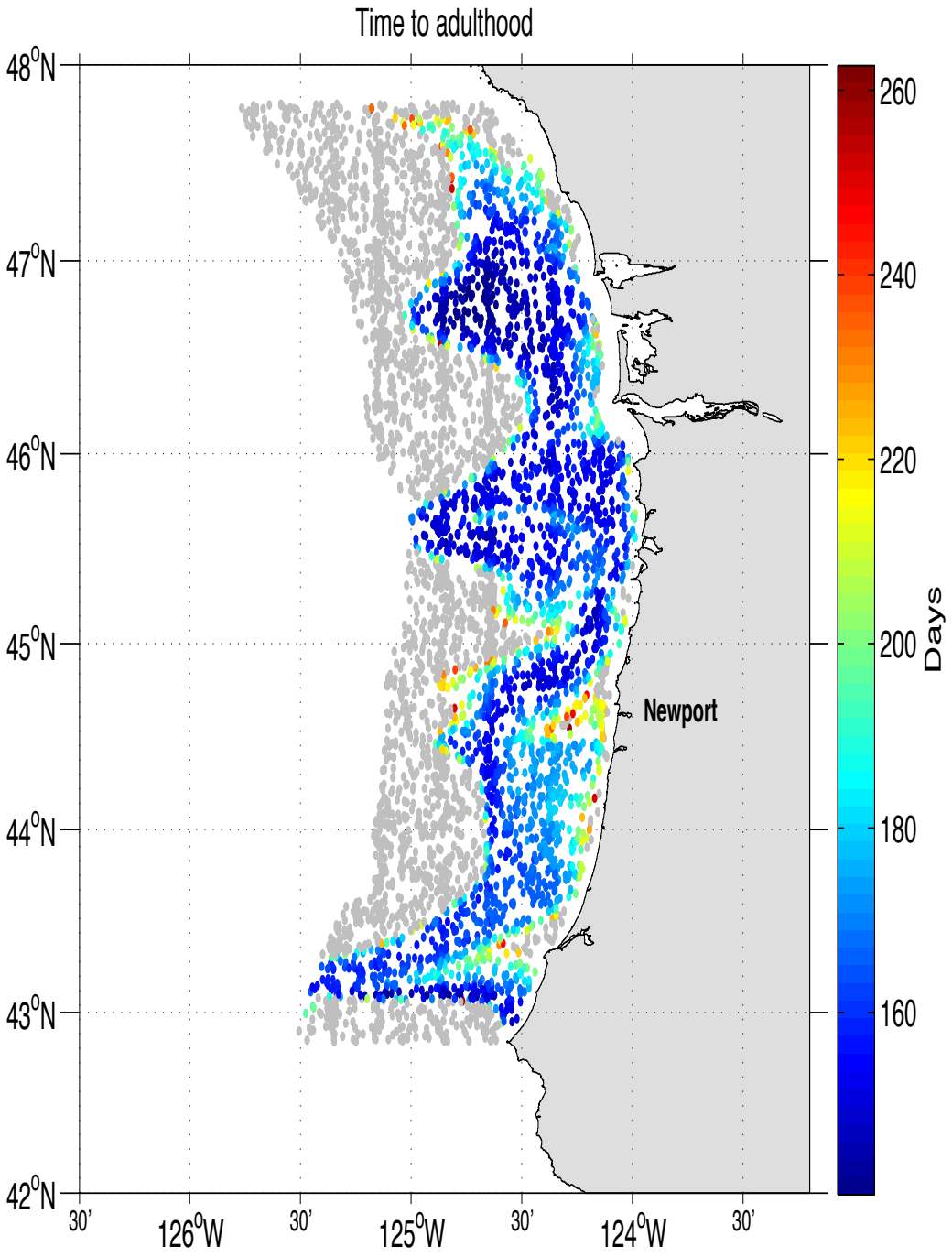

Figure 4.16. Time to adulthood. Grey markers denote krill that did not survive to adult stage.

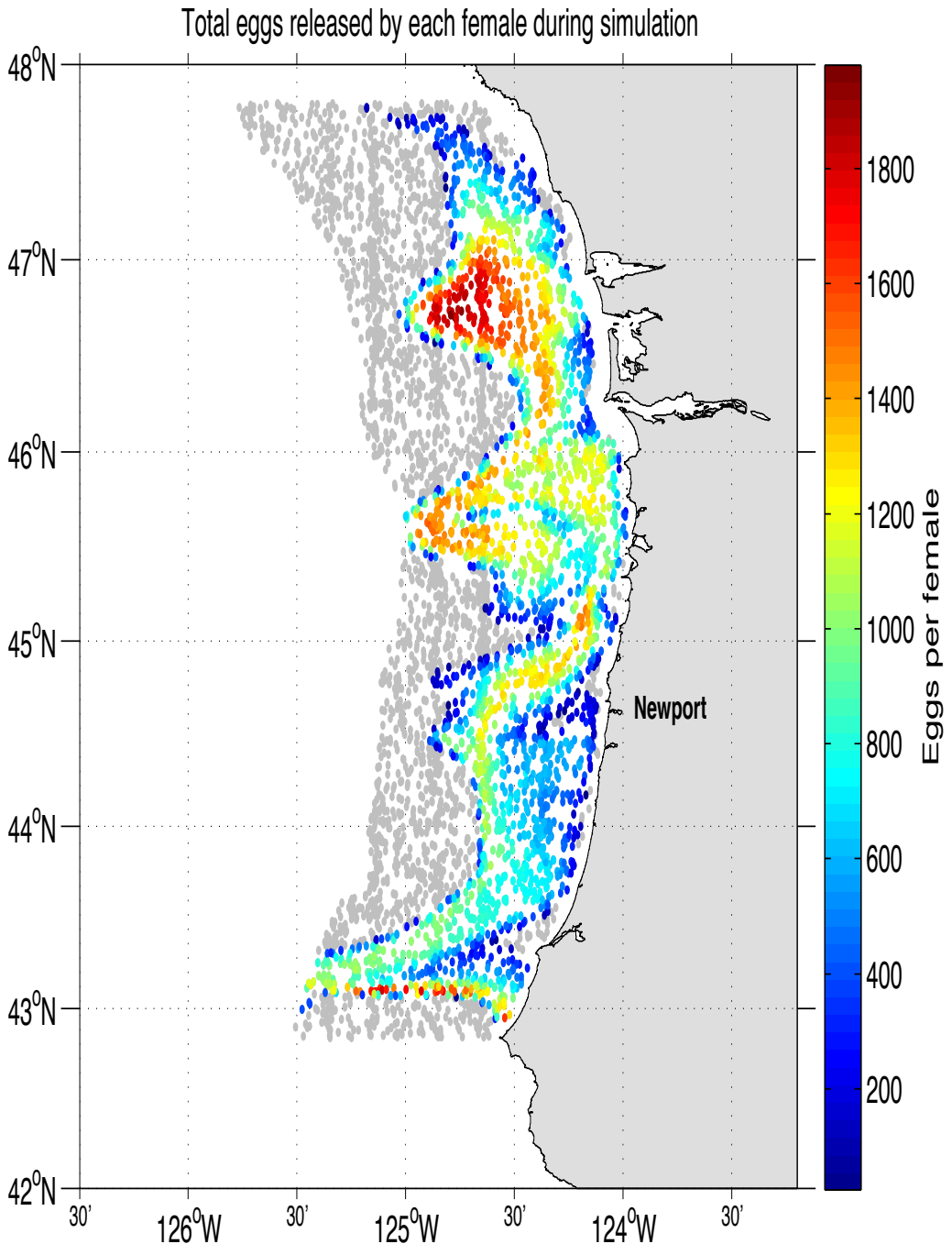

Figure 4.17. Total eggs released by each female during simulation. Grey markers denote krill that did not survive to adult stage or did not reproduce.

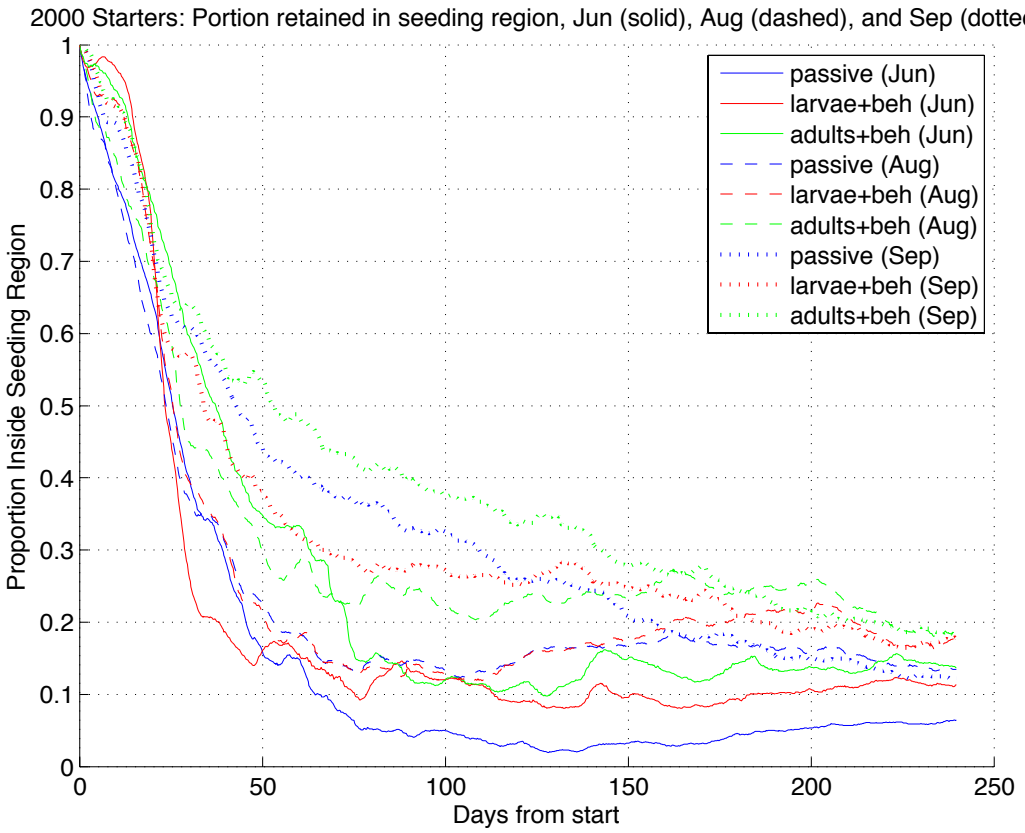

Figure 4.18. 2000 starters: portion retained in seeding region.

Figure 4.19. 2001 starters: portion retained in seeding region.

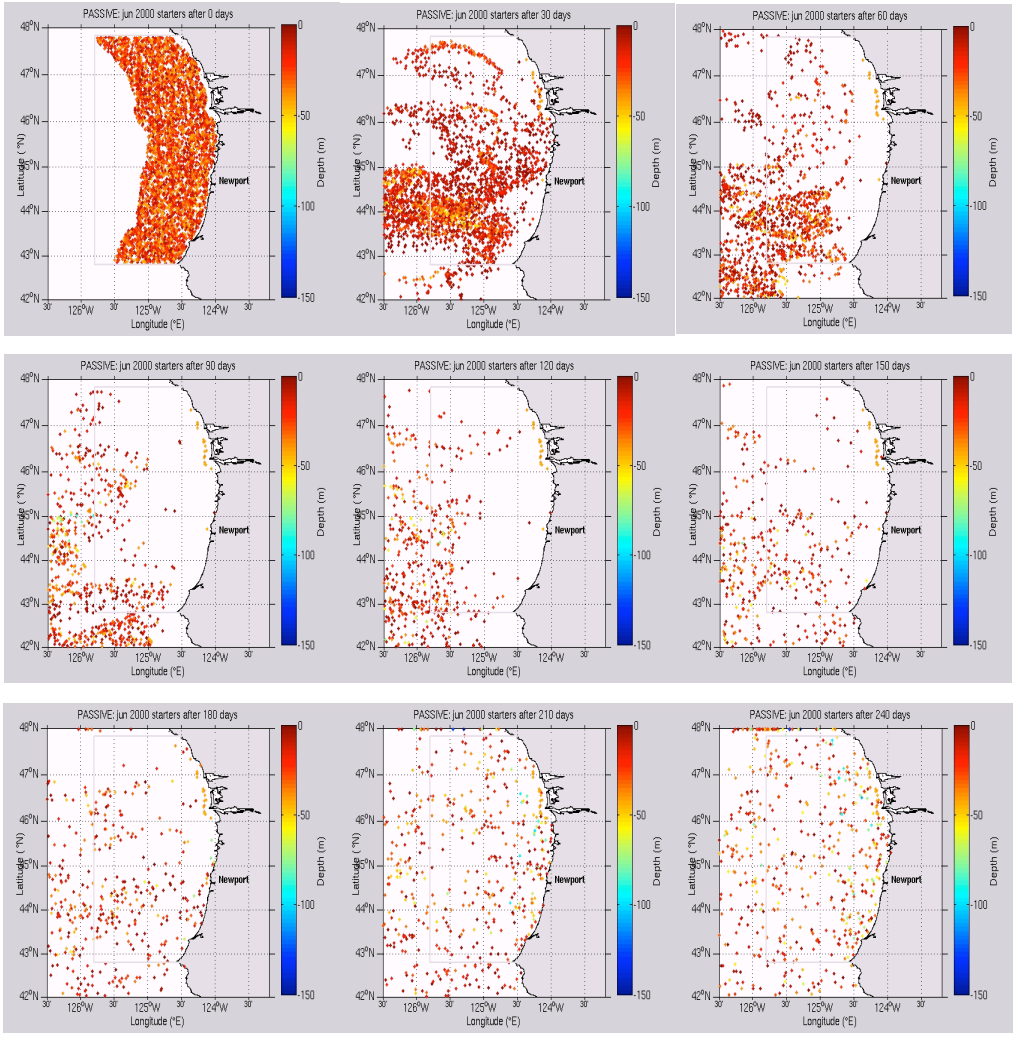

Figure 4.20. Particle tracking model results, June 2000 passive simulation. Snapshots shown from top left are for day 1, then day 30 and every 30th day thereafter. Colors represent particle depth; cool colors are deeper than warm colors.

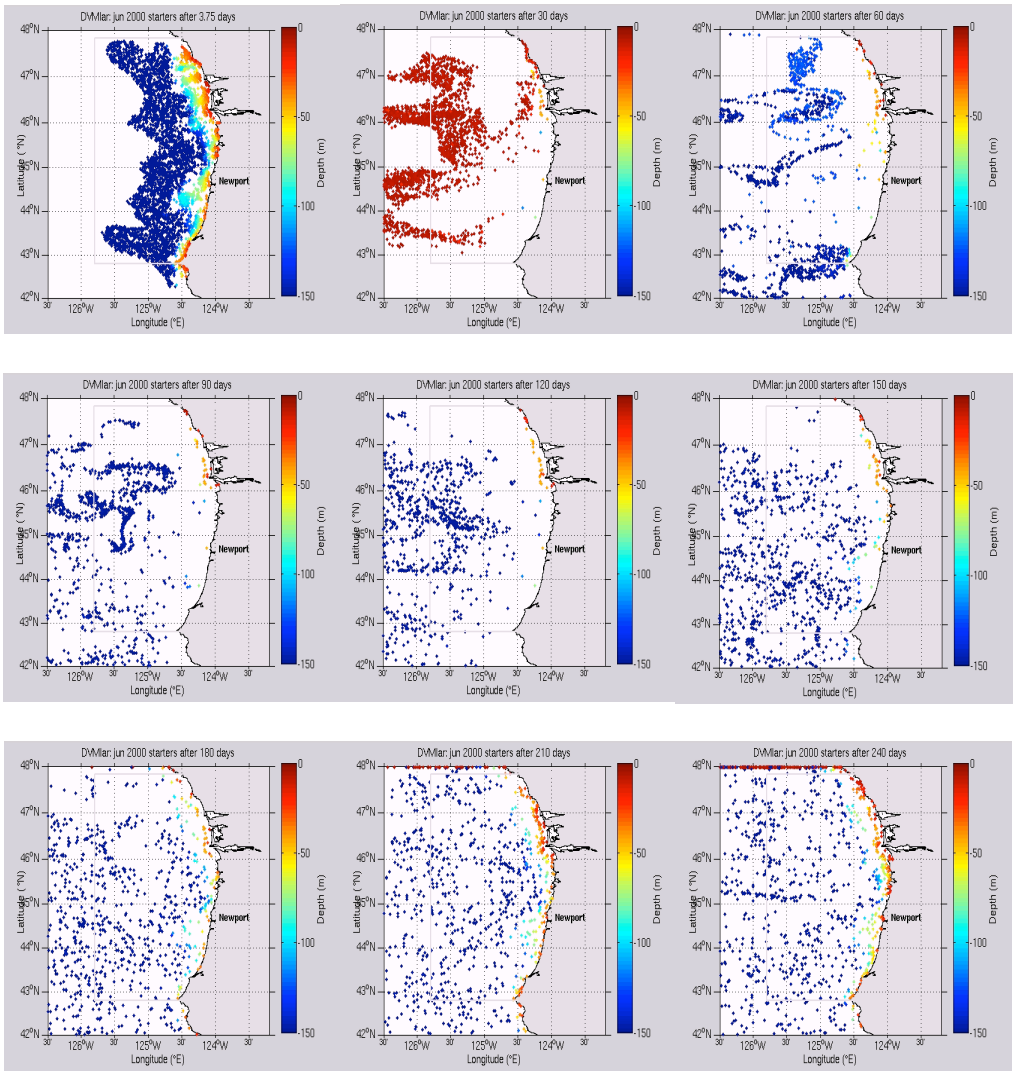

Figure 4.21. Particle tracking model results, June 2000 DVM larvae simulation. Snapshots shown from top left are for day 3.75, then day 30 and every 30th day thereafter. Colors represent particle depth; cool colors are deeper than warm colors.

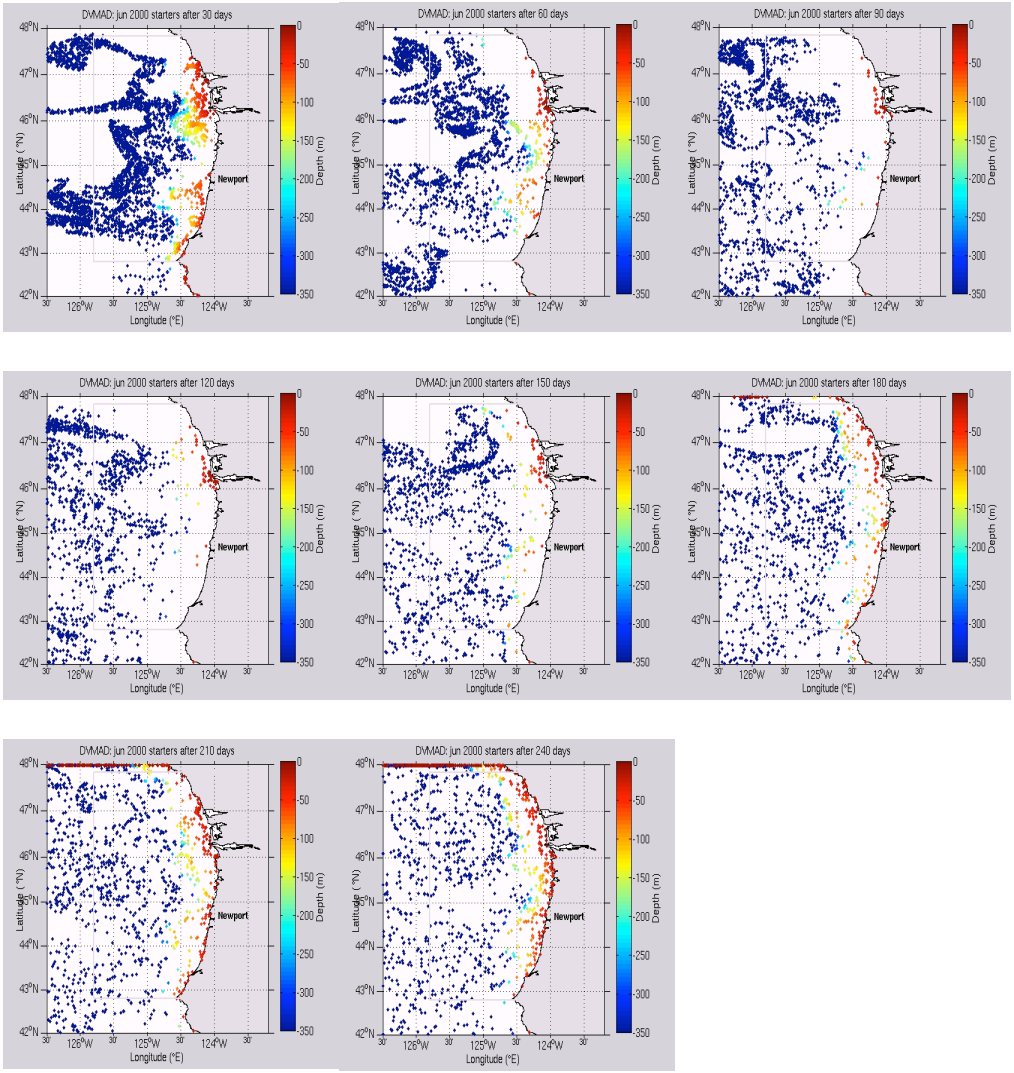

Figure 4.22. Particle tracking model results, June 2000 DVM adults simulation. Snapshots shown from top left are for day 30 and every 30th day thereafter. Colors represent particle depth; cool colors are deeper than warm colors.

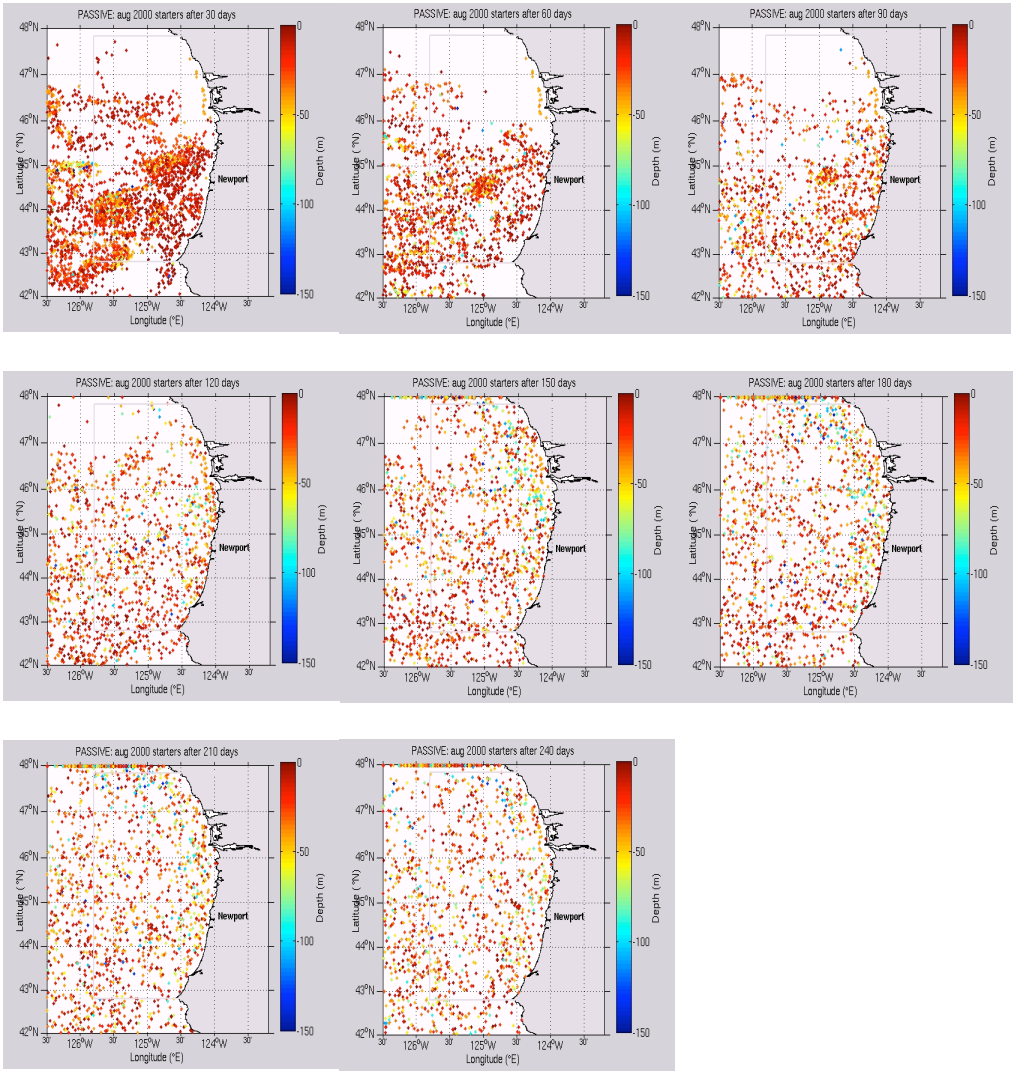

Figure 4.23. Particle tracking model results, August 2000 passive simulation. Snapshots shown from top left are for day 30 and every 30th day thereafter. Colors represent particle depth; cool colors are deeper than warm colors.

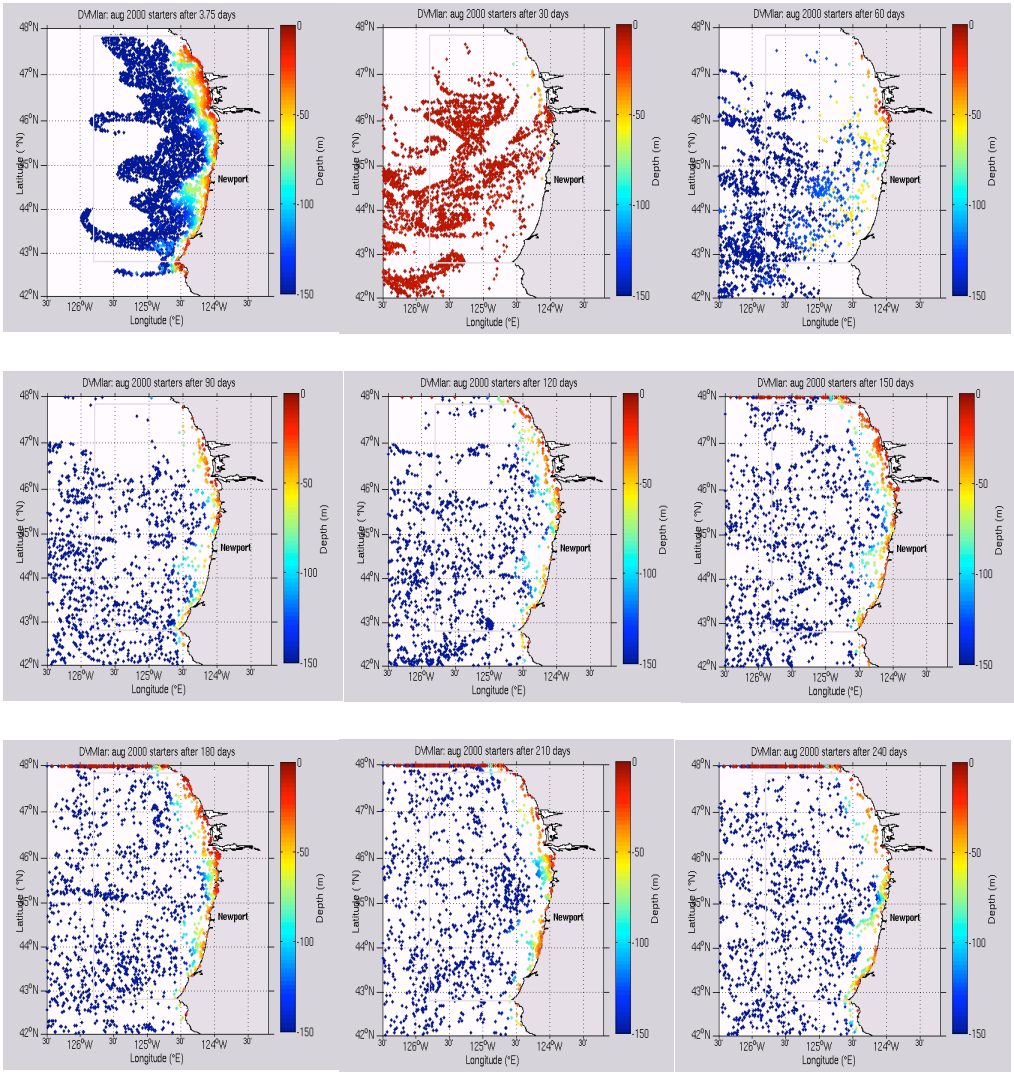

Figure 4.24. Particle tracking model results, August 2000 DVM larvae simulation. Snapshots shown from top left are for day 3.75, then day 30 and every 30th day thereafter. Colors represent particle depth; cool colors are deeper than warm colors.

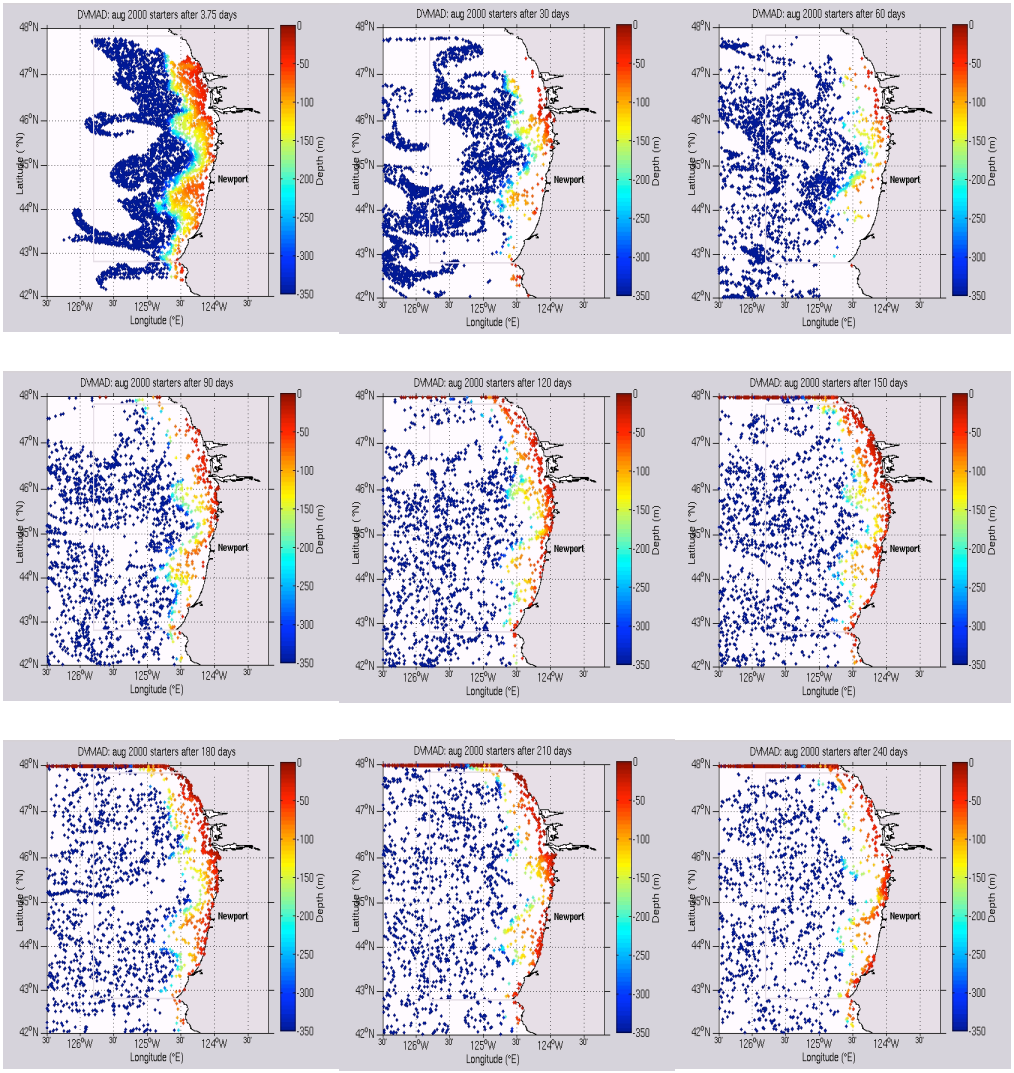

Figure 4.25. Particle tracking model results, August 2000 DVM adults simulation. Snapshots shown from top left are for day 3.25, then day 30 and every 30th day thereafter. Colors represent particle depth; cool colors are deeper than warm colors.

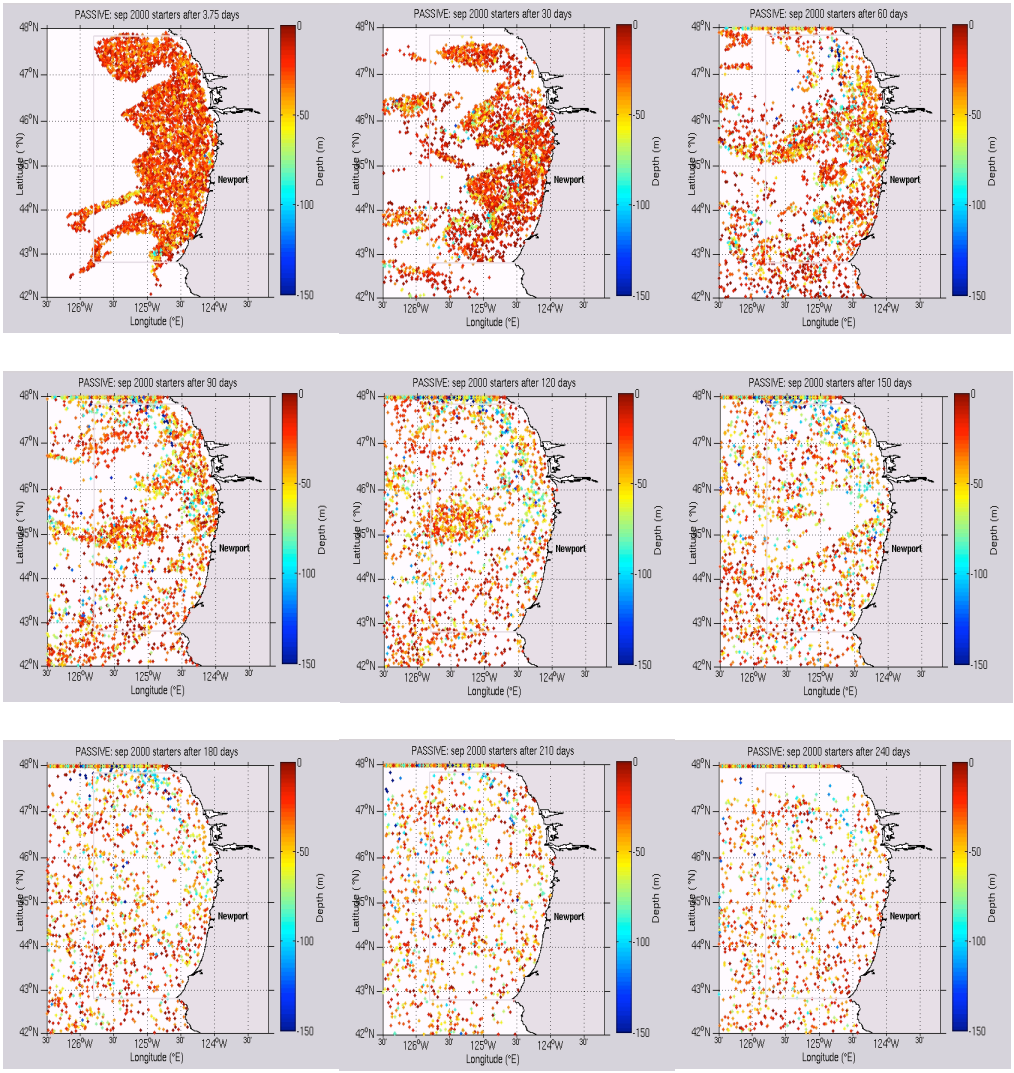

Figure 4.26. Particle tracking model results, September 2000 passive simulation. Snapshots shown from top left are for day 3.25, then day 30 and every 30th day thereafter. Colors represent particle depth; cool colors are deeper than warm colors.

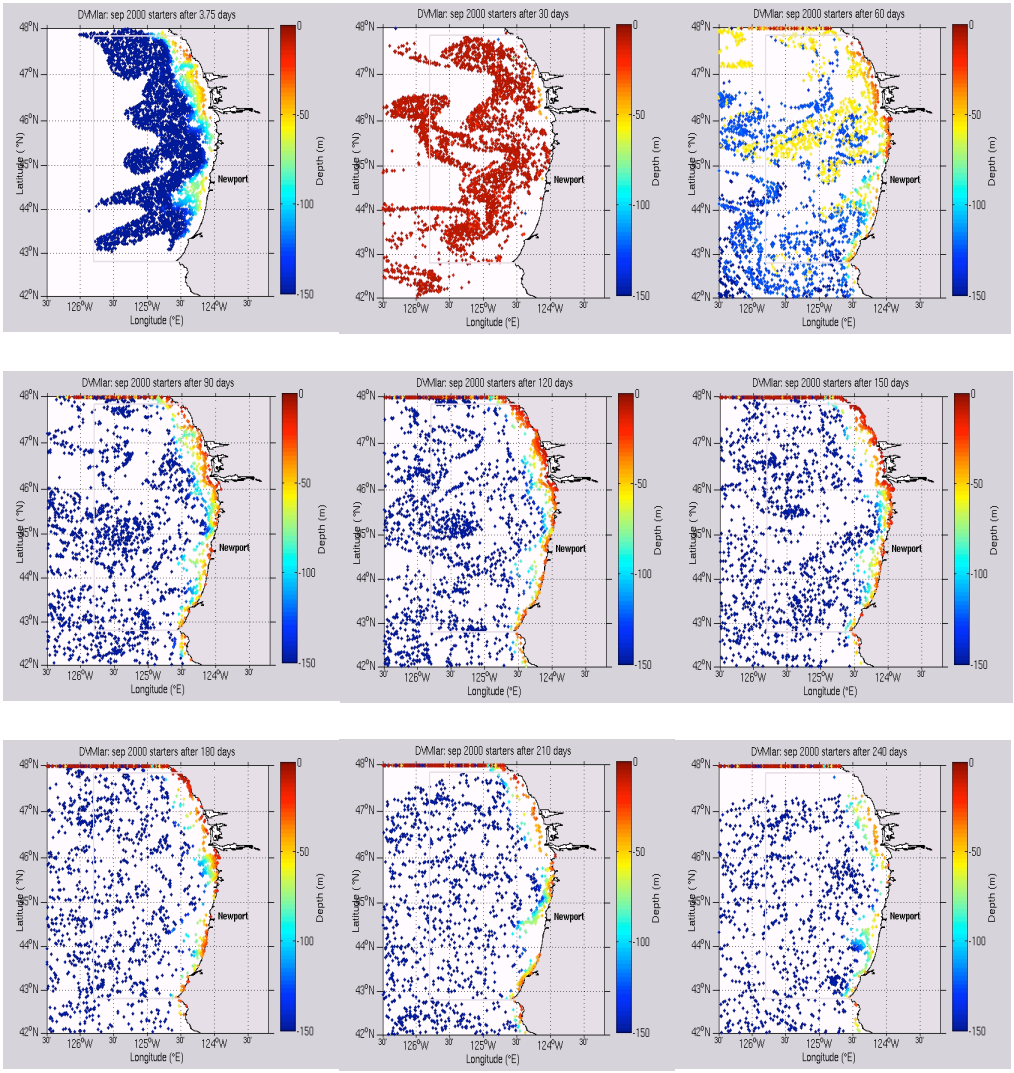

Figure 4.27. Particle tracking model results, September 2000 DVM larvae simulation. Snapshots shown from top left are for day 3.25, then day 30 and every 30th day thereafter. Colors represent particle depth; cool colors are deeper than warm colors.

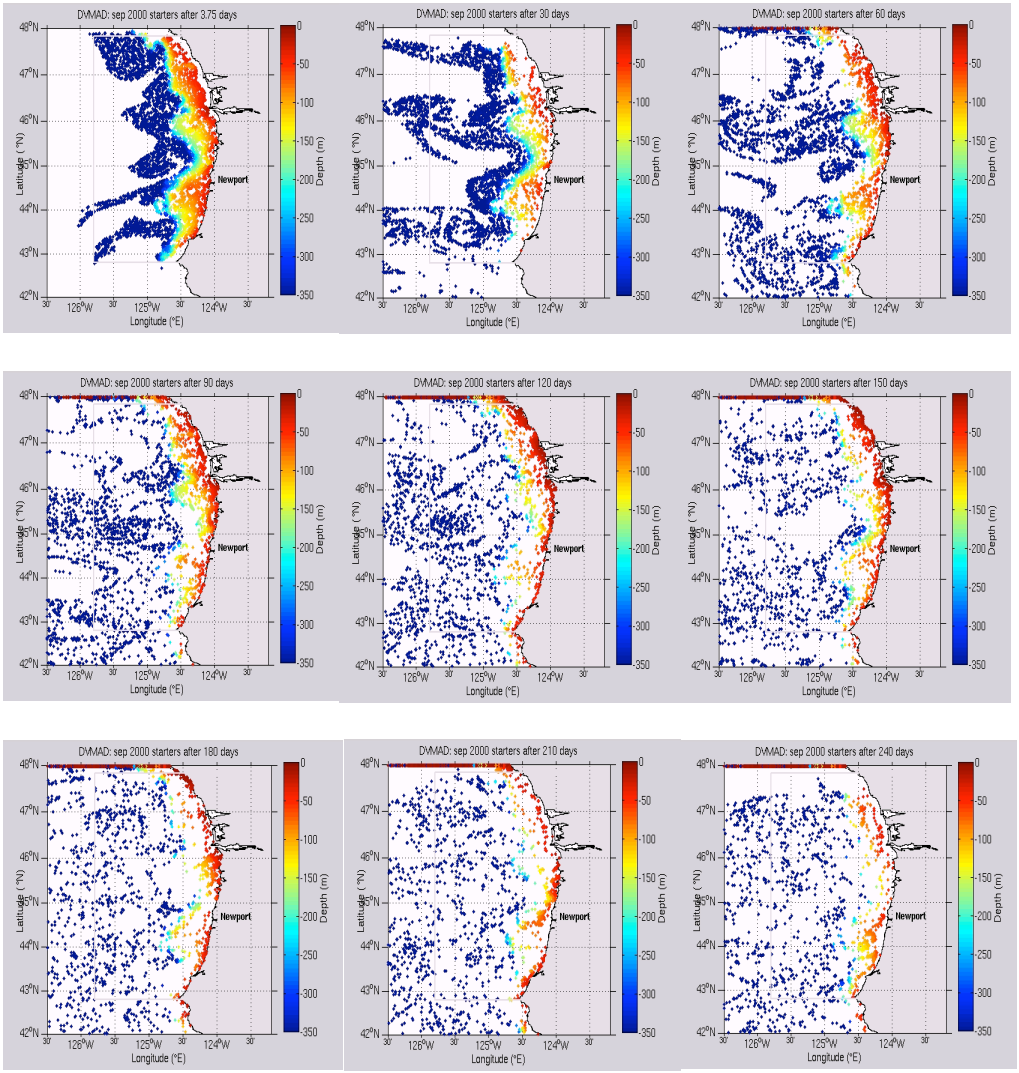

Figure 4.28. Particle tracking model, September 2000 DVM adults simulation. Snapshots shown from top left are for day 3.25, then day 30 and every 30th day thereafter. Colors represent particle depth; cool colors are deeper than warm colors.

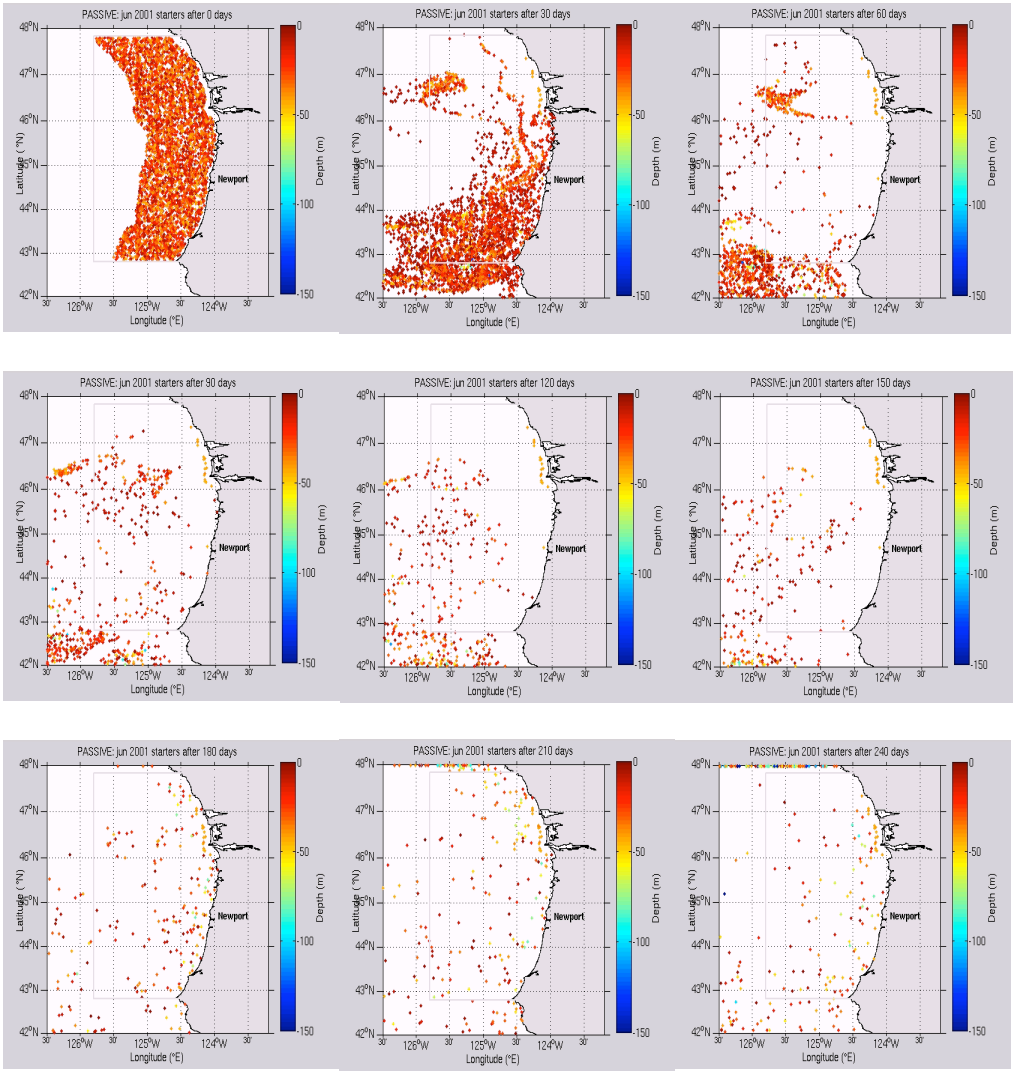

Figure 4.29. Particle tracking model results, June 2001 passive simulation. Snapshots shown from top left are for day 1, then day 30 and every 30th day thereafter. Colors represent particle depth; cool colors are deeper than warm colors.

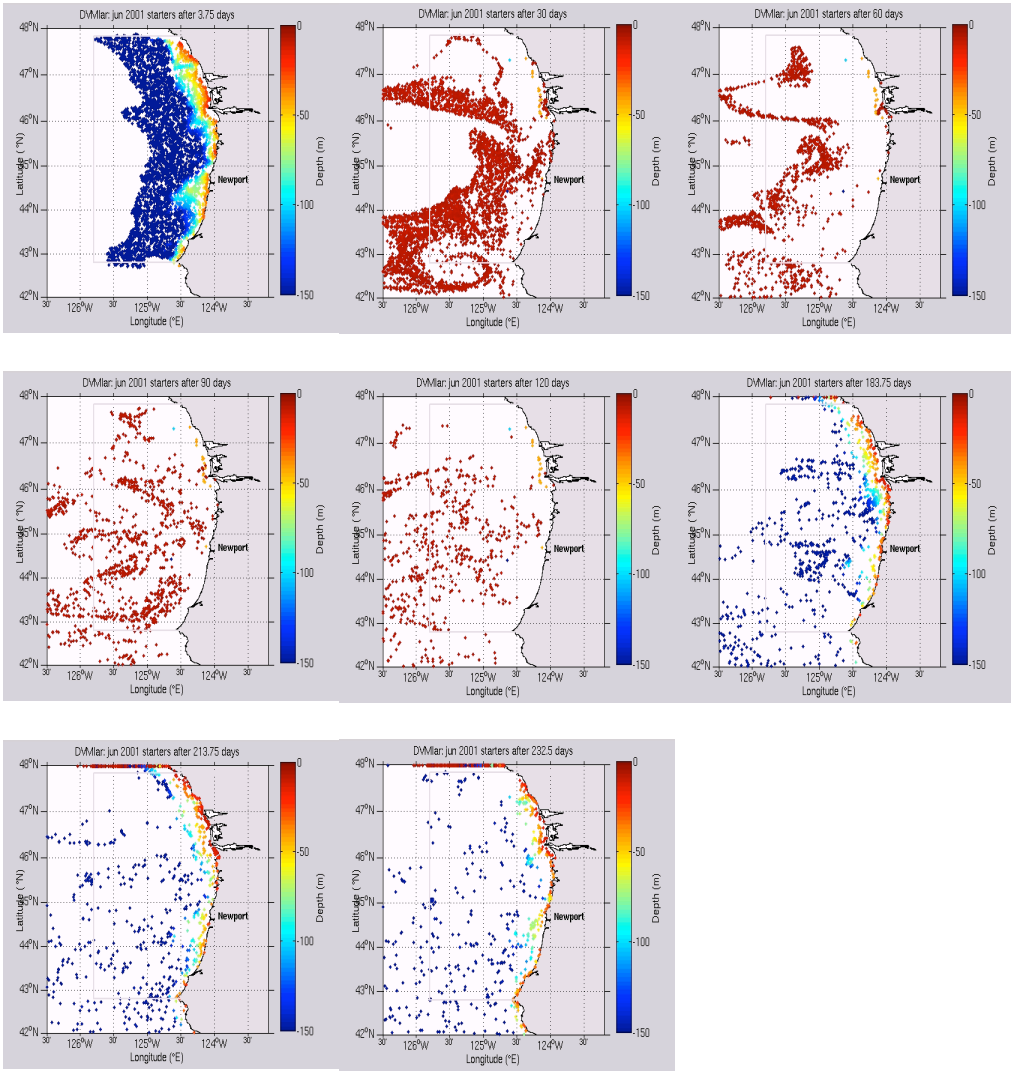

Figure 4.30. Particle tracking model results, June 2001 DVM larvae simulation. Snapshots shown from top left are for day 3.75, then day 30 and every 30th day thereafter. Colors represent particle depth; cool colors are deeper than warm colors.

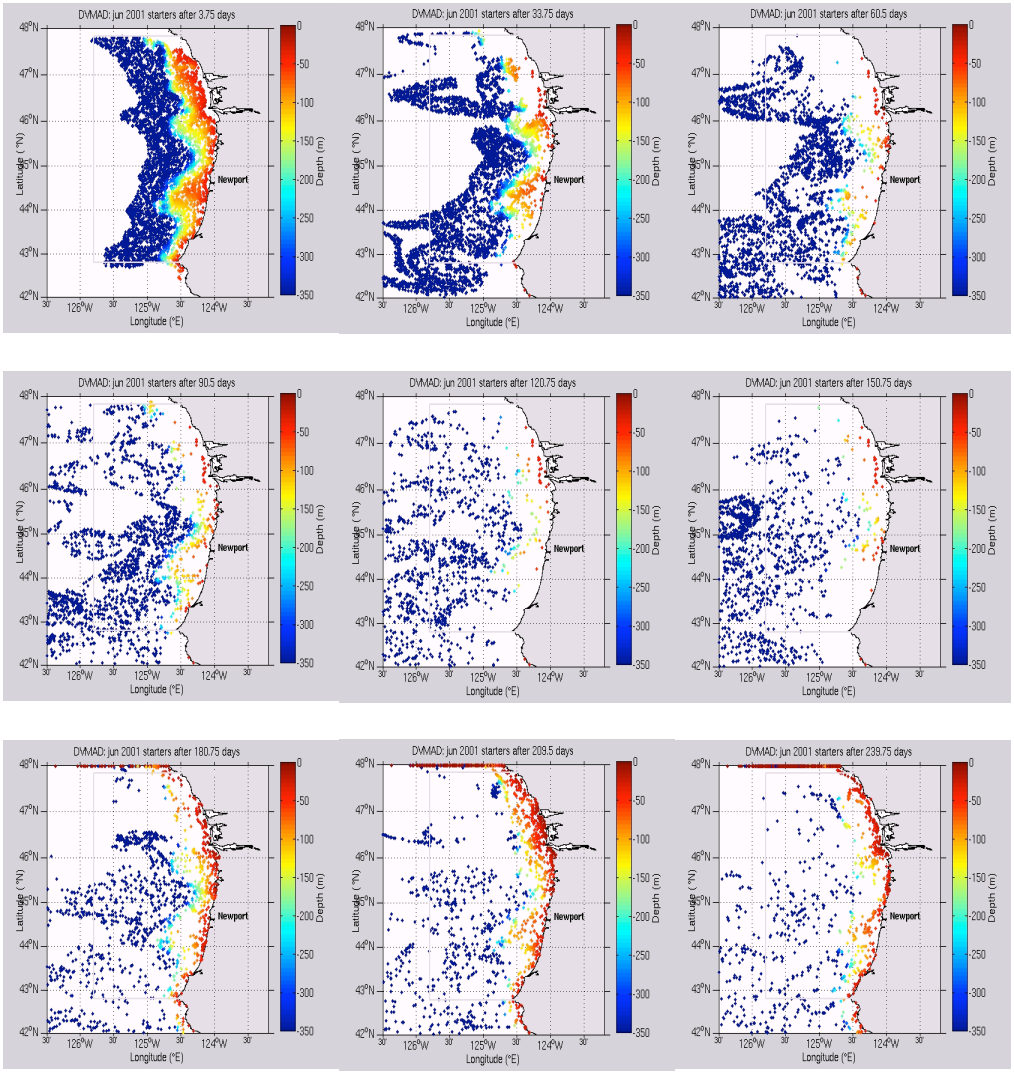

Figure 4.31. Particle tracking model results, June 2001 DVM adults simulation. Snapshots shown from top left are for day 3.75, then day 30 and every 30th day thereafter. Colors represent particle depth; cool colors are deeper than warm colors.

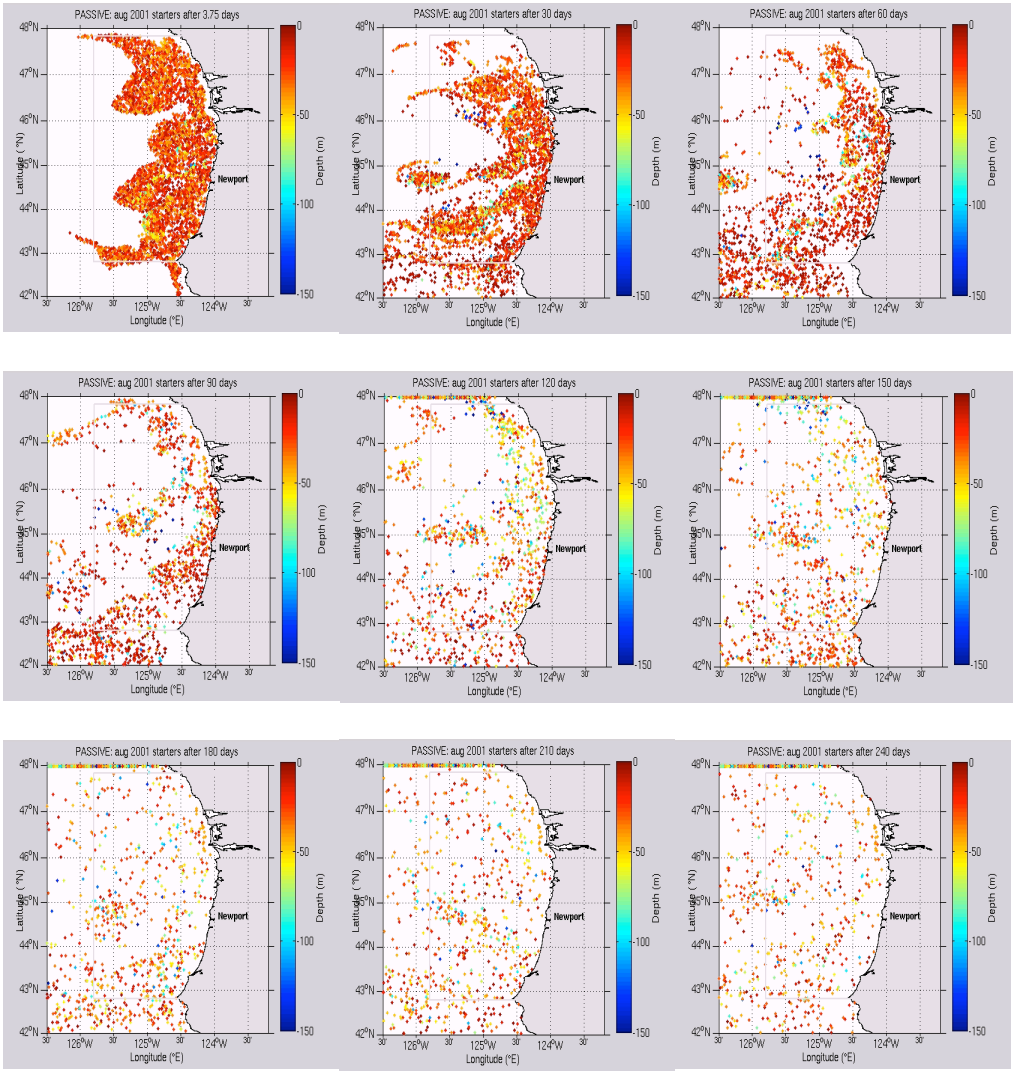

Figure 4.32. Particle tracking model results, August 2001 passive simulation. Snapshots shown from top left are for day 3.75, then day 30 and every 30th day thereafter. Colors represent particle depth; cool colors are deeper than warm colors.

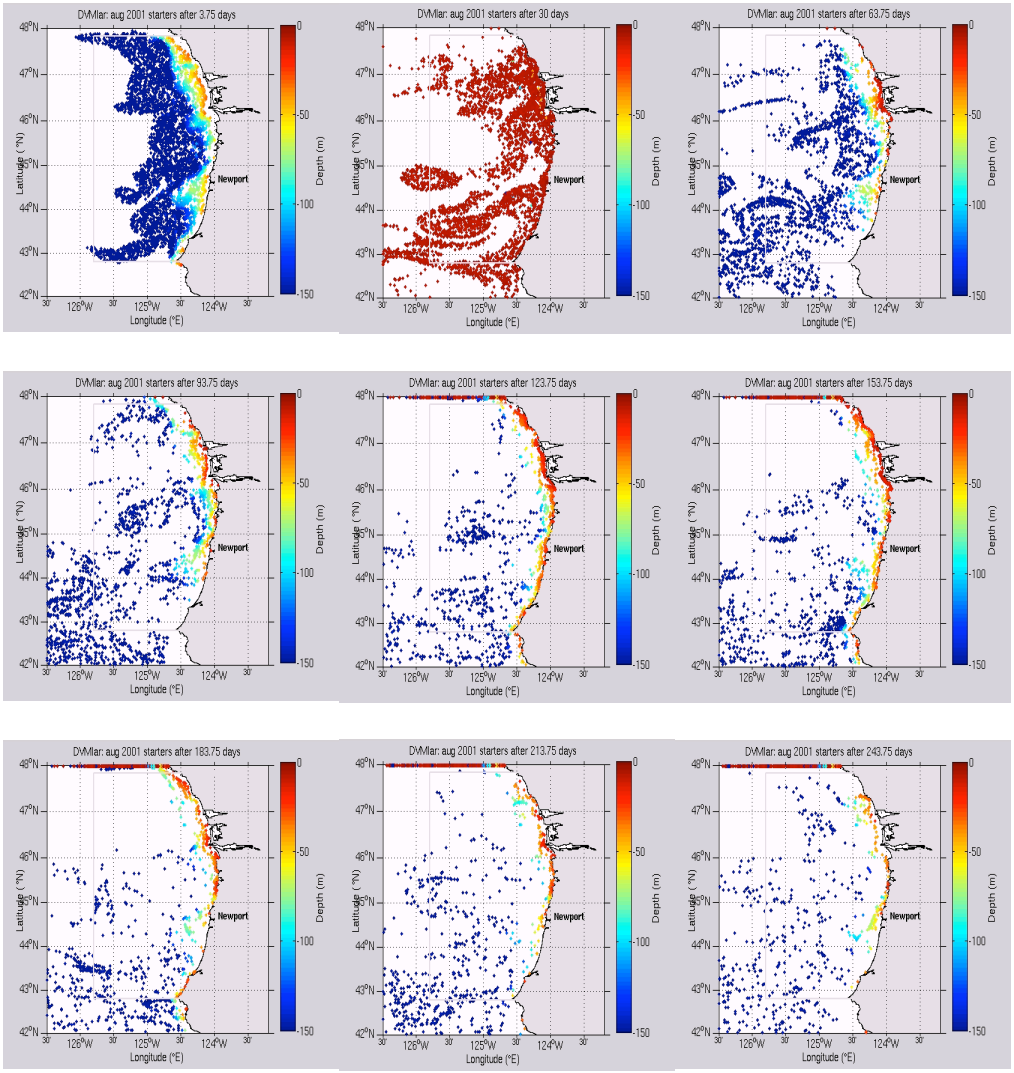

Figure 4.33. Particle tracking model results, August 2001 DVM larvae simulation. Snapshots shown from top left are for day 3.25, then day 30 and every 30th day thereafter. Colors represent particle depth; cool colors are deeper than warm colors.

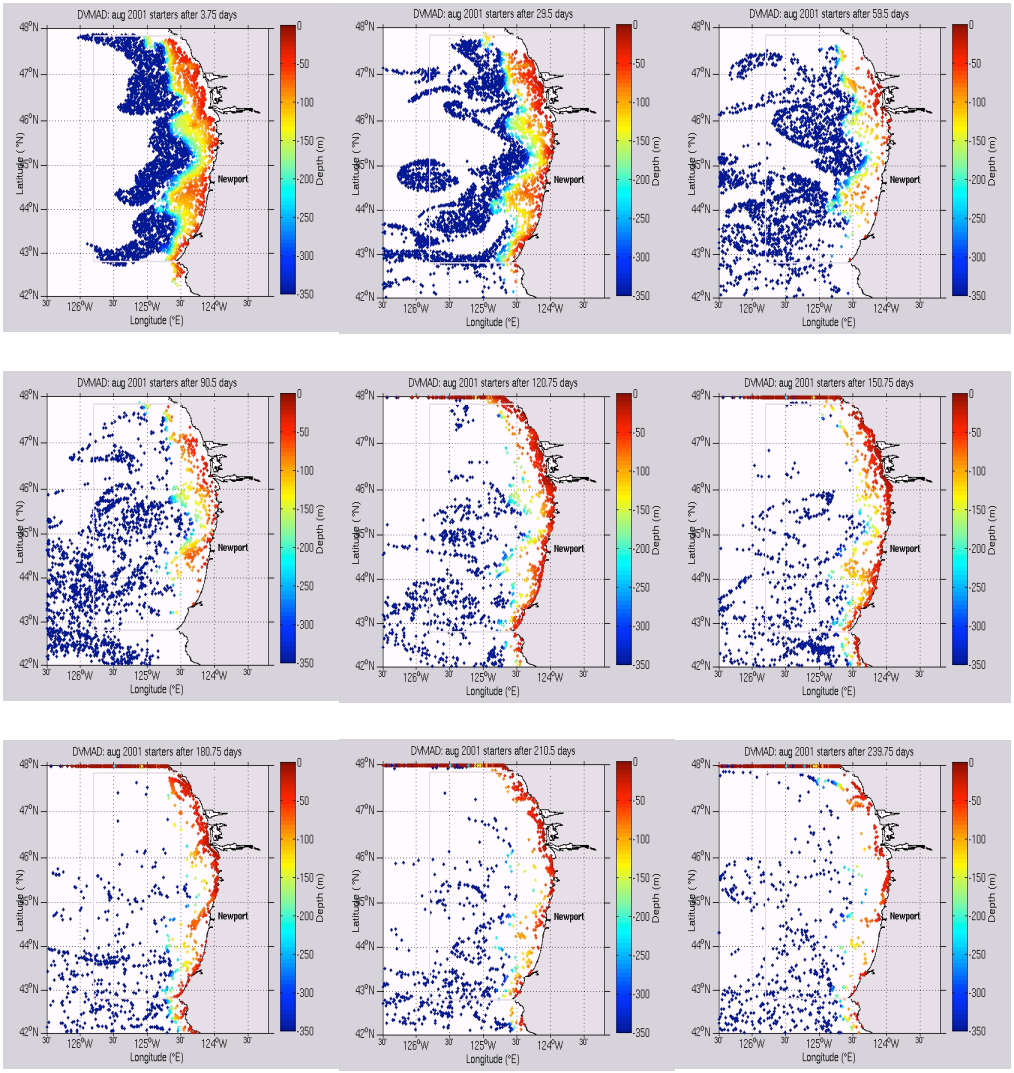

Figure 4.34. Particle tracking model results, August 2001 DVM adults simulation. Snapshots shown from top left are for day 3.75, then day 30 and every 30th day thereafter. Colors represent particle depth; cool colors are deeper than warm colors.

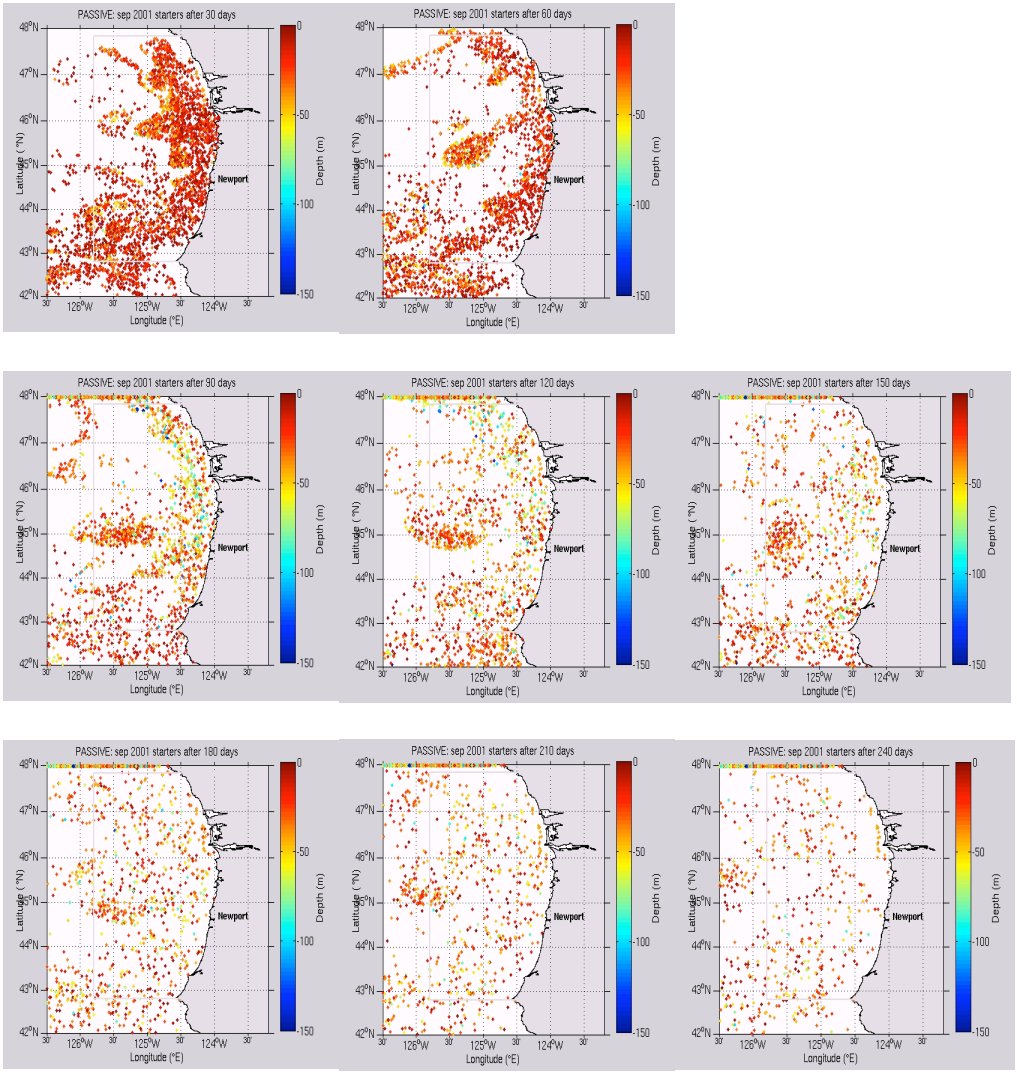

Figure 4.35. Particle tracking model results, September 2001 passive simulation. Snapshots shown from top left begin on day 30 and are shown for every 30th day thereafter. Colors represent particle depth; cool colors are deeper than warm colors.

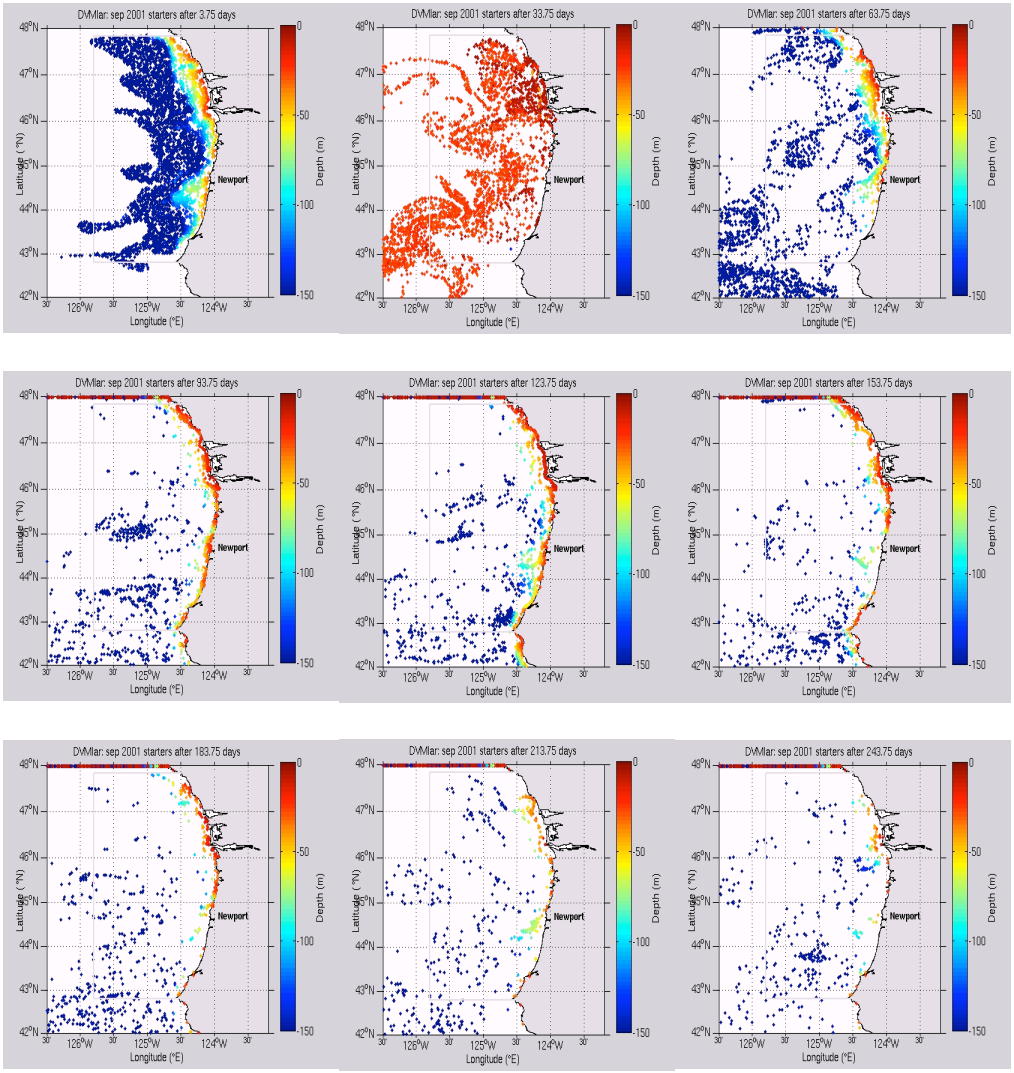

Figure 4.36. Particle tracking model results, September 2001 DVM larvae simulation. Snapshots shown from top left are for day 3.75, then day 30 and every 30th day thereafter. Colors represent particle depth; cool colors are deeper than warm colors.

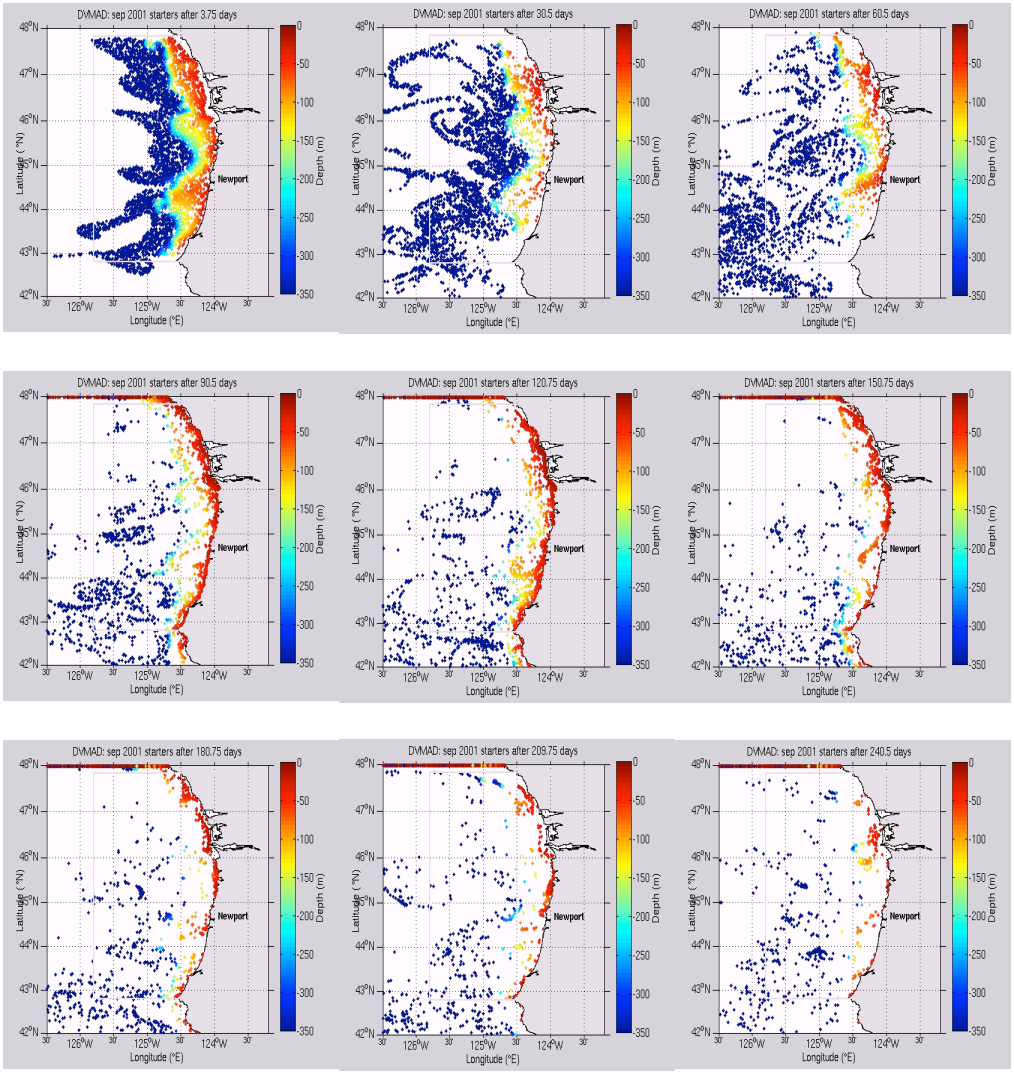

Figure 4.37. Particle tracking model results, September 2001 DVM adults simulation. Snapshots shown from top left are for day 3.75, then day 30 and every 30th day thereafter. Colors represent particle depth; cool colors are deeper than warm colors.

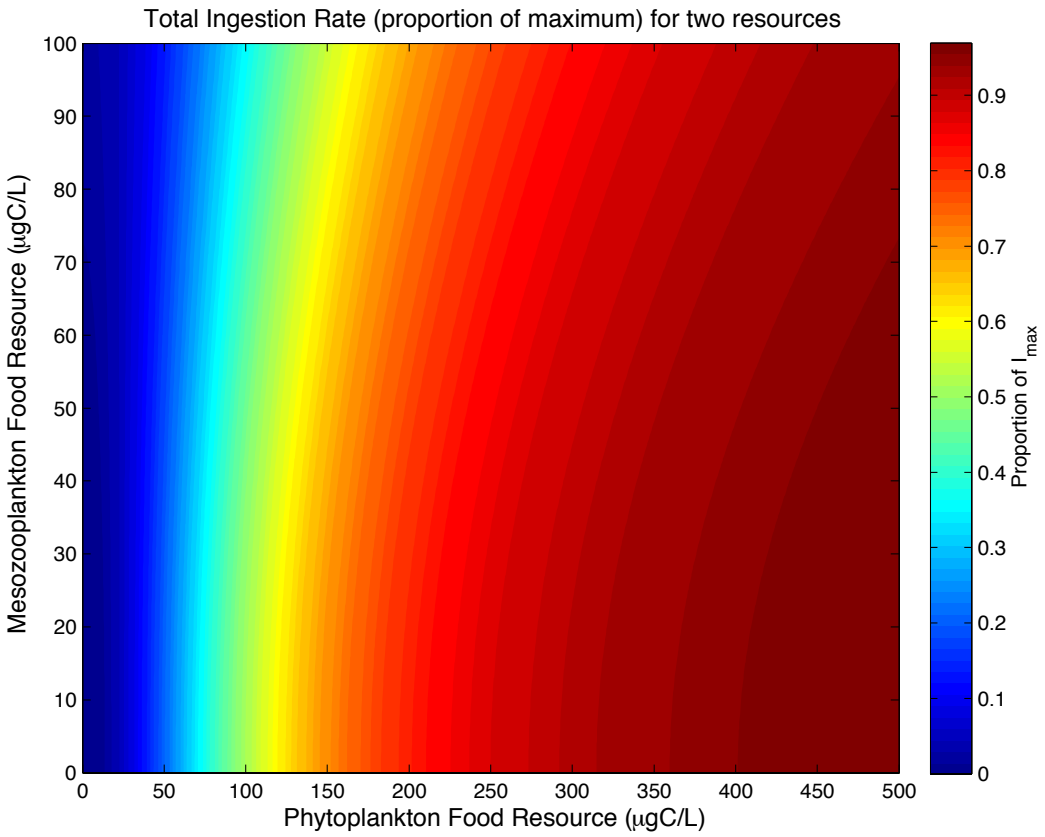

Figure 4.38. Total ingestion rate (proportion of maximum) for two resources.

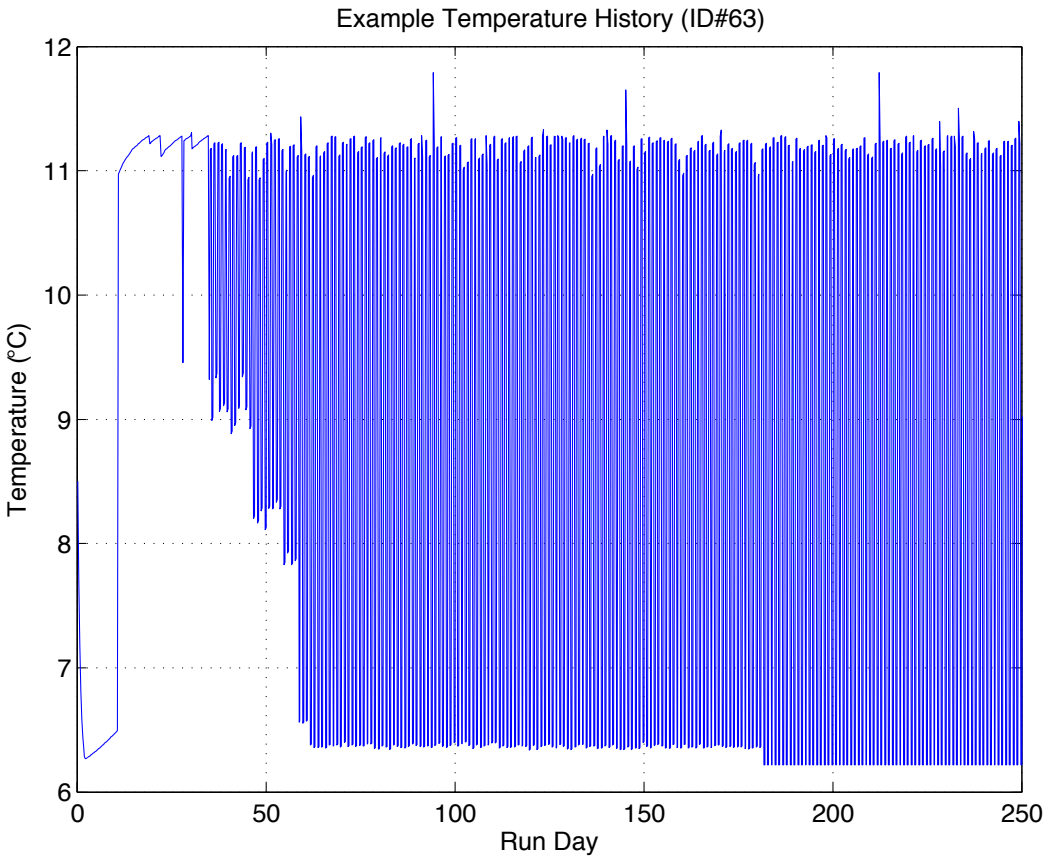

Figure 4.39. Example temperature history.

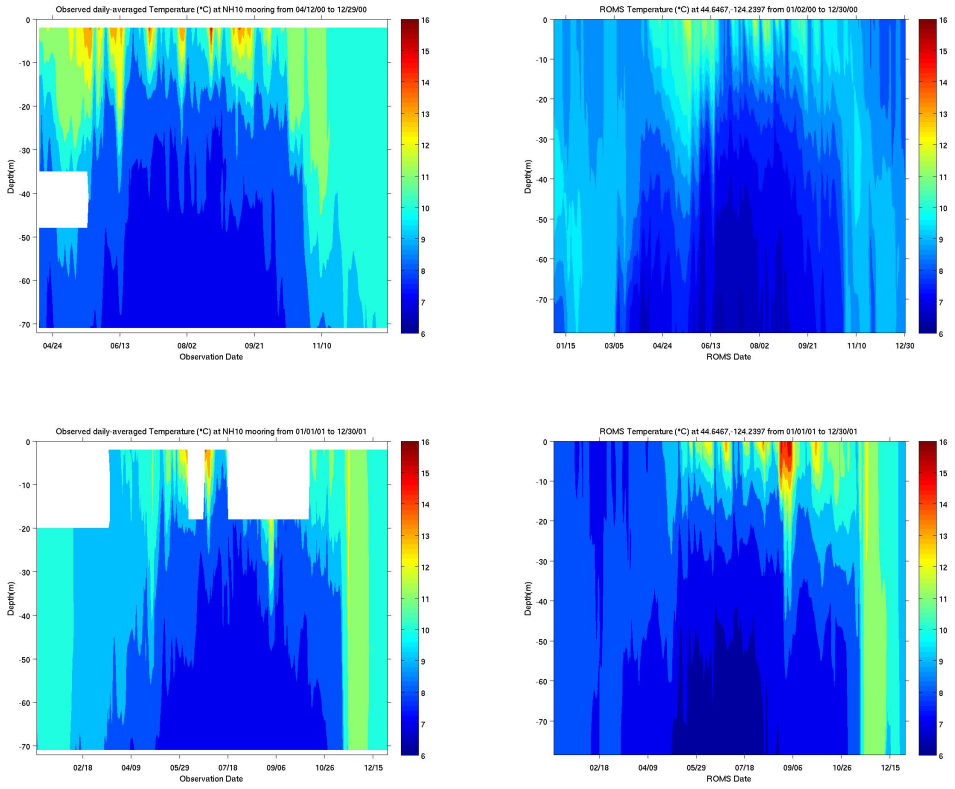

Figure 4.40. Observed and modeled temperatures at NH10, 2000-2001. Temperature in 2000 (top) and 2001 (bottom) at NH10, observed (left) and modeled (right). Data is from National Data Buoy Center station 46094. White areas are periods when no data were reported.

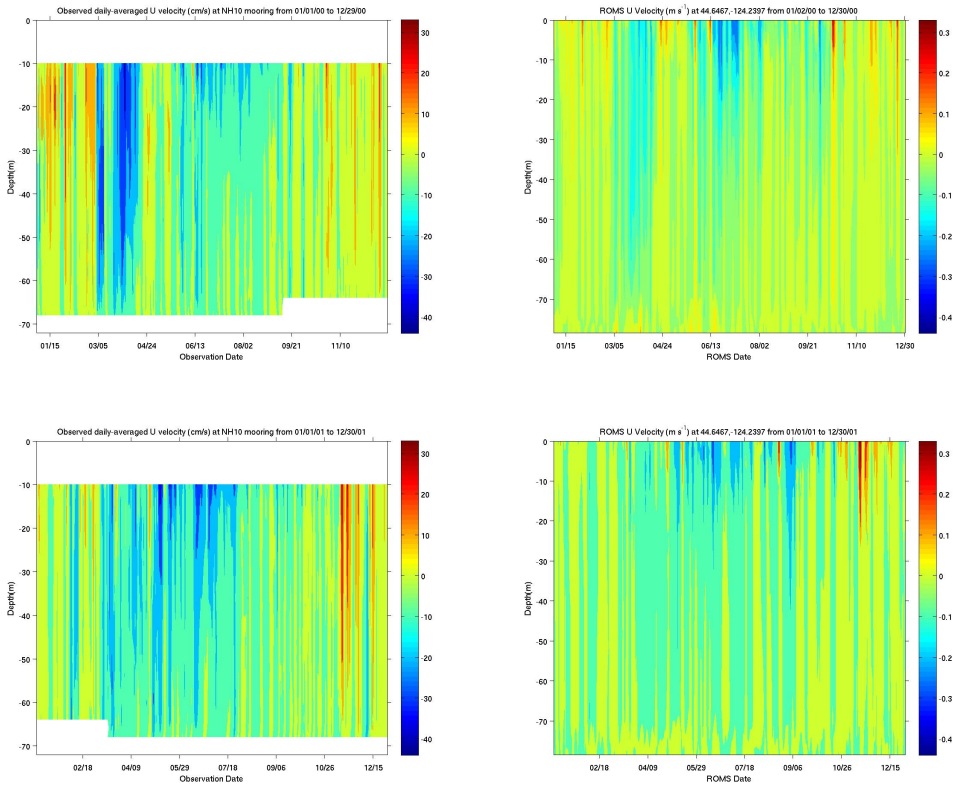

Figure 4.41. Observed and modeled *u*-velocities at NH10, 2000-2001. *U*-velocity in 2000 (top) and 2001 (bottom) at NH10, observed (left) and modeled (right). Data is from National Data Buoy Center station 46094. White areas are periods when no data were reported.

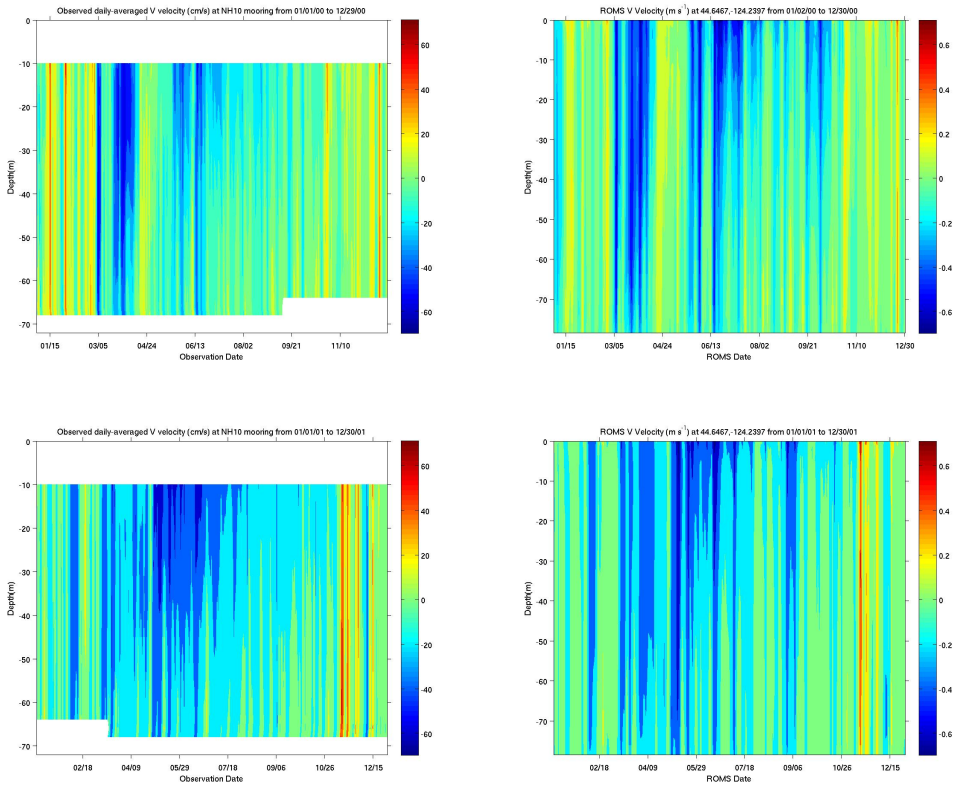

Figure 4.42. Observed and modeled *v*-velocities at NH10, 2000-2001. *V*-velocity in 2000 (top) and 2001 (bottom) at NH10, observed (left) and modeled (right). Data is from National Data Buoy Center station 46094. White areas are periods when no data were reported.

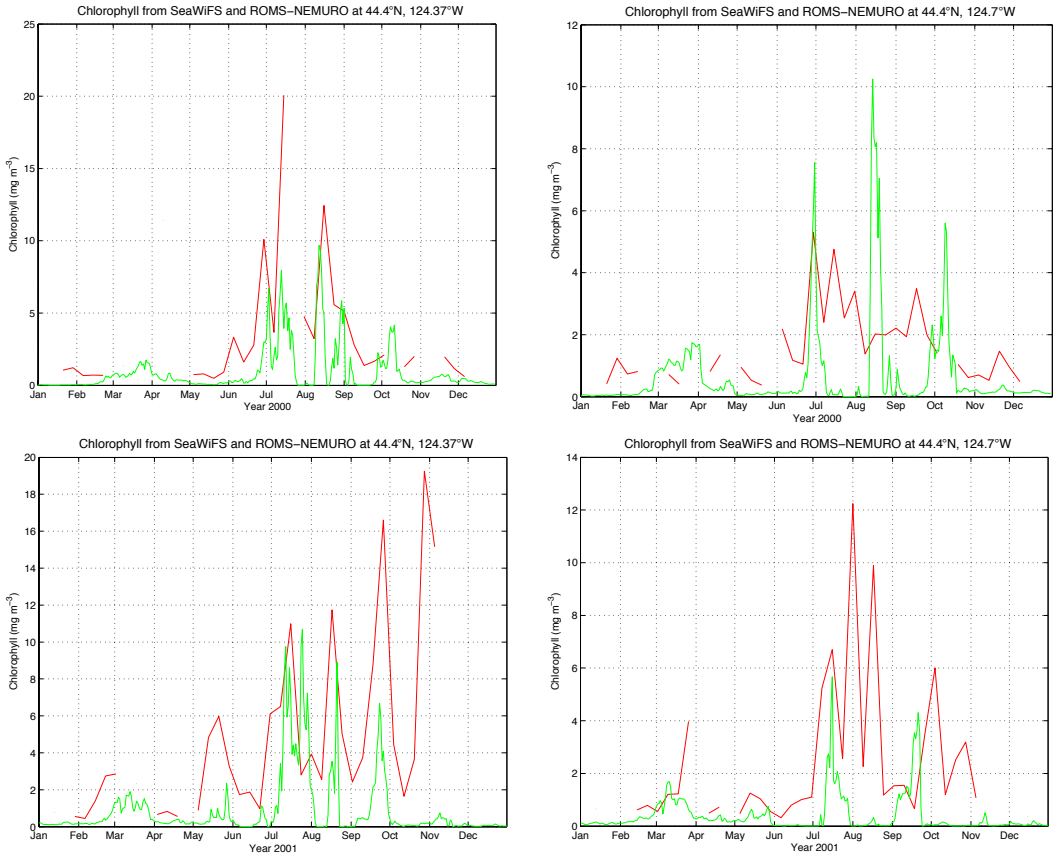

Figure 4.43. Surface chlorophyll comparison between SeaWiFS and ROMS-NEMURO at two locations in the seeding region in 2000 and 2001. Surface chlorophyll at 44.4°N, 124.37°W (left panels) and 44.4°N, 124.7°W (right panels) for 2000 (top) and 2001 (bottom). Green lines are surface chlorophyll in the ROMS-NEMURO model, red lines are surface chlorophyll estimates from SeaWiFS.

Table 4.1. Empirically-determined stage-specific Belehrádek function constants for *E. pacifica.*

Stage	a_i (day $^oC^{-1}$): stage-specific constant to reach next stage
Egg	1217
(N1) nauplius 1	599
(N2) nauplius 2	1423
(MN) metanauplius	2547
(C1) calyptopis 1	5767
(C2) calyptopis 2	2771
(C3) calyptopis 3	2621
(F1) furcilia 1	4045
(F2) furcilia 2	4269
(F3) furcilia 3	8239
(F4/5) furcilia 4/5	5693
(F6) furcilia 6	3296
(F7) furcilia 7	2247

Table 4.2. IBM equations. Listed in the order presented in the text. Where parameters do not change with life stage, they are included. When parameters differ either as a separate function or with development, they are listed in Table 4.3.

(3) $\boldsymbol{R_{TOT} = R_A + R_B}$
(4) $\boldsymbol{R_A = \varphi I}$, where $\boldsymbol{R_A}$ is the active metabolic rate (μgC d^{-1}), $\boldsymbol{\varphi}$ is a proportion (unitless), and I is ingestion rate (μgC d^{-1})
(5) $\boldsymbol{R_B = \alpha W^{\beta}}$, where $\boldsymbol{R_B}$ is the basal metabolic rate (μgC d^{-1}), W is individual weight (μgC)
(6) $\boldsymbol{nP_{available} = nP[max\left(0.2, 0.5 - \left(0.1 * \frac{nP}{0.3}\right)\right)]}$, where nP is the concentration of nanophytoplankton (mmolN m^{-3}), and nP_{avail} is the available concentration of nanophytoplankton (mmolN m^{-3})
(8) $\boldsymbol{I_{max} = 0.249 W^{0.91}}$, where $\boldsymbol{I_{max}}$ is the maximum ingestion rate (μgC d^{-1}) and W is individual weight (μgC)
(9) $\boldsymbol{DW = 0.000795(TL)^{3.239}}$, where DW is dry weight (mgC) and TL is total length (mm)
(10) $\boldsymbol{F_{rep} = max\left(0, \frac{0.078(W-1000)}{W+1000}\right)}$, where F_{rep} is the fraction of ingestion set aside for reproductive material and W is individual weight (μgC)
$\boldsymbol{Brood\ Size = EBSC * R_{rep}}$
(11) $\boldsymbol{EBSC = 3.2(15.135TL - 156.59)}$, where $EBSC$ is the expected brood size (μgC) and TL is the total individual length (mm)
(12) $\boldsymbol{R_{rep} = max\left(0.5, 0.1 \ln\left(\frac{int\_food}{IBP} - 0.001\right) + 1.33\right)}$, where R_{rep} is the food-dependent multiplier for $EBSC$ (unitless), int_food is the integrated food ingested (%weight·days), IBP is the previous interbrood period (days)

Table 4.3. Equation parameters for IBM. Bold numbers in parentheses refer to the equation to which the parameter belongs.

(4) $\boldsymbol{\varphi}$=0.23 (Calyptopis 1 through Furcilia 7) $\boldsymbol{\varphi}$=0.20 (Juveniles) $\boldsymbol{\varphi}$=0.12 (Adults)
(5) $\boldsymbol{\alpha}$=0.09 (Egg through Metanauplius) $\boldsymbol{\alpha}$=0.045 (Calyptopis 1 through Furcilia 7) $\boldsymbol{\alpha}$=0.076 (Juveniles) $\boldsymbol{\alpha}$=0.062 (Adults) $\boldsymbol{\beta}$=0.81 (Egg through Metanauplius) $\boldsymbol{\beta}$=0.95 (Calyptopis 1 through Furcilia 7) $\boldsymbol{\beta}$=0.91 (Juveniles) $\boldsymbol{\beta}$=0.91 (Adults)
(7) c_{filter}=0.001818*0.0585, with units of: $\left(\mathbf{1}/_{[\boldsymbol{\mu gC\ m^{-3}}]^2 \cdot \boldsymbol{day}}\right)$; the first number is a scaling factor so the max I_{TOT} is 1 b_{filter}=0.000105, with units of: $\left(\mathbf{1}/_{[\boldsymbol{\mu gC\ m^{-3}}]^2}\right)$ $c_{capture}$=0.0131*0.0345, with units of: $\left(\mathbf{1}/_{[\boldsymbol{\mu gC\ m^{-3}}]^2 \cdot \boldsymbol{day}}\right)$; the first number is a scaling factor so the max I_{TOT} is 1 $b_{capture}$=0.0001087, with units of: $\left(\mathbf{1}/_{[\boldsymbol{\mu gC\ m^{-3}}]^2}\right)$

Table 4.4. Preferred daytime depths for *E. pacifica* life stages.

Life Stage	Daytime Depth (m)
Calyptopis 2 – 3	15
Furcilia 1 – 2	20
Furcilia 3	25
Furcilia 4/5	40
Furcilia 6	55
Furcilia 7	125
Juvenile	150
Adult	350

5.0 Conclusion

There is still much to learn about *Euphausia pacifica*. This research set out to add to the quickly growing body of knowledge about the important krill species of the North Pacific basin. Specifically, it asked the questions,

1. Can we link differences in larval transport to upwelling in a reliable and quantifiable way?
2. How likely is it that eggs sampled at the inshore station NH05 along the Newport Hydrographic line originated at the surface over the shelf break? and
3. What is the lower range of juvenile stage durations that we might expect to find along the coast at Oregon, and how valid is the assumption that the same population can be sampled on the Oregon continental shelf over a period of more than 200 days? Can *E. pacifica* sustain a population at the Oregon coast without supplementation from adjacent regions?

A metric was proposed to quantify the fraction of migrating late larval stages in net tows and how it was anticipated to vary with upwelling on an event-length time scale, due to differential cross-shelf transport. While the data from one year was consistent with the hypothesized relationship, the other years did not conform to expectations. The concept of differential cross-shelf transport has been applied to *E. pacifica* and other species; results in Chapter 2 suggest there may be other confounding factors operating in the Oregon upwelling zone that make such a process very difficult to observe with field data.

Modeling of egg trajectories demonstrated that females spawning at or beyond the shelf break are unlikely to be the primary source of eggs found at the inner shelf station NH05. We were also able to show that years with strongly positive (warm) Pacific Decadal Oscillation index values are not likely to be years with large fluxes of *E. pacifica* eggs to the nearshore region if they originate at the shelf break or seaward as a result of increased egg development rate.

Finally, optimistic (i.e. no mortality) trajectories of individuals modeled off Oregon suggest that cohort analyses of juvenile and adult *E. pacifica* in the region may not always violate the assumption of resampling a single population, especially if samples are taken during the fall or krill are caught in mesoscale features such as eddies. In these special cases, cohort analysis may be useful for estimating *in situ* growth rates, which might not be expected for a region as dynamic as the Northern California Current. More often, and for a large portion of the seeding region used in Chapter 4, however, those krill that are retained do not stay for very long (order of a month or two)—often for a period shorter than what is generally used for a cohort analysis (several months to more than a year). Simple diel-vertical migration in older modeled *E. pacifica* (especially adults) was shown to offer a population minimal protection from losses to the south and offshore, but was overall not enough to overcome the loss of most of the population from the seeding region. Juvenile stage durations were modeled to be as short as two and a half months for some individuals (assuming sufficient food is available), which would confer the population the advantage of a rapid resupply of young to a highly advective area. As *E. pacifica* in the particle tracking simulations were sometimes transported back into the seeding region from offshore or the south, some potential for self-seeding was shown.

For this potential to be realized, however, *E. pacifica* that are swept offshore must be able to maintain healthy enough body condition during their excursion into warm, low-food areas that reproduction upon re-entry is possible. More observational work exploring coping mechanisms to survive (or not) in conditions like these will yield some of the most important keys to our understanding of *E. pacifica's* ability to thrive in areas and times that, with our current knowledge, seem inhospitable.

A significant challenge lies in correctly parameterizing an individual-based model for a species as plastic as *E. pacifica* with information that accurately captures the important aspects of the species. There are still significant gaps in our understanding of fundamental biological processes for *E. pacifica*, such as how it responds to an ocean environment with generally insufficient food, whether overwintering metabolism is greatly reduced, how consumption rates by larval stages change when multiple food types are available, what mechanisms cause the variability in larval stage diel-vertical migration, and what the impact of different qualities of food might have on egg characteristics such as buoyancy, to name a few. An important missing key is also the degree to which horizontal migration is expressed by this species (if at all) and what cues initiate such behavior. It may be that DVM is less important to spatial distributions than horizontal migrations, yet very little work has been done to explore this behavior in the species.

The last chapter of this dissertation identifies several needs for understanding *E. pacifica* distribution and dynamics. Primary among these is a better understanding of the capacity of *E. pacifica* to cope with unfavorable environments into which transport is likely. While much focus to this point has been on identifying mechanisms that allow this species to remain near the coast to be successful, a shift of our energies toward appreciating how it

might survive excursions away from the coast may now be in order. Perhaps some of the plasticity of *E. pacifica* is a result of its behavior; DVM expressed differently in very warm (less time at the surface regardless of food scarcity at depth) or food-poor environments (remaining in shallow food patches during the day regardless of vulnerability to predation) may be the best way to explain how they can survive for multiple years. Females ready to spawn may behave very differently from the rest of the population, undertaking different vertical migration schedules or ambits. Or perhaps there are fundamental modifications to *E. pacifica's* physiology during different seasons or when encountering severe food shortages; reduction of a starving krill's metabolic needs might extend its life long enough to be advected back into a more favorable environment or to survive until a richer season.

Some of these unknowns can be addressed with laboratory or shipboard experiments. For example, starvation experiments with respiration and growth measurements would clarify whether metabolic needs are reduced beyond what body shrinkage would indicate. Experiments such as these would also give empirical evidence of a point of no return, or a body condition from which this krill could not bounce back or continue growing—this number would be hugely useful in modeling efforts. Behavioral responses to light intensity (measured as swimming speeds—or rate of pleopod beating if the krill is tethered—away from a light source, for instance) under starved and satiated conditions could be measured in a laboratory setting to show whether there is evidence for adaptive behavior to poor food conditions in the ocean. Similarly, responses to a light source in varying water temperatures might indicate how a krill might react in too-warm environments.

In the absence of experiments like these, a model like that presented here would probably benefit from a more mechanistic DVM process. An improved vertical migration behavior would depend not only on light intensity and stage-based preferred depths, but several other factors as well. One might be vertical food distribution; a krill that is able to detect the peak concentration of food in the water column and swim to that depth rather than simply to the surface would be able to take advantage of subsurface chlorophyll maxima, which is more realistic. Another factor might be individual motivations, such as recent feeding history (similar to the way egg brood size is calculated in the model presented in Chapter 4), recent egg production, temperature gradients in the immediate vicinity, or even water velocities (a krill that swims down against an upward flow might encounter different food). The greater flexibility provided by this type of DVM might enable more rapid growth as a result of higher ingestion rates or decreased metabolic rates than is possible in the simplified DVM model used here.

As ever, greater spatial and temporal resolution in a circulation model is desirable. Better ability to resolve small-scale retention features, such as sub-mesoscale eddies, would provide more information about how or whether *E. pacifica* is retained near the coast. A data-assimilative physical model might provide more accurate ocean conditions and provide better forcing for an ecosystem model and thus, hopefully, more representative food resources for an IBM such as the one presented here.

Despite the challenges ahead, Lagrangian individual-based modeling is a useful tool for exploring some of the unanswered questions about *E. pacifica*. With a highly resolved and realistic ecosystem model coupled to the physical circulation model used here, very near-future efforts will include running the individual-based bioenergetic model with an improved DVM

over a winter to examine long-term impacts of the region's circulation on survival of a full cohort of *E. pacifica*. Moving from egg to egg, or linking larval stages to reproducing adults, is a high modeling priority.

6.0 Bibliography

Ainley, D. G., Spear, L. B., and Allen, S. G. (1996). Variation in the diet of Cassin's auklet reveals spatial, seasonal, and decadal occurrence patterns of euphausiids off California, USA. *Marine Ecology Progress Series*, *137*(1), 1-10.

Barnes, H. and Marshall, S.M. (1951) On the variability of replicate plankton samples and some applications of 'Contagious' series to the statistical distribution of catches over restricted periods. *J. Mar. Biol. Assoc.* 30, 233—263.

Barth, J.A. (2003) Anomalous southward advection during 2002 in the northern California Current: evidence from Lagrangian surface drifters. *Geophysical Research Letters* 30, 8024, doi:10.1029/2003GL017511

Batchelder, H. P., and Miller, C. B. (1989). Life history and population dynamics of *Metridia pacifica*: Results from simulation modelling. *Ecological Modelling*, 48(1), 113-136.

Batchelder, H. P., and Williams, R. (1995). Individual-based modelling of the population dynamics of *Metridia lucens* in the North Atlantic. *ICES Journal of Marine Science: Journal du Conseil*, *52*(3-4), 469-482.

Batchelder, H.P., Edwards, C.A. and Powell, T.M. (2002) Individual-based models of copepod populations in coastal upwelling regions: implications of physiologically and environmentally influenced diel vertical migration on demographic success and nearshore retention. *Progress in Oceanography*. 53, 307--333.

Batchelder, H. P. 2006. Forward-in-Time-/Backward-in-Time Trajectory (FITT/BITT) Modeling of Particles and Organisms in the Coastal Ocean. *Journal of Atmospheric and Oceanic Technology* 23, 727--741.

Baums, I.B., Paris, C.B., and Chérubin, L.M., (2006) A bio-oceanographic filter to larval dispersal in a reef-building coral. *Limnology and Oceanography* 51.5 (2006): 1969-1981.

Bernal, P.A. and McGowan, J.A. (1981) Advection and upwelling in the California Current, in Richards, F.A. (ed.), Coastal Upwelling, Vol. 1. *American Geophysical Union*, Washington, DC. pp. 381-389.

Bi, H., Peterson, W. T., and Strub, P. T. (2011). Transport and coastal zooplankton communities in the northern California Current system. *Geophysical Research Letters*, *38*(12).

Boden, B. P., 1950. The post-naupliar stages of the crustacean *Euphausia pacifica* . *T. Am. Microsc. Soc.* 69, 373--386.

Bollens, S.M., Frost, B.W., and Lin, T.S. (1992) Recruitment, growth, and diel vertical migration of *Euphausia pacifica* in a temperate fjord. *Mar. Biol.* 114, 219--228.

Brinton, E. (1962). The distribution of Pacific euphausiids.

Brinton, E. (1967) Vertical Migration and Avoidance Capability of Euphausiids in the California Current. *Limnol. Oceanogr.* 12, 451--483.

Brinton, E. (1976) Population biology of *Euphausia pacifica* off southern California. *Fish. Bull.* 74, 733--762.

Brinton, E., Ohman, M.D., Townsend, A.W., Knight, M.D. (1999) Euphausiids of the world ocean (World Biodiversity Database CD-ROM Series). Expert Centre for Taxonomic Identifications (ETI), University of Amsterdam.

Brinton, E., and Townsend, A. (2003). Decadal variability in abundances of the dominant euphausiid species in southern sectors of the California Current. *Deep Sea Research Part II: Topical Studies in Oceanography*, *50*(14), 2449-2472.

Burrows, M.T., Tarling, G. (2004) Effects of density dependence on diel vertical migration of populations of northern krill: genetic algorithm model. *Mar. Ecol. Prog. Ser.* 277, 209—220.

Carton, J. A., Chepurin, G., and Cao, X. (2000). A simple ocean data assimilation analysis of the global upper ocean 1950-95. Part II: Results. Journal of Physical Oceanography, 30(2), 311-326.

Carlotti, F., and WOLF, K. U. (1998). A Lagrangian ensemble model of *Calanus finmarchicus* coupled with a 1D ecosystem model. Fisheries Oceanography, 7(3-4), 191-204.

Carr, S. D., Capet, X. J., Mcwilliams, J. C., Pennington, J. T., and Chavez, F. P. (2008). The influence of diel vertical migration on zooplankton transport and recruitment in an upwelling region: Estimates from a coupled behavioral-physical model. *Fisheries Oceanography*, *17*(1), 1-15.

Cloern, J. E., Grenz, C., and Vidergar-Lucas, L. (1995). An empirical model of the phytoplankton chlorophyll: carbon ratio-the conservation factor between productivity and growth rate. *Limnology and Oceanography*, *40*(7), 1313-1321.

Conkright, M. E., Garcia, H. E., O'Brien, T. D., Locarnini, R. A., Boyer, T. P., Stephens, C., and Antonov, J. I. (2002). World Ocean Atlas 2001. Volume 4, Nutrients.

Corwith, H.L. and Wheeler, P.A. (2002) El Niño related variations in nutrient and chlorophyll distributions off Oregon. *Prog. Oceanogr.* 54, 361--380.

Coyle, K.O. and Pinchuk, A.I. (2005) Seasonal cross-shelf distribution of major zooplankton taxa on the northern Gulf of Alaska shelf relative to water mass properties, species depth preferences and vertical migration behavior. *Deep Sea Res.* 52, 217-245.

Croll, D. A., Marinovic, B., Benson, S., Chavez, F. P., Black, N., Ternullo, R., and Tershy, B. R. (2005). From wind to whales: trophic links in a coastal upwelling system. *Marine Ecology Progress Series*, *289*(117), 30.

Décima, M. Ohman, M.D., De Robertis, A. (2010) Body size dependence of euphausiid spatial patchiness. *Limnol. Oceanogr.* 55, 777--788.

De Robertis, A. (2002). Size-dependent visual predation risk and the timing of vertical migration: An optimization model. *Limnology and Oceanography*, 925-933.

Di Lorenzo, E. (2003). Seasonal dynamics of the surface circulation in the Southern California Current System. *Deep Sea Research Part II: Topical Studies in Oceanography*, *50*(14), 2371-2388.California Current System. *Deep-Sea Research II* 50 (2003) 2371–2388

Di Lorenzo, Emanuele, Arthur J. Miller, Niklas Schneider, James C. McWilliams, (2005): The Warming of the California Current System: Dynamics and Ecosystem Implications. *J. Phys. Oceanogr.*, 35, 336–362.

Dilling, L., Wilson, J., Steinberg, D., and Alldredge, A. (1998). Feeding by the euphausiid *Euphausia pacifica* and the copepod *Calanus pacificus* on marine snow. Marine Ecology Progress Series, 170, 189-201.

Dorman, J.G., Bollens, S.M. and Slaughter, A.M. (2005) Population biology of euphausiids off northern California and effects of short time-scale wind events on *Euphausia pacifica*. *Mar. Ecol. Prog. Ser.* 288, 183--198.

Drake, P.T., Edwards, C.A., and Barth, J.A. (2011) Dispersion and connectivity estimates along the U.S. west coast from a realistic numerical model. *J. Mar. Res.* 69(1), 1--37.

Durazo, R., Collins, C. A., Hyrenbach, D. K., Schwing, F. B., Baumgartner, T. R., García, J., and Sydeman, W. J. (2001). The state of California current, 2000–2001: a third straight La Niña year.

Emmett, R. L., Krutzikowsky, G. K., and Bentley, P. (2006). Abundance and distribution of pelagic piscivorous fishes in the Columbia River plume during spring/early summer 1998–2003: relationship to oceanographic conditions, forage fishes, and juvenile salmonids. *Progress in Oceanography*, *68*(1), 1-26.

Endo, Y. (1981). Ecological studies on the euphausiids occurring in the Sanriku waters with special reference to their life history and aggregated distribution. Tohoku University, Sendai, 198(1), 166.

Endo, Y. and Yamano, F. (2006) Diel vertical migration of *Euphausia pacifica* (Crustacea, Euphausiacea) in relation to molt and reproductive processes, and feeding activity. *J. Oceanogr.* 62, 693—703.

Fiechter, J., Moore, A.M., Edwards, C.A., Bruland, K.W., Di Lorenzo, E., Lewis, C.V., and Hedstrom, K. (2009). Modeling iron limitation of primary production in the coastal Gulf of Alaska. Deep Sea Research Part II: Topical Studies in Oceanography, 56(24), 2503-2519.

Feinberg, L.R. and Peterson, W.T. (2003) Variability in duration and intensity of euphausiid spawning off central Oregon, 1996-2001. *Prog. Oceanogr.* 57, 363--379.

Feinberg, L.R., Shaw, C.T. and Peterson, W.T. (2006) Larval development of *Euphausia pacifica* in the laboratory: variability in developmental pathways. *Mar. Ecol. Prog. Ser.* 316, 127--137.

Feinberg, L.R., Shaw, C.T., and Peterson, W.T. (2007) Long-term laboratory observations of *Euphausia pacifica* fecundity: comparison of two geographic regions. *Mar. Ecol. Prog. Ser.* 341, 141--152.

Franks, P.J.S. (1992) Sink or swim: accumulation of biomass at fronts. *Mar. Ecol. Prog. Ser.* 82, 1--12.

Gentleman, W., Leising, A., Frost, B., Strom, S., and Murray, J. (2003). Functional responses for zooplankton feeding on multiple resources: a review of assumptions and biological dynamics. *Deep Sea Research Part II: Topical Studies in Oceanography*, *50*(22), 2847-2875.

Gentleman, W. C., and Neuheimer, A. B. (2008). Functional responses and ecosystem dynamics: how clearance rates explain the influence of satiation, food-limitation and acclimation. *Journal of Plankton Research*, 30(11), 1215-1231.

Goericke, R., Venrick, E., Mantyla, A., Bograd, S. J., Schwing, F. B., Huyer, A., and Sydeman, W. J. (2005). The state of the California current, 2003-2004: still cool?. *California Cooperative Oceanic Fisheries Investigations Report*, *46*, 32.

Goericke, R., Venrick, E., Mantyla, A., Bograd, S. J., Schwing, F. B., Huyer, A., and Sydeman, W. J. (2005). The state of the California current, 2004-2005: still cool?. *California Cooperative Oceanic Fisheries Investigations Report*, *46*, 32-71.

Gómez-Gutiérrez, J. (2003) Comparative study of the population dynamics, secondary productivity, and reproductive ecology of the euphausiids

Euphausia pacifica and *Thysanoessa spinifera* in the Oregon Upwelling Region. PhD dissertation, Oregon State University. 245 pp.

Gómez-Gutiérrez, J., Peterson, W.T. and Miller, C.B. (2005) Cross-shelf life-stage segregation and community structure of the euphausiids off central Oregon (1970–1972). *Deep-Sea Res. Pt II* 52, 289--315.

Gómez-Gutiérrez, J., Feinberg, L.R., Shaw, T., Peterson, W.T. (2006) Variability of brood size and female length of *Euphausia pacifica* among three populations in the North Pacific. *Mar. Ecol. Prog. Ser.*, 323, 185-194.

Gómez-Gutiérrez, J., Feinberg, L.R., Shaw, T.C., and Peterson, W.T. (2007) Interannual and geographical variability of the brood size of the euphausiids *Euphausia pacifica* and *Thysanoessa spinifera* along the Oregon coast (1999-2004). *Deep-Sea Res. Pt I* 54, 2145--2169.

Gómez-Gutiérrez, J., Peterson, W.T. and Miller, C.B. (2010) Embryo biometry of three broadcast spawning euphausiid species applied to identify cross-shelf and seasonal spawning patterns along the Oregon coast. *J. Plankton Res.* 32, 739—760.

Hansen, H. J., 1911. The genera and species of the order Euphausiacea, with account of remarkable variation. *Bulletin de l'Institut Océanographique de Monaco* 210, 1--54.

Hare, S.R, N.J. Mantua, and R.C. Francis, (1999): Inverse Production Regimes: Alaska and West Coast pacific salmon. *Fisheries*, 24, 6-14.

Harris, R., Wiebe, P., Lenz, J., Skjoldal, H. R., and Huntley, M. (Eds.). (2000). *ICES zooplankton methodology manual*. Academic Press.

Harvey, H. R., Ju, S. J., Son, S. K., Feinberg, L. R., Shaw, C. T., and Peterson, W. T. (2010). The biochemical estimation of age in Euphausiids: laboratory calibration and field comparisons. *Deep Sea Research Part II: Topical Studies in Oceanography*, *57*(7), 663-671.

Hickey, B. M. (1989). Patterns and processes of circulation over the Washington continental shelf and slope. *Elsevier Oceanography Series*, *47*, 41-115.

Hodur, R.M., J. Pullen, J. Cummings, X. Hong, J.D. Doyle, P. Martin, and M.A. Rennick. 2002. The Coupled Ocean/Atmosphere Mesoscale Prediction System (COAMPS). *Oceanography* 15(1):88–98.

Holt C.A., Mantua N. (2009) Defining spring transition: regional indices for the California Current System. *Mar. Ecol. Prog. Ser.* 393, 285—299

Hunter, J. R., Craig, P. D., and Phillips, H. E. (1993). On the use of random walk models with spatially variable diffusivity. *Journal of Computational Physics*, *106*(2), 366-376.

Huyer, A. (1983) Coastal Upwelling in the California current system. *Prog. Oceanogr.* 12, 259--284.

Iguchi, N., Ikeda, T., and Imamura, A. (1993) Growth and life cycle of a euphausiid crustacean (*Euphausia pacifica* Hansen) in Toyama Bay, Southern Japan Sea. *Bull. Jpn Sea Natl. Fish. Res. Inst.* 43, 69--81.

Iguchi, N., and Ikeda, T. (1994). Experimental study on brood size, egg hatchability and early development of a euphausiid Euphausia pacifica from Toyama Bay, southern Japan Sea. *Bull Jpn Sea Natl Fish Res Inst*, *44*, 49-57.

Ju, S., Harvey, H.R., Gómez-Gutiérrez, J., Peterson, W.T. (2006) The role of lipids during embryonic development of the euphausiids *Euphausia pacifica* and *Thysanoessa spinifera*. *Limnol. Oceanogr.* 51(5), 2398—2408.

Keister, J.E., Vance, P.M., Peterson, W.T. (2001) Vertical Distribution of *Euphausia pacifica* off the Central Oregon coast, U.S. GLOBEC Northeast Pacific Scientific Investigator's Meeting, Seattle, WA.

Keister, J.E. and Peterson, W.T. (2003) Zonal and seasonal variations in zooplankton community structure off the central Oregon coast, 1998-2000. *Prog. Oceanogr.* 57, 341--361.

Keister, J.E., Cowles, T.J., Peterson, W.T., and Morgan, C.A. (2009) Do upwelling filaments result in predictable biological distributions in coastal upwelling ecosystems? *Prog. Oceanogr.* 23, 303--313.

Keister, J. E., Di Lorenzo, E., Morgan, C. A., Combes, V., and Peterson, W. T. (2011). Zooplankton species composition is linked to ocean transport in the Northern California Current. *Global Change Biology*, *17*(7), 2498-2511.

Kim, H. S., Yamaguchi, A., and Ikeda, T. (2010). Population dynamics of the euphausiids *Euphausia pacifica* and *Thysanoessa inspinata* in the Oyashio region during the 2007 spring phytoplankton bloom. *Deep Sea Research Part II: Topical Studies in Oceanography*, *57*(17), 1727-1732.

Kim, S., and J. A. Barth *(*2011*),* Connectivity and larval dispersal along the Oregon coast estimated by numerical simulations, J. Geophys. Res., 116*, C06002, doi:*10.1029/2010JC006741*.*

Kishi, M.J., Kashiwai, M., Ware, D.M., Megrey, B.A., Eslinger, D.L., Werner, F.E., and Zvalinsky, V.I. (2007). NEMURO—a lower trophic level model for the North Pacific marine ecosystem. Ecological Modelling, 202(1), 12-25.

Knight, M.D. (1984) Variation in larval morphogenesis within the Southern California Bight population of *Euphausia pacifica* from winter through summer, 1977-78. *CalCOFI Rep*. 25, 87--99.

Lamb, J., and W. Peterson (2005), Ecological zonation of zooplankton in the

COAST study region off central Oregon in June and August 2001 with consideration of retention mechanisms, *J. Geophys. Res.*, 110, C10S15, doi:10.1029/2004JC002520.

Large, W.G. and Pond, S. (1981) Open Ocean Momentum Flux Measurements in Moderate to Strong Winds. *J. Phys. Oceanogr.* 11, 324--336.

Lasker, R. (1966). Feeding, growth, respiration, and carbon utilization of a euphausiid crustacean. *Journal of the Fisheries Board of Canada*, *23*(9), 1291-1317.

Lavaniegos-Espejo, B. E., Lara-Lara, J. R., and Brinton, E. (1989). Effects of the 1982-83 El Niño event on the euphausiid populations of the Gulf of California. *Reports of California Cooperative Oceanic Fisheries Investigations*,*30*, 73-87.

Liu, H. L., and Sun, S. (2010). Diel vertical distribution and migration of a euphausiid *Euphausia pacifica* in the Southern Yellow Sea. *Deep Sea Research Part II: Topical Studies in Oceanography*, *57*(7), 594-605.

Lu, B., Mackas, D., and Moore, D.F. (2003) Cross-shore separation of adult and juvenile euphausiids in a shelf-break alongshore current. *Progr. Ocean.* 57, 381-404.

Mackas, D.L., Kieser, R., Saunders, M., Yelland, D.R., Brown, R.M., and Moore, D.F. (1997) Aggregation of euphausiids and Pacifica hake (*Merluccius productus*) along the outer continental shelf off Vancouver Island. *Can. J. Fish. Aquat. Sci.* 54, 2080-2096.

Mantua, N. J., Hare, S. R., Zhang, Y., Wallace, J. M., and Francis, R. C. (1997). A Pacific interdecadal climate oscillation with impacts on salmon production. *Bulletin of the American Meteorological Society*, *78*(6), 1069-1079.Mauchline, J. and Fisher, L.R. (1969) The biology of euphausiids. *Adv. Mar. Biol.* 7, 1--454.

Marta-Almeida, M., Dubert, J., Peliz, A. and Queiroga, H. (2006) Influence of vertical migration pattern on retention of crab larvae in a seasonal upwelling system. *Mar. Ecol. Prog. Ser.* 307, 1--19.

Marinovic, B., and Mangel, M. (1999). Krill can shrink as an ecological adaptation to temporarily unfavourable environments. Ecology Letters, 2(5), 338-343.

Mauchline, J. (1967). Feeding appendages of the *Euphausiacea* (*Crustacea*). Journal of Zoology, 153(1), 1-43.

Mauchline, J. and Fisher, L.R. (1969) The biology of euphausiids. *Adv. Mar. Biol.* 7, 1--454.

Mauchline, J. (1998) The Biology of Calanoid Copepods, *Advances in Marine Biology*, 33, 1-707.

McLaren, I. A., Corkett, C. J., and Zillioux, E. J. (1969). Temperature

adaptations of copepod eggs from the arctic to the tropics. *The Biological Bulletin*, *137*(3), 486-493.

Miller, C. B., Lynch, D. R., Carlotti, F., Gentleman, W., and Lewis, C. V. (1998). Coupling of an individual-based population dynamic model of *Calanus finmarchicus* to a circulation model for the Georges Bank region. Fisheries Oceanography, 7(3-4), 219-234.

Mouillott, D., Culioli, J.M., Thang, D.C. (2002) Indicator species analysis as a test of non-random distribution of species in the context of marine protected areas. *Environ. Conserv.* 29, 385--390.

Nakagawa, Y., Endo, Y., and Taki, K. (2001). Diet of *Euphausia pacifica* Hansen in Sanriku waters off northeastern Japan. *Plankton Biology and Ecology*, *48*(1), 68-77.

Nakagawa, Y., Endo, Y., and Taki, K. (2002). Contributions of heterotrophic and autotrophic prey to the diet of euphausiid, *Euphausia pacifica* in the coastal waters off northeastern Japan. *Polar Bioscience*, 52-65.

Nakagawa, Y., Endo, Y., and Sugisaki, H. (2003). Feeding rhythm and vertical migration of the euphausiid *Euphausia pacifica* in coastal waters of north-eastern Japan during fall. *J. Plankton Res.* 25, 633—644.

Nakagawa, Y., Ota, T., Endo, Y., Taki, K., and Sugisaki, H. (2004). Importance of ciliates as prey of the euphausiid *Euphausia pacifica* in the NW North Pacific. *Marine ecology. Progress series*, *271*, 261-266.

Nemoto, T. (1957). Foods of baleen whales in the northern Pacific. *Sci. Rep. Whales Res. Inst*, *12*, 33-89.

North, E. W., Schlag, Z., Hood, R. R., Li, M., Zhong, L., Gross, T., and Kennedy, V. S. (2008). Vertical swimming behavior influences the dispersal of simulated oyster larvae in a coupled particle-tracking and hydrodynamic model of Chesapeake Bay. *MARINE ECOLOGY-PROGRESS SERIES-*, *359*, 99.

Ohman, M. D. (1984). Omnivory by *Euphausia pacifica*: the role of copepod prey. Marine ecology. Progress series, 19(1-2), 125-131.

Papastephanou, K.M., Bollens, S.M. and Slaughter, A.M. (2006) Cross-shelf distribution of copepods and the role of event-scale winds in a northern California upwelling zone. *Deep-Sea Res. Pt II* 53, 3078--3098.

Passow, U., and Alldredge, A. L. (1999). Do transparent exopolymer particles (TEP) inhibit grazing by the euphausiid *Euphausia pacifica*?. Journal of plankton research, 21(11), 2203-2217.

Pearcy, W. G., and Small, L. F. (1968). Effects of pressure on the respiration of vertically migrating crustaceans. *Journal of the Fisheries Board of Canada*,*25*(7), 1311-1316.

Peterson, W.T., Miller, C.B. and Hutchinson, A. (1979) Zonation and maintenance of copepod populations in the Oregon upwelling zone. *Deep-Sea Res.* 26, 467--494.

Peterson, W. (1998) Life cycle strategies of copepods in coastal upwelling zones. *J. Marine Syst.* 15, 313--326.

Peterson, W. T., and Schwing, F. B. (2003). A new climate regime in northeast Pacific ecosystems. *Geophysical Research Letters*, *30*(17).

Pfeiffer-Herbert, A. S., McManus, M. A., Raimondi, P. T., Chao, Y., and Chai, F. (2007). Dispersal of barnacle larvae along the central California coast: A modeling study. *Limnology and oceanography*, *52*(4), 1559-1569

Pierce, S. D., J. A. Barth, R. E. Thomas, and G. W. Fleischer (2006) Anomalously warm July 2005 in the northern California Current: historical context and the significance of cumulative wind stress, *Geophys. Res. Lett.* 33, L22S04, doi:10.1029/2006GL027149.

Pillar, S.C., Armstrong, D.A. and Hutchings, L. (1989) Vertical migration, dispersal and transport of *Euphausia lucens* in the southern Benguela Current. *Mar. Ecol. Prog. Ser.* 53, 179--190.

Pinchuk, A.I. and Hopcroft, R.R. (2006) Egg production and early development of *Thysanoessa inermis* and *Euphausia pacifica* (Crustacea: Euphausiacea) in the northern Gulf of Alaska. *J. Exp. Mar. Bio. and Ecol.* 332, 206-215.

Pinchuk, A. I., and Hopcroft, R. R. (2007). Seasonal variations in the growth rates of euphausiids (*Thysanoessa inermis, T. spinifera, and Euphausia pacifica*) from the northern Gulf of Alaska. Marine Biology, 151(1), 257-269.

Platt, T. G. C. L., Gallegos, C. L., and Harrison, W. G. (1981). Photoinhibition of photosynthesis in natural assemblages of marine phytoplankton.

Roemmich, D., and McGowan, J. (1995). Climatic warming and the decline of zooplankton in the California Current. *SCIENCE-NEW YORK THEN WASHINGTON-*, 1324-1324.

Ross, R.M. (1981) Laboratory culture and development of *Euphausia pacifica*. *Limnol. Oceanogr*. 26, 235--246.

Ross, R.M., Daly, K.L., and English, T.S. (1982) Reproductive cycle and fecundity of *Euphausia pacifica* in Puget Sound, Washington. *Limnol. Oceaonogr.* 27, 304-314.

Ross, R.M. (1982*a*) Energetics of *Euphausia pacifica*. I. Effects of body carbon and nitrogen and temperature on measured and predicted production. *Marine Biology*, 68(1), 1-13.

Ross, R.M. (1982*b*) Energetics of *Euphausia pacifica*. II. Complete carbon and nitrogen budgets at 8 and 12 C throughout the life span. *Marine*

Biology, 68(1), 15-23.
Schwing, F. B., Murphree, T., and Green, P. M. (2002). The Northern Oscillation Index (NOI): a new climate index for the northeast Pacific. *Progress in Oceanography*, *53*(2), 115-139.
Sharqawy, Mostafa H., John H. Lienhard V and Syed M. Zubair. "The thermophysical properties of seawater: A review of existing correlations and data." Desalination and Water Treatment, 16 (April 2010) 354–380.
Shaw, T., Feinberg, L.R., and Peterson, W.T. (2010) Growth of *Euphausia pacifica* in the upwelling zone off the Oregon coast. *Deep Sea Res., pt II* 57, 584-593.
Siegel, V. (2000) Krill (Euphausiacea) life history and aspects of population dynamics. *Can. J. Fish. Aquat. Sci.* 57, 130--150.
Smiles, M. C. and Pearcy, W. G. (1971) Size structure and growth rate of *Euphausia pacifica* off the Oregon coast. *Fish. Bull.* 69, 79-86.
Smith, W. H. F. and Sandwell, D. T. (1997) Global seafloor topography from satellite altimetry and ship depth soundings, Science, v. 277, p. 1957-1962.
Song, Y. and Haidvogel, D. (1994). A semi-implicit ocean circulation model using a generalized topography-following coordinate system. *Journal of Computational Physics*, *115*(1), 228-244.
Steinberg, D. K., Carlson, C. A., Bates, N. R., Goldthwait, S. A., Madin, L. P., and Michaels, A. F. (2000). Zooplankton vertical migration and the active transport of dissolved organic and inorganic carbon in the Sargasso Sea. *Deep Sea Research Part I: Oceanographic Research Papers*, *47*(1), 137-158.
Suh H.L., Soh H.Y., Hong S.Y. (1993) Larval development of the euphausiid *Euphausia pacifica* in the Yellow Sea. *Mar. Biol.* 115, 625--633.
Taki, K. (2008) Vertical distribution and diel migration of euphausiids from Oyashio Current to Kuroshio area off northeastern Japan. *Plankton Benthos Res.* 3, 27—35.
Tanasichuk, R. W. (1998). Interannual variations in the population biology and productivity of Thysanoessa spinifera in Barkley Sound, Canada, with special reference to the 1992 and 1993 warm ocean years. *Marine Ecology Progress Series*, *173*, 181-195.
Tarling, G.A., Cuzin-Roudy, J., and Buchholz, F. (1999) Vertical migration behavior in the northern krill *Meganyctiphanes norvegica* is influenced by moult and reproductive processes. *Mar. Ecol. Prog. Ser.* 190, 253--262.
Thygesen, U.H. (2011) How to reverse time in stochastic particle tracking

models. *J. Mar. Sys.* 88, 159-168.

Vance, P.M., Keister, J.E. and Peterson, W.T. (2003) Seasonal and annual variation in the population composition and depth distributions of the euphausiid, *Euphausia pacifica*. *EOS Trans,* American Geophysical Union, Honolulu, HI, 84(52) OS21B-19.

Visser, A.W. (1997) Using random walk models to simulate the vertical distribution of particles in a turbulent water column. *Mar. Ecol. Prog. Ser.* 158, 275-281.

Wiebe, P. H., Ashjian, C. J., Lawson, G. L., Piñones, A., and Copley, N. J. (2011). Horizontal and vertical distribution of euphausiid species on the Western Antarctic Peninsula US GLOBEC Southern Ocean study site. *Deep Sea Research Part II: Topical Studies in Oceanography*, *58*(13), 1630-1651.

Yamanaka, Y., Yoshie, N., Fujii, M., Aita, M. N., and Kishi, M. J. (2004). An ecosystem model coupled with Nitrogen-Silicon-Carbon cycles applied to Station A7 in the Northwestern Pacific. *Journal of Oceanography*, *60*(2), 227-241.